



4-2006

Comparative Genomic Analyses and Expression of a Set of Overlapping Open Reading Frames of Frog Virus 3, Type Species of *Ranavirus* (Family *Iridoviridae*)

Wendy Guat Hoon Tan
Western Michigan University

Follow this and additional works at: <https://scholarworks.wmich.edu/dissertations>



Part of the Animal Sciences Commons, Biology Commons, and the Cell and Developmental Biology Commons

Recommended Citation

Tan, Wendy Guat Hoon, "Comparative Genomic Analyses and Expression of a Set of Overlapping Open Reading Frames of Frog Virus 3, Type Species of *Ranavirus* (Family *Iridoviridae*)" (2006). *Dissertations*. 995.

<https://scholarworks.wmich.edu/dissertations/995>

This Dissertation-Open Access is brought to you for free and open access by the Graduate College at ScholarWorks at WMU. It has been accepted for inclusion in Dissertations by an authorized administrator of ScholarWorks at WMU. For more information, please contact wmu-scholarworks@wmich.edu.



COMPARATIVE GENOMIC ANALYSES AND EXPRESSION OF A SET OF
OVERLAPPING OPEN READING FRAMES OF FROG VIRUS 3,
TYPE SPECIES OF *RANAVIRUS* (FAMILY *IRIDOVIRIDAE*)

by

Wendy Guat Hoon Tan

A Dissertation
Submitted to the
Faculty of The Graduate College
in partial fulfillment of the
requirements for the
Degree of Doctor of Philosophy
Department of Biological Sciences
Dr. Karim Essani, Advisor

Western Michigan University
Kalamazoo, Michigan
April 2006

COMPARATIVE GENOMIC ANALYSES AND EXPRESSION OF A SET OF
OVERLAPPING OPEN READING FRAMES OF FROG VIRUS 3,
TYPE SPECIES OF *RANAVIRUS* (FAMILY *IRIDOVIRIDAE*)

Wendy Guat Hoon Tan, Ph.D.

Western Michigan University, 2006

Frog virus 3 (FV3) is the type species member of the genus *Ranavirus* (family *Iridoviridae*). To better understand the molecular mechanisms involved in the replication of FV3, including transcription of its highly methylated DNA genome, the complete nucleotide sequence of the FV3 genome has been determined. The FV3 genome is 105,903 base pairs long excluding the terminal redundancy. The G+C content of FV3 genome is 55% and it encodes 98 non-overlapping potential open reading frames (ORFs) containing 50 to 1293 amino acids. Eighty-four ORFs have significant homology to known proteins of other iridoviruses, whereas 14 are unique FV3 ORFs. Of these, 12 ORFs do not share homology to any known proteins and only two FV3 specific ORFs shared some degree of homology with other organisms. A microsatellite containing a stretch of 34 tandemly repeated CA dinucleotide in a non-coding region was detected. To-date, no such sequence has been reported in any animal virus. A set of overlapping reading frames (ORF 55R and 55L) has also been identified and shown to express both at

the RNA and protein levels by RT-PCR and baculovirus expression system respectively. Both were classified as immediate-early genes and the function of ORF 55L protein has been shown to be a DNA nuclease, and possible exonuclease activity for ORF 55R protein.

UMI Number: 3211707

Copyright 2006 by
Tan, Wendy Guat Hoon

All rights reserved.

INFORMATION TO USERS

The quality of this reproduction is dependent upon the quality of the copy submitted. Broken or indistinct print, colored or poor quality illustrations and photographs, print bleed-through, substandard margins, and improper alignment can adversely affect reproduction.

In the unlikely event that the author did not send a complete manuscript and there are missing pages, these will be noted. Also, if unauthorized copyright material had to be removed, a note will indicate the deletion.

UMI[®]

UMI Microform 3211707

Copyright 2006 by ProQuest Information and Learning Company.

All rights reserved. This microform edition is protected against unauthorized copying under Title 17, United States Code.

ProQuest Information and Learning Company
300 North Zeeb Road
P.O. Box 1346
Ann Arbor, MI 48106-1346

Copyright by
Wendy Guat Hoon Tan
2006

ACKNOWLEDGMENTS

I would like to thank Dr. Karim Essani for his constructive criticism and guidance for this research and its completion. Many thanks to my committee members Drs. Bruce Bejcek, Todd Barkman and Rob Eversole for their advice and scientific input to complete this project and for their critical review of this manuscript. I am especially grateful to Dr. Todd Barkman whose guidance with lots of patience made the initiation of this research work much less insurmountable. Drs. John Stout and John Barrett, whose expert technical assistance and guidance in many of the molecular and electron microscopy works in this project deserve many thanks. I want to thank Drs. Zvi Kelman and Jae-Ho Shin for their expertise in the helicase assays, Drs. Charles Ide and Anna Jelaso for their technical assistance in real-time RT-PCR. My sincerest thanks to Vivian Locke, Hui Lin Lee, Michael Franz and Jean Hsiao, whose help and friendship was invaluable, especially during my down times. I am very thankful for Don Debat, whose love for computer arts helped me in many of the graphic presentations in this manuscript. I also sincerely thank many other individuals who have assisted me directly or indirectly and their names are too numerous for this space. This work is dedicated to my parents, whose lifetime suffering from debilitating diseases inspired me to seek knowledge in an attempt to find ways to alleviate suffering from diseases.

Wendy Guat Hoon Tan

TABLE OF CONTENTS

ACKNOWLEDGMENTS	ii
LIST OF FIGURES	vii
INTRODUCTION.....	1
Iridoviruses	1
REVIEW OF LITERATURE.....	5
Discovery of FV3.....	5
Unique Features	5
Ultra-Structure	7
Replication Strategy.....	8
Nongenetic Reactivation	14
Modification of Host Cell Enzymatic Activities.....	15
Inhibition of Host Cell Macromolecular Synthesis.....	16
Temporal and Quantitative Control of Transcriptions	17
Host Cell Cytoskeleton Rearrangement.....	18
MATERIALS AND METHODS	21
Cells and Viruses.....	21
Cells.....	21
FV3	21
100X Concentration and Titeration of FV3	22
Recombinant Baculovirus	23
Isolation of FV3 Genomic DNA.....	23

Table of Contents—continued

Cloning of FV3 DNA Fragments	24
Transposon Priming of Genomic DNA Fragments.....	25
Alkaline-lysis Mini-preps	26
PCR Reactions	28
DNA Sequencing	28
Computer-assisted Analyses	29
Nucleotide Sequence Accession Number.....	30
FV3 Infected Cell Extracts	30
Isolation of Total RNAs	31
2-Step RT-PCR of ORFs 55L and 55R.....	33
Construction of Recombinant Baculovirus Expressing FV3 55L and 55R	35
No Myc-His Tag Version	35
Myc-His Tag Version.....	36
Isolation of Bacmid DNA.....	37
Transfection of Recombinant Baculovirus DNA.....	39
Western Blot of Recombinant 55L and 55R Proteins	41
Purification of Recombinant Proteins.....	42
Preparation of Helicase Substrates	43
DNA Helicase Assay.....	44
DNase Assay	45
Preparation of Substrate.....	45
Nuclease Assay	45

Table of Contents—continued

RESULTS	47
FV3 Genomic Organization	47
Microsatellites and Repeated Sequences	51
Regulatory sequences – Putative Promoter Sequences, Transcriptional Start and Termination Sequences and RNA Polymerase II Binding Sites	52
Transcriptional Regulation	53
DNA Replication, Repair, Modification and Processing	54
Protein Modifications	55
Host-virus Interactions	56
FV3 Specific Proteins	57
Structural and Other Genes	58
Nucleotide Differences as Compared to Published Sequences	58
Relatedness of FV3 Genome to Other Iridoviruses	61
Analyses of ORFs 55L and 55R	65
Is There Helicase Activity in FV3 Infected Cells?	68
Infected Cells Helicase Assays	68
Are Both FV3 ORFs 55L and 55R Expressed at the RNA Level?	70
2-Step RT-PCR	70
Temporal Classification of ORFs 55L and 55R Transcripts	72
Are Both ORFs 55L and 55R Expressed at the Protein Level?	73
Expression of FV3 ORFs 55L and 55R Proteins	73

Table of Contents—continued

Helicase Assays of Recombinant ORFs 55L and 55R Proteins.....	77
DNase Assay.....	78
DISCUSSION	83
APPENDICES	
A. List of FV3 ORFs.....	85
B. Radiation Safety Compliance.....	91
C. Recombinant DNA Biosafety Approval	93
BIBLIOGRAPHY	95

LIST OF FIGURES

1. Electron micrograph of FV3 virions showing icosahedral morphology	9
2. Replication cycle of FV3 in an infected cell.....	11
3. Baculovirus expression system for producing the recombinant FV3 55L and 55R proteins.....	40
4. <i>KpnI</i> and <i>HindIII</i> restriction maps of FV3 genomic DNA	48
5. Computer generated restriction map of FV3 genome from completely aligned genomic sequence	49
6. Linear ORF map of FV3 genome.....	50
7. Partial nucleotide sequence alignments of FV3 and aza-C ^r DNA methyltransferase gene	60
8. DNA dot matrix plots comparing FV3 genome with TFV genome.....	62
9. Parsimony bootstrap tree of the major capsid protein of representative iridoviruses	64
10. Parsimony bootstrap trees of 6 conserved genes of FV3, TFV, LCDV1, ISKNV and CIV	65
11. Super family 2 (SF2) helicases conserved motifs and amino acids sequence alignment of ORF 55L with other known helicases.....	67
12. Helicase assay of FV3 infected cells and uninfected cells.....	69
13. Agarose gel electrophoretic analysis of 2-Step RT-PCR amplifications of total RNAs extracted from FV3-infected FHM cells.....	71
14. Agarose gel electrophoretic analysis of RT-PCR amplifications of total RNAs extracted from FV3-infected FHM cells treated with cycloheximide and fluorophenylalanine	74
15. UV fluorescent microscopy of recombinant baculovirus infected Sf-21 cells	75

List of Figures—continued

16. Western blot of AcFV3-55L and AcFV3-55R recombinant proteins	76
17. Helicase assay of purified recombinant FV3 55L and 55R proteins	78
18. DNA nuclease activity assays of FV3 55L and 55R purified recombinant proteins with pcDNA3.1myc-hisA plasmid DNAs	80

INTRODUCTION

Iridoviruses

Iridoviruses are large DNA viruses that infect cold-blooded lower vertebrates and insects. The family *Iridoviridae* consists of four genera: *Iridovirus* and *Chloriridovirus* that infect insects; and *Ranavirus* and *Lymphocystivirus* that infect lower vertebrates [Williams *et al.*, 2000]. To date, no iridoviruses have been isolated from higher vertebrates. Iridoviruses are large icosahedral viruses whose genomes consist of linear, double-stranded DNA that is both circularly permuted and terminally redundant [Goorha and Murti, 1982; Darai *et al.*, 1983, 1985; Delius *et al.*, 1984]. The genomes of *Ranavirus* and *Lymphocystivirus* have been shown to be highly methylated [Willis and Granoff, 1980; Darai *et al.*, 1983; Tidona and Darai, 1997]. Recently, many virulent iridoviruses have been isolated and characterized from fish, reptiles, amphibians and turtles. These viruses cause serious systemic diseases and high mortality rates in cultured fish, frogs and turtles, and have become economically important pathogens [Berry *et al.*, 1983; Ahne *et al.*, 1989; Hedrick *et al.*, 1992; Hengstberger *et al.*, 1993; Marschang *et al.*, 1999; He *et al.*, 2000, 2001; Chinchar, 2002]. Most of the viruses isolated from fish, amphibians and reptiles were tentatively classified as members of the genus *Ranavirus* [Williams *et al.*, 2000].

Currently, eight of the lower vertebrate iridovirus genomes have been completely sequenced. These include lymphocystis disease virus 1 (LCDV1), Accession No. L634545 and AY380826; infectious spleen and kidney

necrosis virus (ISKNV), Accession No. AF371960; Grouper iridovirus, Accession No. AY666015; Orange-spotted grouper iridovirus, Accession No. AY894343; Rock bream iridovirus, Accession No. AY532606; *Abystoma tigrinum virus*, Accession No. AY150217 and tiger frog virus (TFV), also called *Rana tigrina ranavirus*, Accession No. AF389451. The genome sizes range from 103,000 base pairs (bp) for LCDV1 [Tidona and Darai, 1997] to 140,000 bp for Grouper iridovirus [Tsai *et al.*, 2005] encoding from 105 to 124 non-overlapping potential open reading frames (ORFs) in various genomes.

Frog virus 3 (FV3), the type species of the genus *Ranavirus* and one of the most extensively studied iridovirus at the molecular level, was originally isolated from a renal tumor of a leopard frog, *Rana pipiens* [Granoff *et al.*, 1966]. It was first thought that the virus caused the kidney tumor. However, later studies revealed that FV3 did not cause any detectable disease in frogs [Naegele *et al.*, 1974]. FV3 replicates in a wide variety of cell lines of human, simian, rodent, piscine, avian and amphibian origin [Granoff, 1969]. However, it has a stringent replication temperature requirement of 32°C or less, with an optimal temperature of 26°C - 30°C [Gravell and Granoff, 1970].

FV3 DNA replicates in two stages, and utilizes both the nucleus and the cytoplasm of the host cell [Goorha, 1982]. First stage of DNA synthesis takes place in the nucleus that results in the synthesis of genome size molecules. Later, progeny DNA is exported to the cytoplasm where second stage DNA synthesis results in the formation of concatemeric DNA [Goorha *et al.*, 1978; Goorha, 1982]. One unique feature of FV3 is its highly methylated DNA. All internal cytosines in the tetranucleotide sequence CCGG are methylated [Willis and Granoff, 1980]. FV3 shows one of the

highest levels of DNA methylation known. Since its isolation [Granoff *et al.*, 1966], FV3 has been the subject of many studies related to its highly ordered and tightly coordinated expression of immediate early, delayed early and late genes [Willis *et al.*, 1977; Elliot and Kelly, 1980]. Since host RNA polymerase II (RNAP II) is utilized for FV3 mRNA synthesis and is unable to transcribe methylated DNA, it has been of great interest to understand how the highly methylated FV3 genome is transcribed (reviewed in Willis *et al.* 1989). A FV3 trans-activating protein has been implicated in the transcription of the methylated viral template [Willis and Granoff, 1985; Thompson *et al.*; 1986; Spangler and Essani, 1994]. The purpose of this study was to sequence the genome of FV3 to facilitate the identification of the gene(s) encoding this protein(s) and other proteins that might play important roles in virus replication, particularly the transcription of viral DNA. Additionally, the FV3 genomic sequence will also be helpful in understanding molecular mechanisms involved in viral pathogenesis, and in elucidating phylogenetic relationships among different iridovirus species and genera.

Many cellular processes such as DNA methylation and DNA replication protein machinery such as polymerases, exonucleases, endonucleases, helicases and histones are important in maintaining genome stability. Mutations in some of these enzymatic proteins have been implicated in early lethality and causing severe diseases in animals, including humans. For example, mutations in at least three of the human RecQ helicases caused genetic disorders associated with cancer predisposition and premature aging [Karow *et al.*, 2000]. Many important discoveries relating to the molecular mechanisms involved in disease processes have been discovered as a result

of studies on viruses. It was believed that by dissecting the genetic make-up of FV3, other important functions of various genes conserved in humans can be elucidated. The long term objective of this research is to contribute to the growing understanding of the molecular mechanisms involved in the regulation of eukaryotic gene expression.

REVIEW OF LITERATURE

Discovery of FV3

FV3 is classified in the genus *Ranavirus*; in the family *Iridoviridae*. FV3 was originally isolated by Granoff *et al.* [1966] from a kidney tumor of a leopard frog, *Rana pipiens*. Other frog viruses (FV1, FV2, FV5-24) were also isolated from normal frog kidney and liver. FV3 was further studied as it was thought to be the causative agent for the frog adenocarcinoma. However, later investigation has shown that FV3 did not cause nor have any relationship to the development of the kidney tumor. It was discovered that the tumor was the result of *Lucké* herpesvirus infection [Naegele *et al.*, 1974]. Nevertheless, FV3 possessed several interesting characteristics that made it an attractive model for detailed scientific investigations. Since its discovery in 1966, FV3 has become the most studied type species of *Ranavirus* in many biochemical and biological studies, both at the molecular and organismal level.

Unique Features

FV3 genomic DNA is linear, double-stranded and 105,903 bp in size, excluding the terminal redundancy [Tan *et al.*, 2004]. FV3 DNA was shown to be circularly permuted and terminally redundant by biochemical and electron microscopic studies [Goorha and Murti, 1982]. Circular permutation of FV3 genomic DNA was demonstrated when native virion DNA was completely denatured and slowly renatured, producing circular duplexes with

different lengths of single-stranded ends when viewed with electron microscope. These single stranded ends were presumably the terminal repeats of the DNA molecules [Goorha and Murti, 1982]. Further, when the native DNA was subjected to lambda 5' endonuclease treatment and renatured, observations by electron microscopy showed that the DNA was linear with single stranded ends. Since the DNA did not circularize, this suggested that the terminal redundancy is composed of direct repeats as opposed to inverted repeats. This terminal repeat was calculated to be about 4% of the genome [Goorha and Murti, 1982]. Additionally, restriction maps of the virion DNA created by *EcoRI*, *HindIII*, *KpnI* and *XbaI* restriction enzymes demonstrated that the virion DNA was circular [Lee and Willis, 1983].

Another striking feature of FV3 is that every internal cytosine residue of the CpG sequences is methylated [Willis and Granoff, 1980]. This methylation pattern is most commonly found in eukaryotic DNA. In eukaryotes, promoter-region methylation is implicated in down regulation of gene expression [Meehan *et al.*, 1992; Razin and Cedar, 1991; Selker, 1990; Volpe *et al.*, 1993] especially when CpGs are methylated; with the exception of the chicken lysozyme gene [Wölf *et al.*, 1991]. However, methylation in FV3 DNA was suggested to play a role in protecting its DNA from endonucleolytic activity; as Goorha *et al.* [1984] found that FV3 DNA replicated in the presence of 5-azacytidine (a drug that inhibits DNA methylation) showed many breaks and was not properly encapsidated into virus shells, resulting in reduced production of infectious FV3 particles.

Interestingly, FV3 messenger RNA (mRNA) does not have poly A tails, a characteristic that resembles most prokaryotic mRNAs [Willis and Granoff,

1976b]; eukaryotic histone messages [Adesnik and Darnell, 1972]; Reovirus mRNAs [Stoltzfus *et al.*, 1973] and some herpesvirus mRNAs [Silverstein *et al.*, 1973]. This feature has enabled FV3 mRNAs to be resolved into very distinct bands on denaturing polyacrylamide gels [Willis, 1985]. FV3 mRNA also contained 5' methylated caps commonly found in both eukaryotic and prokaryotic mRNA; and was internally methylated [Raghow and Granoff, 1980]. However, the internal methylation of mRNA was found mostly in early transcripts but late transcripts are devoid of internal methylated nucleotides [Raghow and Granoff, 1980]. It is not clear why late transcripts are not internally methylated. One possibility is that early transcripts are synthesized in the nucleus and that internal methylation was catalyzed by cellular [Schibler *et al.*, 1977] or viral enzymes available only in the nucleus; and late transcripts are only made in the cytoplasm. Also, no intronic regions of the FV3 genome were found when colinearity of the gene and transcript were examined by electron microscopy and S1 nuclease analysis, suggesting that FV3 transcripts are not spliced [Willis, 1985]. Thus, FV3 possesses both prokaryotic and eukaryotic characteristics, filling a unique niche in the evolutionary hierarchy.

Ultra-Structure

FV3 virions are icosahedral and are approximately 150 nm from vertex to vertex of the icosahedron (Figure 1). The icosahedral lattice is made up of tightly packed subunits that can be released by treatment of Nonidet-40 (NP-40) and observed after negative staining [Willis, 1985]. These surface subunits are composed mainly of the major capsid protein encoded by the

virus. The outer covering of the virion is an envelope acquired from the host cell membrane which encloses the icosahedral capsid. Freeze-etching of unfixed FV3 showed that beneath the capsid is a lipid membrane that encircled the DNA-protein core in a sphere-like shape [Darcy-Tripier *et al.*, 1984]. When FV3 infected cells were subjected to freeze-etching, cross-sectional and longitudinal views of the virus core showed filaments of about 10 nm in width that were randomly oriented. It was suggested that these filamentous rods were part of the viral DNA-protein complex [Darcy-Tripier *et al.*, 1984]. When crude virus suspensions were subjected to sucrose gradient equilibrium centrifugation, two different bands of viruses were obtained. The upper band consisted of enveloped (extracellular) FV3 and the lower band composed mainly of naked, non-enveloped (intracellular) FV3 [Braunwald *et al.*, 1979]. Some cylindrical aberrant forms of FV3 were also reported [Stoltz, 1973; Kelly and Atkinson, 1975; Moura Nunes *et al.*, 1975; Devauchelle, 1973; Tripier *et al.*, 1977]. Both enveloped and non-enveloped forms of FV3 are infectious, unless subjected to heat-inactivation (56°C, 30 minutes) or UV-irradiation [Gravell and Naegele, 1970].

Replication Strategy

During infection, enveloped FV3 has been shown to be adsorbed to host cell membranes and were taken up via receptor-mediated endocytosis by clathrin-coated pits and vesicles [Houts *et al.*, 1974; Braunwald *et al.*, 1985]. Once inside the cell, the virion uncoats and releases its core DNA into the cytoplasm (Figure 2). In cultured rat liver Kupffer cells, it was shown that unenveloped (naked) FV3 can be engulfed into phagocytic vacuoles and



Figure 1.

Electron micrograph of FV3 virions showing icosahedral morphology. Shown here are two non-enveloped (naked) particles. The disrupted envelope debris can be found below the virus particle on the top.

then release its virion core into the cytoplasm (Figure 2) [Gendrault *et al.*, 1981]. The viral genomic DNA was transported to the nucleus, where the initial stage of DNA replication and initiation of early mRNA synthesis catalyzed by the host cell RNAP II occurs (Figure 2) [Goorha *et al.*, 1978]. The DNA replicated in the nucleus is only of genome or twice genome size and these molecules served as precursors for the second stage of DNA replication and late viral mRNA synthesis in the cytoplasm (Figure 2) [Goorha, 1982]. It was suggested that the initial viral DNA synthesized in the

nucleus was transported [Martin *et al.*, 1984] to the cytoplasm as a template for further replication where FV3 encoded polymerases might have participated in the second stage of DNA replication. In the cytoplasm, the progeny DNA molecules produced are large concatemers. The concatemers were cleaved and then encapsidated into preformed virus shells (Figure 2) [Goorha, 1982]. Since FV3 genome is circularly permuted and terminally redundant [Goorha and Murti, 1982], it was assumed that it utilizes a 'headful' packaging method that is similar to bacteriophage T4 [Streisinger *et al.*, 1967; Goorha, 1982]. The assembly of the virions occurred in specific sites or viroplasm established in the cell cytoplasm (Figure 2). The assembled virions either bud out of the cell, acquiring a part of the plasma membrane as its envelope; or are found accumulated in paracrystalline arrays, which are released during cell lysis (Figure 2) [Granoff, 1969; Moura Nunes *et al.*, 1975].

The time of viral DNA synthesis in FV3-infected cells varies in different cell lines [Maes and Granoff, 1967; McAuslan and Smith, 1968; Kucera, 1970; Goorha *et al.*, 1978]. However, in Fathead minnow (FHM) cells, viral DNA replication begins 2 hours post infection (hpi) and peaks around 4-5 hpi [Goorha *et al.*, 1978]. Initiation and continuous replication of viral DNA are contingent upon viral protein synthesis [Goorha *et al.*, 1979]. At between 0-2 hpi, FV3 DNA is synthesized exclusively in the nucleus. The nuclear viral DNA is not methylated until it has been transported to the cytoplasm, where the FV3 encoded DNA methyltransferase might catalyze the reaction [Willis and Granoff, 1980; Willis *et al.*, 1984a; Kaur *et al.*, 1995]. The second stage

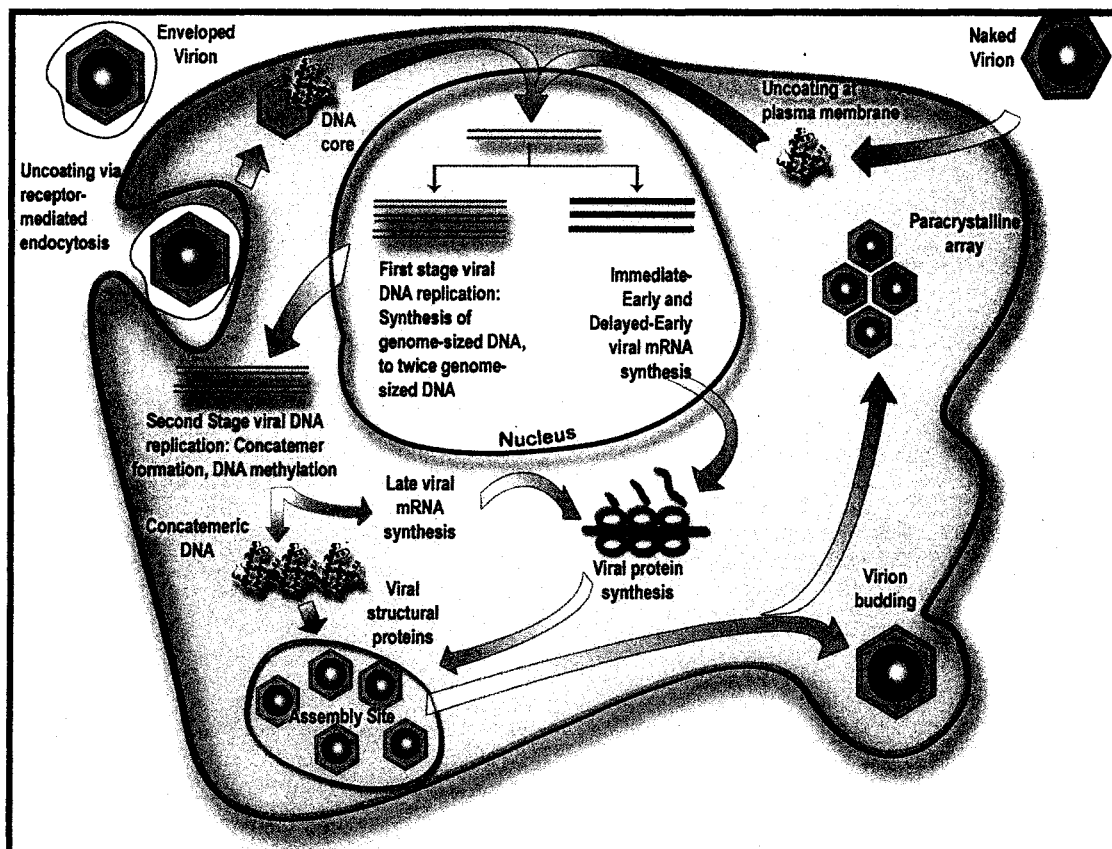


Figure 2.

Replication cycle of FV3 in an infected cell. Enveloped virion enter cell via receptor mediated endocytosis in clathrin-coated pits. Non-enveloped (naked) virion is engulfed into the cell. Both forms of virions uncoat and released its virion core into the cytoplasm and the DNA is transported to the nucleus for 1st stage viral DNA and mRNA synthesis. The progeny DNA molecules from 1st stage DNA replication were then transported into the cytoplasm where 2nd stage DNA replication, late mRNA synthesis and protein synthesis occur. Mature virions are assembled in specialized area formed by reorganization of the cellular cytoskeleton. Mature virions either bud out of the cell and acquiring an envelope from the host cell membrane or align in paracrystalline array and are released during cell lysis, which produce naked virion. Modified from Chinchar, V. G. [2000].

of DNA replication in the cytoplasm occurs concurrently with continuous first stage replication in the nucleus [Goorha, 1982]. DNA replicated in the cytoplasm are large concatemers more than 10 times the genome size [Willis and Granoff, 1980; Goorha, 1982]. In order to maintain the integrity of the

genome, viruses that have linear genomes regenerate the ends of their DNA molecules by concatemeric replication [Watson, 1971]. The large concatemers of the FV3 genome may have served similar purposes [Willis, 1985] or as templates for synthesis of mature viral DNA molecules [Becker and Murialdo, 1978]. Viruses employ 2 known mechanisms for DNA synthesis. One of the mechanisms is rolling circle replication, where circular or linear viral DNA begin replication as a circle and then by rolling circles; producing concatemers [Eisen *et al.*, 1968; Gilbert and Dressler, 1968; Skalka, 1977]. In the second mechanism, unit length progeny molecules are formed from a linear replicating complex and then these units recombined to form large concatemeric structures. During this stage, DNA replication and recombination of progeny molecules occurs simultaneously [Luder and Mosig, 1982; Miller, 1975].

The mechanism of FV3 concatemer formation was studied by experiments using a temperature-sensitive (ts) mutant that is defective in DNA transport at the non-permissive temperature. The viral DNA molecules from cells infected with the ts mutant after 30 minutes of shift-down to permissive temperature was collected and pelleted by centrifugation. Analysis of these DNA molecules suggested that the DNAs were of at least 10 times the genome size, given the centrifugation conditions used [Goorha and Dixit, 1984]. It was hypothesized that these concatemers could not have been produced via rolling circle replication in such a short time. Therefore, it favors the conclusion that the concatemers were produced by recombination [Goorha and Dixit, 1984]. This conclusion can also be supported by the identification of a FV3 sequence that potentially encodes an integrase. If

concatemers were made by recombination as suggested, it is possible that this enzyme might function as an integrase-resolvase [Goorha and Dixit, 1984; Parsons *et al.*, 1988; Rohozinski and Goorha, 1992].

Since FV3 DNA replicates in different stages and at two different sites, it must be that one or more viral protein(s) in the cytoplasm is/are required for transition from stage 1 to stage 2. Indeed, Elliot and Kelly [1980] and Martin *et al.* [1981] found at least 2 viral proteins in FV3 infected cell cytoplasm but are not found in the nucleus that might be involved in this transition. Unlike many large DNA viruses, it was noted that FV3 continues to transcribe its early mRNAs throughout the infectious cycle [Willis *et al.*, 1977]. Studies with *ts* mutants showed that although normal level of DNA synthesis were found at non-permissive temperature, no virus particles were formed. However, when the *ts* mutants were shifted to the permissive temperature, mature virus particles were only formed when RNA and protein synthesis was not inhibited [Purifoy *et al.*, 1973].

The FV3 genome encodes different classes of proteins essential for controlling temporal expression of its genes and for host-virus interaction during its replication cycle. Among these are trans-acting proteins that allowed transcription of methylated DNA [Thompson *et al.*, 1986, 1987]; trans-acting protein that interact with RNAP II or specific DNA sequences [Willis and Thompson, 1986]; regulatory proteins that control synthesis of specific viral proteins at specific time [Elliot and Kelly, 1984; Goorha and Granoff, 1974a, 1974b; Goorha *et al.*, 1977] and DNA binding proteins that might have important functions in the viral replication cycle [Goorha, 1981b; Aubertin *et al.*, 1983]. The endowment of these proteins provides FV3 with

various capabilities to respond in many ways during its infectious cycle. Some of these abilities are described below:

Nongenetic Reactivation

Although both enveloped and non-enveloped forms of FV3 are infectious, naked viral DNA is not infectious [Willis *et al.*, 1976b]. However, when the infected cells are coinfecting with UV-irradiated FV3, the naked viral DNA can be nongenetically reactivated to produce progeny virus with the genome acquired from the naked viral DNA [Willis *et al.*, 1979b].

It has been shown that UV-irradiated and heat inactivated (56°C, 30 minutes) FV3 can kill tissue culture cells without producing progeny viruses [Willis, 1985]. However, when both of these types of inactivated viruses are coinfecting into cells, one of the partners can be reactivated nongenetically and infectious viruses are produced [Fenner and Woodroffe, 1960; Gravell and Naegele, 1970]. The genotype of the progeny of this coinfection is that of the heat-inactivated FV3 but not the UV-irradiated partner [Gravell and Cromeans, 1971]. Initially, it was thought that a virion RNA polymerase that functions in this activity was inactivated by the heat and that the polymerase activity was restored by the UV-irradiated virus during coinfection. This hypothesis was rejected when it was demonstrated that in anucleated cells, FV3 replication does not occur, confirming that a host cell nucleus is required [Goorha *et al.*, 1977, 1978]. Later, Goorha [1981a] also showed that a functional host cell RNAP II is required to transcribe the viral genome, at least in the initial stage of viral replication. Therefore this nongenetic reactivation can be attributed to the possibility that an immediate-early viral gene product

is required for this type of reactivation [Willis *et al.*, 1979b].

Modification of Host Cell Enzymatic Activities

Goorha *et al.* [1981a] has demonstrated the requirement of host RNAP II in FV3 mRNA synthesis by using a mutant cell line of Chinese hamster ovary (CHO) cells that is resistant to α -amanitin (a toxic polypeptide that inhibits mammalian RNAP II). Infection of the mutant CHO cells with FV3 in the presence of α -amanitin showed no inhibitory effect on RNA synthesis while FV3 infected CHO wild-type cells were sensitive to the α -amanitin treatment [Goorha 1981a].

Since naked DNA is not infectious and a functional host RNAP II is required for viral replication, it was hypothesized that a FV3 protein(s) modified the host RNAP II before transcription of its methylated template. Indeed, Campadelli-Fiume *et al.* [1975] demonstrated that RNAP II molecules extracted from FV3 infected cells had reduced availability of α -amanitin binding sites, but no reduced ability in RNA synthesis. This demonstrated that infection with FV3 somehow modified the α -amanitin binding site of the RNAP II molecule. It was suggested that either a FV3 protein had bound to the site or had irreversibly altered it. Somehow, this modification of RNAP II enabled transcription of methylated FV3 template. It is also possible that critical viral promoter regions are not methylated, thus allowing transcription [Willis, 1985]. Conversely, other viral proteins such as methylcytosine binding proteins (MeCPs) might work in concert or play a role in processing methylated DNA for transcription.

Inhibition of Host Cell Macromolecular Synthesis

In many molecular and biochemical studies, FV3 has been shown to possess an exquisite ability to orchestrate and sequentially express and regulate its genes while at the same time, inhibit host cell macromolecular synthesis. One other remarkable phenomenon of heat-inactivated and UV-irradiated FV3 is the ability to rapidly inhibit host cell DNA, RNA and protein synthesis within the first hour of infection [Maes and Granoff, 1967; Guir *et al.*, 1970; Gravell and Naegele, 1970; Willis *et al.*, 1976a; Raghov and Granoff, 1979]. When cells were infected with heat-inactivated or UV-irradiated FV3 for 2 hours, host macromolecular synthesis was 90% shut-down but no infectious virus particles were made. However, normal viral replication occurred when this was followed up with super-infection of active FV3 [Goorha and Granoff, 1974a]. Additionally, Aubertin *et al.* [1973] and Cordier *et al.* [1981] also demonstrated that cells infected with a solubilized FV3 protein extract inhibited RNA synthesis as well. It was suggested that a single FV3 protein molecule was responsible for shutting down all 3 types of host cell macromolecular synthesis [Drillien *et al.*, 1980]. However, Aubertin *et al.* [1976] showed another solubilized FV3 protein extract that has inhibitory effects on RNAP II in infected cells and prevented RNA synthesis. Therefore, it is more likely that more than one viral protein is involved in eliminating host macromolecular synthesis. Since heat-inactivated or UV-irradiated FV3 can completely eliminate host cell macromolecular synthesis by 2 hpi, it provides a very useful system to study details of viral replication and macromolecular synthesis in infected cells. In cells that are infected with heat inactivated or UV irradiated FV3, newly synthesized macromolecules

post infections with active FV3 are virus specific [Willis, 1985].

Temporal and Quantitative Control of Transcriptions

FV3 mRNA synthesis is classified into three classes: immediate-early, delayed-early and late [Willis *et al.*, 1977]. This classification has been made possible with the use of the protein synthesis inhibitor, cycloheximide and an amino acid analog, fluorophenylalanine (FPA) which inhibits the functions of proteins containing phenylalanine at critical sites. When FV3 was infected in the presence of cycloheximide, only immediate-early transcripts were made when the mRNAs were extracted from infected cells for polyacrylamide gel electrophoresis (PAGE) analysis. This treatment inhibited protein synthesis and late transcripts, which are dependent upon immediate-early and delayed-early regulatory proteins for transcriptions, were absent [Willis and Granoff, 1978]. PAGE analysis of FV3 mRNAs produced in the presence of FPA yielded additional three species of mRNAs that were not present in the immediate-early class. In the absence of inhibitors, all classes of viral mRNAs are synthesized after about 5-6 hpi [Willis and Granoff, 1978]. Also, Willis *et al.* [1977, 1978] found that viral DNA synthesis does not occur in the presence of FPA treatment. Initially, it was presumed that a viral polymerase or protein required for DNA synthesis was inactivated by FPA and thus, this affects the synthesis of late transcripts. However, Willis *et al.* [1979a] had isolated a DNA-positive ts mutant that also failed to synthesize late mRNAs at the non-permissive temperature. Therefore, late viral transcription is not dependent upon DNA synthesis, but that specific viral protein(s) is also required for the transition from delayed-early to late transcription [Goorha *et*

al., 1979].

The regulation and control of viral RNA synthesis is both temporal and quantitative. In the presence of cycloheximide, FV3 was shown to over-produce a particular species of RNA identified as ICR489 [Willis and Granoff, 1978]. This effect was not seen when mRNAs were extracted after 1 hour of normal infection nor in the presence of FPA [Willis and Granoff, 1978]. From these data, it was suggested that this particular species of immediated-early RNA is regulated by a delayed-early viral protein. This exemplifies sequential and quantitative controls for each temporal class of viral mRNAs.

Host Cell Cytoskeleton Rearrangement

Electron microscopy has shown that FV3 induces selective and sequential major organizational changes in the cell cytoskeleton composed mainly of microtubules, intermediate filaments and microfilaments [Murti *et al.*, 1983, 1984]. At 6 hpi, there was a marked decrease in microtubules; the intermediate filaments were retracted from the cell periphery and surrounded newly formed virus assembly sites; while the microfilament stress fibers that normally stretched along the cell axis disappeared and are recruited to form microvilli-like projections on the cell surface at later time in infection [Murti *et al.*, 1983].

The first of these virus-induced visible changes were the assembly sites. FV3 has the ability to reorganize the cellular cytoplasmic organelles such that the assembly sites were devoid of any organelles and the periphery of the sites were bounded by bundles of intermediate filaments, mitochondria and lysosomes [Murti *et al.*, 1983]. Within these assembly sites were

filaments of various diameters (about 2-3 nm) and contained dense viral DNA and proteins, where the assembly of virions took place. At first, these filaments were thought to be produced by the virus, as antibodies directed against the cell cytoskeletal filament proteins in immunofluorescence studies were negative within these sites [Murti *et al.*, 1984]. However, when infected cell cytoskeleton was viewed under high-voltage electron microscope, it appeared that this fibrous matrix was part of the cellular microtrabecular lattice [Murti *et al.*, 1984]. The microtrabecular lattice is a motile network of proteins that play important roles in mediating and regulating cellular interactions and transport, and integrating cellular components into a functional unit [Porter and Tucker, 1981]. From these data, it appeared that FV3 had hijacked this cellular 'highway' as its own network for viral capsomeres, genomes and virus shells to interact in an orderly manner to assemble mature virions.

The second type of virus-induced structure appeared late in FV3 infection as projections on the surface of the infected cells which resembled cellular microvilli [Murti *et al.*, 1983]. These projections contain cellular microfilaments where mature FV3 are released by budding. Of all the 3 major components of the cytoskeleton, it was shown that microtubules do not have any major function in the virus replication cycle. This was demonstrated when FV3 infected cells were treated with high concentration of colchicine to disrupt most cellular microtubules. No marked differences in the production and release of virus in FV3 infected cells treated with colchicine or untreated cells were shown [Murti *et al.*, 1984]. However, electron and immunofluorescence microscopic studies suggested that intermediate

filaments were crucial in organizing and maintaining the virus assembly sites and the microfilaments were important for virus release [Murti *et al.*, 1984].

Organisms must tightly regulate the timing of expression of each of their genes; otherwise their development might go awry with potentially lethal consequences. The mechanisms that control these important events have been of great interest to investigators. Hence, since 1966, about 100 different biochemical, molecular and electron microscopic studies using FV3 have been conducted to further understand the various underlying mechanisms involved in cellular events during FV3 infection. However, many events regarding cellular mediation during viral infections are still not well understood. The many interesting characteristics of FV3 such as replication both in the nucleus and cytoplasm; transcription of methylated DNA; the ability to inhibit host cell molecular synthesis; the ability to reorganize host cell cytoskeleton; being partially eukaryotic and partially prokaryotic and other features, warrant more detailed studies of FV3 as a model system to fully understand eukaryotic gene expression. By studying how FV3 regulates these activities, it might help to uncover important aspects of the genetic basis of various cellular components that play important roles in gene expression and regulation, immune responses and viral pathogenesis.

MATERIALS AND METHODS

Cells and Viruses

Cells

Fat head minnow (FHM) cell monolayers were grown in Eagle's minimum essential medium (EMEM) supplemented with antibiotics-antimycotic (Invitrogen) as suggested by the manufacturer and 10% fetal bovine serum (FBS) (growth medium). Cells were incubated at 30°C with 5% CO₂ until confluent monolayered. *Spodoptera frugiperda* (Sf-21) and *Trichopulsia ni* (Hi-5, Invitrogen) cells were grown in Insectagro (Media-tech) serum free insect cells medium (growth medium) supplemented with antibiotic-antimycotic (Invitrogen) and incubated at 28°C until confluent monolayers were attained.

FV3

FV3 was originally obtained from Dr. Allan Granoff and a clone of 5 azacytidine resistant (aza-C^r) mutant derived from FV3 was obtained from Dr. Rakesh Goorha. Each virus was previously plaque purified 3 times and propagated in FHM cell monolayers at 30°C with 5% CO₂ in EMEM medium supplemented with 2% FBS and antibiotic-antimycotic (Invitrogen) (maintenance medium). FHM cell monolayers were infected with FV3 or aza-C^r mutant (1-50 plaque forming units (pfu/ml), adsorbed for 1 hour at room

temperature and were incubated at 30°C with 5% CO₂ in maintenance medium.

100X Concentration and Titeration of FV3

Both wild-type and aza-C^r FV3 were concentrated into 100X by the following procedures: Supernatant was collected from initial centrifugation of infected cell cultures and cell cytoplasmic lysates in an eppendorf tabletop centrifuge (Model 5804) at 5000 rpm (4100 x g) at 4°C for 20 minutes per run. The cells were lysed by resuspending the pellet in sterile deionized water and freeze in dry ice, subsequently thawed in 30°C waterbath. The freeze-thaw procedure was repeated thrice. Additionally, the suspension was subjected to homogenization with a dounce homogenizer and then the suspension was centrifuged at 5000 rpm (4100 x g) at 4°C for 15 minutes to remove cellular debris. The supernatant was collected and combined with the supernatant collected from the initial centrifugation of the infected cell culture. The combined supernatant was ultracentrifuged using a TI 45 rotor at 40000 rpm (125,000 x g) for 90 minutes in a Beckman Coulter ultracentrifuge. The virion pellets were collected and resuspended in RSB (10 mM NaCl; 10 mM Tris-HCl, pH 7.5; 1.5 mM MgCl₂) or TE (10 mM Tris-HCl, pH 7.5; 10 mM NaCl) and stored at 4°C or -80°C until use.

Virus titers were calculated by using plaque assay with serial dilutions of 100X FV3 using standard procedure. Virus dilutions from 10⁻¹ to 10⁻¹⁵ were made in maintenance medium. FHM cells were seeded in 6-well dishes until monolayered. Duplicate wells of FHM cells were infected with 100 µl of 10⁻⁵ to 10⁻¹⁵ dilutions of 100X FV3 and adsorbed at room temperature for 1

hour. After the adsorption period, the medium was aspirated and maintenance medium with 0.5% methylcellulose (4000 centipoise) was added very carefully to prevent breaking the monolayers. The plates were incubated at 30°C with 5% CO₂ for 3-6 days until plaques were visible under inverted compound light microscope. The medium was then aspirated away and the infected cells stained with 0.1% crystal violet plus 10% formaldehyde in deionized water and let stand for 20 minutes. The plates were then rinsed in buckets of deionized water gently and air dried. The plaques were counted from the wells with a lightbox to obtain the number of pfu/ml.

Recombinant Baculovirus

Recombinant baculoviruses expressing the FV3 ORFs 55R and 55L were propagated on Sf-21 or Hi-5 cells using insect cell growth medium and incubated at 28°C for 72 to 144 hours. Plaque identification was done by visualizing recombinant baculoviruses with UV light microscope for green colored virus particles.

Isolation of FV3 Genomic DNA

Genomic DNA from FV3 and aza-C^r mutant was isolated from 100X FV3 resuspended in RSB to a final volume of 3ml. To the virus concentrate, one-tenth the volume of 1 M MgCl₂ was added to a final concentration of 10 mM and DNase was added to a final concentration of 200 ug/ml, to remove any cellular DNA. The virus suspension was incubated for 1 hour at 37°C and then 500 mM EDTA was added to a final concentration of 50 mM to chelate Mg²⁺. The treated virions were layered over a 10 ml cushion of 20%

sucrose in RSB and centrifuge for 1.5 hour at 4°C with a SW 41 rotor at 30,000 rpm (111,000 x g) in a Beckman Coulter ultracentrifuge. The supernatant was aspirated away and the pellet resuspended in TE. Sodium dodecyl sulfate (SDS) was added to the virus suspension to a final concentration of 1%, proteinase K to a final concentration of 200 µg/ml, and DNase-free RNase to a final concentration of 40 µg/ml and digested overnight at 37°C. DNA was extracted on the next day from the digested virions once with phenol, and twice with phenol-chloroform. The extracts were combined and one-fifth the volume of 300 mM sodium acetate and 2.5 volumes of 100% ethanol were added to precipitate the DNA at -80°C overnight. The next day, the extracts were centrifuged in an eppendorf microfuge at 12000 rpm (13,400 x g) for 20 minutes to pellet the viral DNA. The supernatant was discarded and pellet washed twice with 70% ethanol, spinned down at 12000 rpm (13,400 x g) for 5 minutes and then vacuum dried. The DNA was then resuspended in sterile deionized water or 10 mM Tris-HCl, pH 8.0, for PCR and restriction digestion.

Cloning of FV3 DNA Fragments

The viral DNA was digested with *KpnI* and *HindIII* restriction enzymes and fractionated on 1% agarose gel and electrophoresed at 100 V for 1.5 hours and the fragments were cut out from the gel and extracted by using QIAEXII gel extraction kit (Qiagen). The gel extracted DNA fragments were ligated into *KpnI* or *HindIII* sites of pKB111, pBR322 or pGEM4Z vectors. Ligation mixtures were transformed into DH5- α -MCR (Invitrogen) *E. coli* cells and plated on LB agar with 50 µg/ml ampicillin or kanamycin and selected for

ampicillin or kanamycin resistance. Selected transformants were grown in liquid LB medium supplemented with 50 µg/ml ampicillin or kanamycin for 16 hours. Plasmid DNAs containing the viral DNA inserts was isolated using the alkaline-lysis mini-preps method (Maniatis *et al.*, 1982) as described in this section and resuspended in deionized water for sequencing. The plasmid DNA concentration was quantified by using a spectrophotometer.

Transposon Priming of Genomic DNA Fragments

KpnI fragments A, D, E, M and *HindIII* G fragments were sequenced using New England Biolabs (NEB) GPS 1.1 transposon genome priming system kit. Briefly, the cloned FV3 DNA fragments from the *HindIII* and *KpnI* libraries were used for transposition and transformation into DH5α *E. coli* competent cells. FV3 cloned restriction fragments were transposed in a mass ratio of 1:4 donor: target. Each transposition reaction mixture of 2 µl 10X GPS buffer (250 mM Tris-HCl, pH 8.0; 20 mM DTT; 20 mM ATP), 1 µl pGPS1.1 (0.02 µg) donor DNA, 0.08 µg FV3 DNA fragment, 1 µl TnsABC transposase (7 µg/ml-A, 10 µg/ml-B, 20 µg/ml-C) and water to a final volume of 19 µl was incubated at 37°C for 10 minutes. After incubation, 1 µl Start solution (300 mM magnesium acetate) was added to each tube, gently mixed and incubated for 1 hour at 37°C. Thereafter, the reaction was heat inactivated at 75°C, and 1 µl and 10 µl of the transposition reaction was used for transformation into DH5α *E. coli* competent cells. Litmus 28 control target plasmid (80 µg/ml) and donor plasmid GPS1.1 were used as positive control for the transposition reaction. A negative control was also performed without the transposase. Plasmid pUC (supplied with the kit) was used for

transformation control. The transformation mixture was diluted into 1 ml of LB without antibiotics to outgrow for 1 hour at 37°C with aeration. The transformation mixture was then plated on LB agar with 15 µg/ml chloramphenicol and incubated at 37°C overnight. Random clones of the transposition-transformation reactions were selected from chloramphenicol resistance colonies and the plasmid DNAs were extracted using alkaline-lysis method. DNA sequencing was performed by using transposon-specific primers N and S (3.2 pmol/µl) provided in the transposition kit, using similar sequencing reaction protocols as described in DNA sequencing.

Alkaline-lysis Mini-preps

E.coli cultures (20 ml) were centrifuged at 5000 rpm (4100 x g) for 10 minutes to pellet the cell and the supernatant discarded. The cells was washed once with cold PBS and centrifuged at 12000 rpm (13,400 x g) for 10 minutes to pellet the cells. The bacterial pellet was resuspended in 125 µl of lysis buffer (25 mM Tris, pH 8.0; 10 mM EDTA; 50 mM Glucose) and another 125 µl of lysis buffer with 10 mg/ml lysozyme and incubated on ice for 5 minutes. After incubation, 500 µl of Alkali-SDS (0.5 ml of 3.0 M NaOH; 0.5 ml of 20% SDS; 0.9 ml of water, final concentration 0.2N NaOH + 1% SDS) was added and the tubes inverted 10 times gently and incubated on ice for 5 minutes. After incubation, 400 µl of 3.0 M sodium acetate pH 4.8 was added and the tubes were inverted 10 times and centrifuged immediately at 12000 rpm (13,400 x g) for 5 minutes and incubated on ice for 15 minutes. After incubation, the suspension was pelleted by centrifugation at 12000 rpm (13,400 x g) for 5 minutes at room temperature or 4°C. The supernatant was

removed and transferred to fresh tubes, without loosening the pellet. To the supernatant, 400 μ l of isopropanol was added, mixed gently and then placed at -80°C for 30 minutes and pelleted by centrifugation for 10 minutes at 4°C , and the supernatant discarded. The pellet was resuspended in 225 μ l of deionized water and 125 μ l of phenol-isoamyl-chloroform was added and vortexed to mix. The mixture was centrifuged at 12000 rpm (13,400 x g) for 10 minutes to separate the phases. The top phase was collected and transferred to a fresh tube and 200 μ l of 7.0 M ammonium acetate was added and incubated on ice for 10 minutes. After incubation, the mixture was centrifuged at 12000 rpm (13,400 x g) for 10 minutes and the supernatant collected and transferred to another fresh eppendorf tube. To the supernatant, 800 μ l of 100% ethanol was added and inverted several times and kept at -80°C overnight to precipitate the DNA. The following day, the precipitate was collected by centrifugation at 12000 rpm (13,400 x g) for 10 minutes and resuspended in 150 μ l of 0.3 M sodium acetate, and 450 μ l of 100% ethanol was added and incubated on dry ice for 10 minutes. The precipitate was centrifuged at 12000 rpm (13,400 x g) for 10 minutes and the supernatant discarded, the pellet vacuum dried and resuspended in 25-50 μ l of 10 mM Tris-HCl pH 8 or sterile deionized water. RNase I (1 unit/100 ng DNA) (Promega) was added to the resuspended DNA with an appropriate amount of 10X buffer as suggested and supplied by the manufacturer. The mixture was incubated at 37°C for 30 minutes to digest any residual RNAs. After digestion, the mixture was again phenol-chloroform extracted and ethanol precipitated, vacuum dried and resuspended in sterile deionized water and stored at -20°C until use. The DNA concentration was quantified by

spectrophotometry and an appropriate concentration was used for DNA sequencing as described in 'DNA Sequencing'.

PCR Reactions

Wild type FV3 and aza-C^r mutant genomic DNA was used as a template to obtain PCR fragments for sequencing from a region covering the *HindIII* H fragment. PCR products were also used for junctions between 2 non-overlapping restriction fragments to obtain linkage of the contigs. The thermal cycling conditions for PCR were: Initial denaturation of the templates at 94°C for 2 minutes, followed by 35 cycles of denaturing at 94°C for 30 seconds; annealing at 55°C for 45 seconds and extension of templates at 72°C for 1 minute and 20 seconds and final extension at 72°C for 10 minutes.

DNA Sequencing

Both strands of all plasmid DNAs and PCR products were sequenced using a CEQ2000XL (Beckman-Coulter) automated DNA sequencer by following manufacturer's protocol. Each sequencing reaction was prepared by using 6.5-325 ng (depending on size of fragment) of DNA template with 1 µl each of 5' and 3' primer (10 µmol), and 4 µl of DyeTerminator Cycle Sequencing (DTCS) mastermix and water to a final volume of 20 µl on a 96-well plate and then subjected to 30 cycles of thermal cycling conditions: 96°C for 20 seconds, 50°C for 20 seconds, and 60°C for 4 minutes and holding at 4°C at the end of the cycle. After the thermal cycling, the reactions were stopped by adding 2 µl of freshly prepared Stop solution (1.5 M NaOAc; 50 mM EDTA) and 1 µl of 20 mg/ml glycogen. To precipitate the sequencing

reaction, 60 μ l of 95% ethanol (v/v ethanol/water) stored at -20°C was added and the 96-well plate inverted several times and stored at -20°C for 30 minutes to 1 hour to precipitate the DNA. The 96-well plate was centrifuged at 14000 rpm (33,750 x g) at 4°C for 15 minutes with an eppendorf swing bucket rotor, and the supernatant removed with a micropipette. The samples were further rinsed twice with 70% ethanol (v/v ethanol/water) and centrifuged at 14000 rpm (33,750 x g) at 4°C for 10 minutes each time. After centrifugation, the supernatant was carefully removed with a micropipette and the sample vacuum dried for 40 minutes. The samples were resuspended in 20 μ l of loading buffer (provided with the DTCS mastermix) and overlaid with a drop of light mineral oil (Sigma Cat. M5904). The sample plate was then loaded on the sequencer for automated sequencing. Each sequence read was linked using the primer walking method. Sequences across restriction fragment junctions were obtained by sequencing PCR products amplified from wild-type FV3 and aza-C^r mutant genomic DNA with primers for the appropriate regions flanking the junctions. Each nucleotide was sequenced 2 to 16 times.

Computer-assisted Analyses

Individual primer reads were aligned into contigs by using Sequencher 4.1 (Genecodes). The open reading frames (ORFs) and their amino acids sequences were predicted using MacVector 7.0 (Oxford Molecular Ltd). DNA and protein database searches were conducted using the BLASTX, BLASTP and RPS-Blast at the NCBI website (<http://www.ncbi.nlm.nih.gov/>) [Altschul *et al.*, 1997]. Alignment of amino acid sequences of DNA polymerase, RNA

polymerase II, ribonucleotide reductase small subunit, ribonuclease III, DNA methyltransferase and major capsid protein were obtained by using CLUSTAL-X 1.81 [Thompson *et al.*, 1997]. Trees were estimated for each aligned amino acid sequence using PAUP 4.0 [Swofford, 2003]. The DNA dot matrix was obtained using the Pustell DNA matrix algorithm within MacVector 7.0 (Oxford Molecular Ltd). Prediction of transmembrane helices and secretory domains of proteins were done using TMpred [Hofmann and Stoffel, 1993], TMAP [Persson and Argos, 1994], and TMHMM 2.0 [Sonnhammer *et al.*, 1998].

Nucleotide Sequence Accession Number

The nucleotide sequence of the wild type FV3 genome has been deposited in GenBank and assigned the Accession number AY548484.

FV3 Infected Cell Extracts

FHM cell monolayers in 35 mm petri dish were infected at a multiplicity of infection of 50 pfu/cell of FV3 and adsorbed at room temperature for 1 hour after which, EMEM maintenance medium was added and the dishes incubated at 30°C with 5% CO₂ for 2 hours; 4 hours; 6 hours; 12 hours and 24 hours respectively. After the appropriate incubation period, the medium was removed from the cell monolayer. To each infected cell monolayer, 200 µl of 1% NP-40 was added to disrupt the cell membrane and the cell-lysate was collected on ice and then centrifuged at 12000 rpm (13,400 x g) at 4°C for 5 minutes to separate cellular debris and supernatant. The supernatant (cytosolic fraction) was then collected and used for helicase activity assays.

The remaining cell pellet containing the nuclei was used for extracting the nuclear fraction. The nuclei of the infected cells were resuspended with sterile deionized water and then passed through a 26 gauge syringe several times to disrupt the nuclear membranes. The suspension was then centrifuged at 12000 rpm (13,400 x g) at 4°C and the supernatant (nuclear fraction) collected for helicase activity assays.

Isolation of Total RNAs

FHM cells were first infected with heat inactivated FV3 by subjecting the viruses to heat incubation in a water bath at 56°C for 30 minutes. Cells were infected with 50 pfu/cell of heat inactivated FV3, adsorbed for 1 hour at room temperature and then incubated at 30°C with 5% CO₂ in maintenance medium for 4 hours. The use of heat inactivated FV3 was to curtail host cells DNA replication and protein synthesis as previously observed by Maes and Granoff [1967]; Guir *et al.* [1970]; Gravell and Naegele [1970]; and Willis *et al.*, [1976a]. After the 4 hours incubation, the cells were washed twice with maintenance medium to remove excess heat inactivated FV3. The cells were then infected with 100 pfu/cell of active FV3 and adsorbed at room temperature for 1 hour and EMEM maintenance medium was added and incubated at 30°C with 5% CO₂ for 6 hours. Mock-infected cells were treated in an identical manner and incubated for 6 hours.

For treatment with fluorophenylalanine (FPA) which inhibits protein function, 100 µg/ml of FPA was added to L-phenylalanine free EMEM maintenance medium after the adsorption and incubated at 30°C with 5% CO₂ for 6 hours. For treatment with cycloheximide (CHX) which inhibits

protein synthesis, 10 $\mu\text{g/ml}$ of CHX was added to the EMEM maintenance medium after the adsorption and incubated at 30°C for 6 hours with CO₂.

After 6 hours incubation, total RNAs were extracted from FV3 infected and mock-infected FHM cells using TRI REAGENT (Molecular Research Center Inc, Ohio) or TRIZOL reagent (Invitrogen) by following manufacturers' protocol. Briefly, the maintenance medium was removed and 1 ml per 10cm² of surface area of TRI REAGENT or TRIZOL was added to disrupt the cells in a 50 ml polypropylene centrifuge tube. The homogenate was then allowed to react with the chemicals for 5 minutes at room temperature after which, 0.2 ml of chloroform per 1 ml of TRI REAGENT or TRIZOL used for the initial homogenization was added and the samples shaken vigorously for 15-30 seconds and let stand at room temperature for 2-15 minutes. The sample was then centrifuged at 6300 rpm (5000 x g) at 4°C for 25 minutes to separate the phases. The top aqueous phase was transferred to a fresh tube and 0.5 ml of isopropanol per 1 ml of TRI REAGENT or TRIZOL used for the initial homogenization was added to precipitate the RNAs. The sample was mixed gently and let stand at room temperature for 5-10 minutes and then centrifuged at 6300 rpm (5000 x g) at 4°C for 25 minutes. The supernatant was aspirated and the RNA pellet was washed with 1 ml of 75% ethanol per 1 ml of TRI REAGENT or TRIZOL used for initial homogenization by vortexing and then centrifuged at 7600 rpm (7500 x g) at 4°C for 15 minutes. The ethanol was removed and the RNA pellet was briefly air dried for 3-5 minutes. Diethyl pyrocarbonate (Dep-C, 0.1%) treated and autoclaved sterile deionized water or RNase-free water was added to resuspend the RNAs and incubated at 55-60°C for 15 minutes to solubilize the pellet in a total volume of 87.5 μl .

The total RNAs was then subjected to DNase treatment to remove any trace DNA contamination. A total of 10 μ l of RDD buffer supplied with DNase I from Qiagen and 2.5 μ l of DNase I was added to the solubilized RNAs and incubated at room temperature for 15-30 minutes. One-fifth volume (20 μ l) of 3.0 M sodium acetate made with Dep-C deionized water was added and mixed gently with the solubilized RNAs. An equivalent of 2.5 volumes of 100% ethanol was added and mixed gently and kept at -20°C overnight to precipitate the RNAs. The ethanol precipitated RNAs was then centrifuged at 9700 rpm (12000 x g) for 10 minutes at room temperature and wash once with 2.5 volumes of 70% ethanol, centrifuged and supernatant removed. The pellet was briefly air-dried and resuspended in 50 μ l RNase free water and aliquots of 10 μ l each were stored at -80°C until use. RNA concentration was quantified by spectrophotometry. All labwares used for RNA isolation were treated with Dep-C deionized water and autoclaved before use.

2-Step RT-PCR of ORFs 55L and 55R

cDNA amplifications of ORFs 55R and 55L were performed by using cytoplasmic total RNAs as templates for reverse-transcriptase reaction using Improm II reverse transcriptase kit (Promega) by following the manufacturer's protocol. For each reverse transcription reaction, 1 μ g each of mock-infected; CHX treated; FPA treated; and no inhibitor treatment cytoplasmic total RNAs was added in each tube. In each individual reaction, 1 μ l of 3' or 5' gene specific 10 μ M primer was added and sterile Dep-C treated deionized water or RNase free water was used to make up to a total volume of 5 μ l. The template mixtures were then denatured by heating at 70°C for 15 minutes

and chilled on ice immediately for 5 minutes. The tubes were then briefly centrifuged to collect the condensate and maintain the original volume. A mixture of 1 μ l reverse transcriptase, 4 μ l Improm II 5X reaction buffer, 20 units of recombinant RNasin ribonuclease inhibitor, 1.5 μ l 25 mM MgCl₂, 1 μ l 10 mM dNTP mix and Dep-C treated deionized water to a total volume of 15 μ l was added to each denatured total RNA template reaction tube. Each reaction mixture was incubated at 25°C for 5 minutes to enable the primer to anneal to the template. Extension of the templates was carried out on an Eppendorf thermal cycler at 42°C for 1 hour and then heated to 70°C for 15 minutes to inactivate the enzymatic reaction of the reverse transcriptase. Subsequently, 1.5 μ l of each cDNA was used as template for PCR amplifications with both 3' and 5' gene specific primers (10 μ M) and Dynazyme Ext (Finnzymes) Taq polymerase by following the manufacturer's protocol in the following reaction conditions: 5 μ l 10X reaction buffer with 15 mM MgCl₂; 1 μ l each of 5' and 3' gene specific primers (10 μ mol); 1 μ l 100 mM dNTP mix (USB); 1.5 μ l cDNA template; 1 μ l Dynazyme EXT Taq Polymerase (1 unit/ μ l) and water to a final volume of 50 μ l per reaction using thermal cycling conditions described in PCR.

The following primers were used for all reverse transcriptions and PCR amplifications of ORFs 55R and 55L and GAPDH, a constitutive house-keeping gene: ORF 55R anti-sense primer *EcoRI*-3R 5'-GCGGAATTCTTAAGGCTCAACGCGATAGATGG-3' (*EcoRI* site underlined) and sense primer *Bam*HI-5R 5'-GCGGGATCCATGCTTCCTCAGAACTCC CAG-3' (*Bam*HI site underlined); ORF 55L anti-sense primer *EcoRI*-3L 5'-GCGGAATTCCTACCTCTGTGGCCGTCGGGTTCG-3' (*EcoRI* site

underlined) and sense primer *Bam*HI-5L 5'-GCGGGATCCATGCAAAAC TTTTAAGGCTC-3' (*Bam*HI site underlined); GAPDH anti-sense primer GAP3 5'-CTCGTGGTTCACACCCATCACA-3' and sense primer GAP5 5'-CCAGTATTGACCTCCCACTCACCGG-3'. Each RT-PCR amplification was fractionated on 1% agarose gel in TBE buffer at 100 volts constant for 1 hour. The gels were then stained for 20 minutes with 10 mg/ml ethidium bromide mixed with deionized water. De-staining of the gels was done with de-ionized water for 20 minutes on an orbital shaker and then drained and photographed from a UV light transilluminator.

Construction of Recombinant Baculovirus Expressing FV3 55L and 55R

No Myc-His Tag Version

FV3 ORFs 55R and 55L were amplified by PCR from FV3 genomic DNA by using Dynazyme EXT Taq polymerase (Finnzymes) with the same primers used for RT-PCR as described above (*Bam*HI-5R, *Bam*HI-5L, *Eco*RI-3R, *Eco*RI-3L) which amplified the entire ORF. The resulting PCR products and plasmid pFastBac-Dual-eGFP (a gift from Dr. Grant McFadden) containing a baculovirus polyhedrin promoter for over expression of recombinant protein and a mini-transposon *Tn7* for transposition, were digested with the restriction enzymes *Bam*HI and *Eco*RI. Both the digested PCR products and pFastBac-Dual-eGFP plasmid DNA were electrophoresed on a 1% low melt agarose gel and the appropriate band was excised and purified using QIAEXII gel extraction kit (Qiagen). The gel purified PCR products of 55L and 55R were ligated into the *Bam*HI and *Eco*RI sites of pFastBac-Dual-eGFP and transformed into DH5- α (Invitrogen) competent *E.*

coli cells with 50 µg/ml ampicillin selection. Transformants were selected and grew in 20 ml LB broth supplemented with 50 µg/ml ampicillin and the plasmid DNA isolated by alkaline-lysis mini-preps.

The pFastbac plasmid DNA containing the FV3 55R and 55L gene inserts were sequenced to check for amino acid sequence integrity with the wildtype and then transformed-transposed into DH10-Bac (Invitrogen) competent *E.coli* cells with 50 µg/ml kanamycin, 7 µg/ml gentamicin, 10 µg/ml tetracycline, 100 µg/ml blue-gal and 40 µg/ml IPTG selection on LB agar plates incubated at 37°C for 48 hours. White colonies were picked for analysis by re-streaking on fresh LB agar plates with 50 µg/ml kanamycin, 7 µg/ml gentamicin, 10 µg/ml tetracycline, 100 µg/ml blue-gal and 40 µg/ml IPTG to confirm true transformations. True transformants were grown in LB broth with the same antibiotics, Blue-gal and IPTG and the bacmid DNA isolated as described in this section.

Myc-His Tag Version

A Myc-His tag version of both genes were cloned by PCR using 55R sense primer (*Bam*HI-5R) and anti-sense primer *Xho*I-3R 5'- GCGCTCGAG AGGCTCAACGCGATAGATGG-3' (*Xho*I site underlined); 55L sense primer (*Bam*HI-5L) and anti-sense primer *Xho*I-3L 5'-GCGCTCGAGCCTCTGTG GCCGTCTGGGTTTCG-3' (*Xho*I site underlined) into pcDNA3.1myc-hisA (Invitrogen). Both the PCR products and the pcDNA3.1myc-hisA plasmid DNA were digested with *Bam*HI and *Xho*I, electrophoresed in a 1% low melt agarose gel in TBE buffer and the appropriate bands excised and purified with QIAEX II gel purification kit (Qiagen). The gel purified PCR products and

pcDNA3.1myc-hisA plasmid were ligated and transformed into DH5- α (Invitrogen) competent *E. coli* cells with ampicillin (50 μ g/ml) selection. Isolated pcDNA3.1/myc-hisA plasmid DNA containing the FV3 55R and 55L gene inserts were used for PCR amplification using the same sense primers *Bam*HI-5R and *Bam*HI-5L, but with the anti-sense primer JB3902 5'-GCGGAATTCTCAATGGTGATGGTGATGATGACCG-3' which adds an *Eco*RI site (underlined) for both genes.

The PCR products amplified from pcDNA3.1myc-hisA were digested with *Bam*HI and *Eco*RI, electrophoresed, and gel purified as described before and ligated into *Bam*HI and *Eco*RI sites of pFastBac-Dual-eGFP as described above. The pFastbac plasmid DNA with the inserted FV3 55R or 55L gene were isolated using alkaline-lysis method as described before and sequenced using primers *Bam*HI-5R or *Bam*HI-5L with JB3902 for FV3 55R and 55L respectively. The sequencing was to check for maintenance of each gene's amino acid sequence integrity through the cloning process, before transformation and transposition into DH10Bac *E. coli* cells as described above.

Isolation of Bacmid DNA

The analyzed white colonies of DH10-Bac *E.coli* containing the inserted FV3 55L or 55R genes were cultured in 2 ml liquid LB medium containing 50 μ g/ml kanamycin, 7 μ g/ml gentamicin, 10 μ g/ml tetracycline, 100 μ g/ml blue-gal and 40 μ g/ml IPTG in a shaker at 37° overnight. The cultures were centrifuged at 13000 rpm (14000 x g) on a refrigerated table top Eppendor centrifuge for 1 minute to pellet cells and the supernatant

removed. The cells were resuspended in 300 μ l of Solution I (15 mM Tris-HCl, pH 8.0; 10 mM EDTA, 100 μ g/ml RNase A; filter-sterilized and stored at 4°C) and gently vortexed to resuspend. To the suspension, 300 μ l of Solution II (0.2 N NaOH; 1% SDS; filter-sterilized) was added and gently mixed and incubated at room temperature for 5 minutes. After incubation, 300 μ l of 3.0 M potassium acetate, pH 5.5 was added and mixed gently during addition. The sample was then incubated on ice for 10 minutes and centrifuged for 10 minutes at 13000 rpm (14000 x g). The supernatant was transferred to a microcentrifuge tube containing 800 μ l isopropanol and inverted a few times to mix, and stored at -20°C overnight. The sample was centrifuged the following day at 13000 rpm (14000 x g) for 15 minutes at room temperature and the supernatant removed. The pellet was washed twice with 500 μ l of 70% ethanol by inverting the tube several times and then centrifuged for 5 minutes at 14000 x g at room temperature. The DNA was air dried at room temperature for 5-10 minutes and resuspended in 50 μ l of 10 mM Tris-HCl or sterile deionized water and by tapping the tubes gently to prevent shearing the DNA. After resuspension, the bacmid DNA was stored at 4°C until transfection. The bacmid DNA was analyzed for proper insertion and transposition by PCR analysis using M13 forward primer M13F 5'-GTTTTCCCAGTCACGAC-3' or M13 reverse primer M13R 5'-CAGGAAACAGCTATGAC-3' with FV3 55L or 55R gene specific 5' or 3' primers (BamHI-5R or 5L, EcoRI-3R or 3L) with Taq polymerase in reaction conditions as described in RT-PCR and PCR with similar thermal cycling conditions.

Transfection of Recombinant Baculovirus DNA

Bacmid DNAs isolated for both pFastBac-Dual-eGFP FV3 55R and 55L genes (both myc-his tag and non-tag versions) were used for transfection into Sf-21 cells with Cellfectin (Invitrogen) to produce recombinant eGFP baculoviruses by the following: a 6-well plate was seeded with 9×10^5 Sf-21 cells per well in 2 ml of insect cell growth medium. The cells were allowed to attach at 28°C for 1 hour. The purified bacmid DNA (1 µg) was diluted in 100 µl of insect cell growth medium without antibiotics. Cellfectin (Invitrogen) was mixed thoroughly before aliquoting 6 µl for dilution in 100 µl of insect cell antibiotics-free growth medium, mixed gently and then combined with the diluted DNA and incubated at room temperature for 45 minutes. After 1 hour, the seeded cells were washed once with 2 ml of insect cell antibiotics-free growth medium and removed. After incubation of the DNA: Cellfectin complex, 0.8 ml of insect cell antibiotics-free growth medium was added, mixed gently and added to each well of seeded cells and incubated for 5 hours at 28°C. After incubation, the DNA: cellfectin complex was removed from the cells and 2 ml of complete insect cell growth medium was added to the cells and incubated for 72 hours with daily checks for recombinant baculovirus plaques using UV light microscope. Identification of recombinant baculovirus was done by visualizing infected Sf-21 cells under UV-light microscope for expression of green fluorescent protein (eGFP) and the cloned FV3 55L or 55R protein. Recombinant baculoviruses were referred to as AcFV3-55RNT (no-tag); AcFV3-55RT (Myc-His tag); AcFV3-55LNT (no-tag) and AcFV3-55LT (Myc-His tag). After several passages of the recombinant viruses, large scale propagation of the recombinant viruses were

generated from infection of Sf-21 or Hi-5 cells grown in insect cell growth medium. The entire process of the expression system is summarized here in Figure 3.

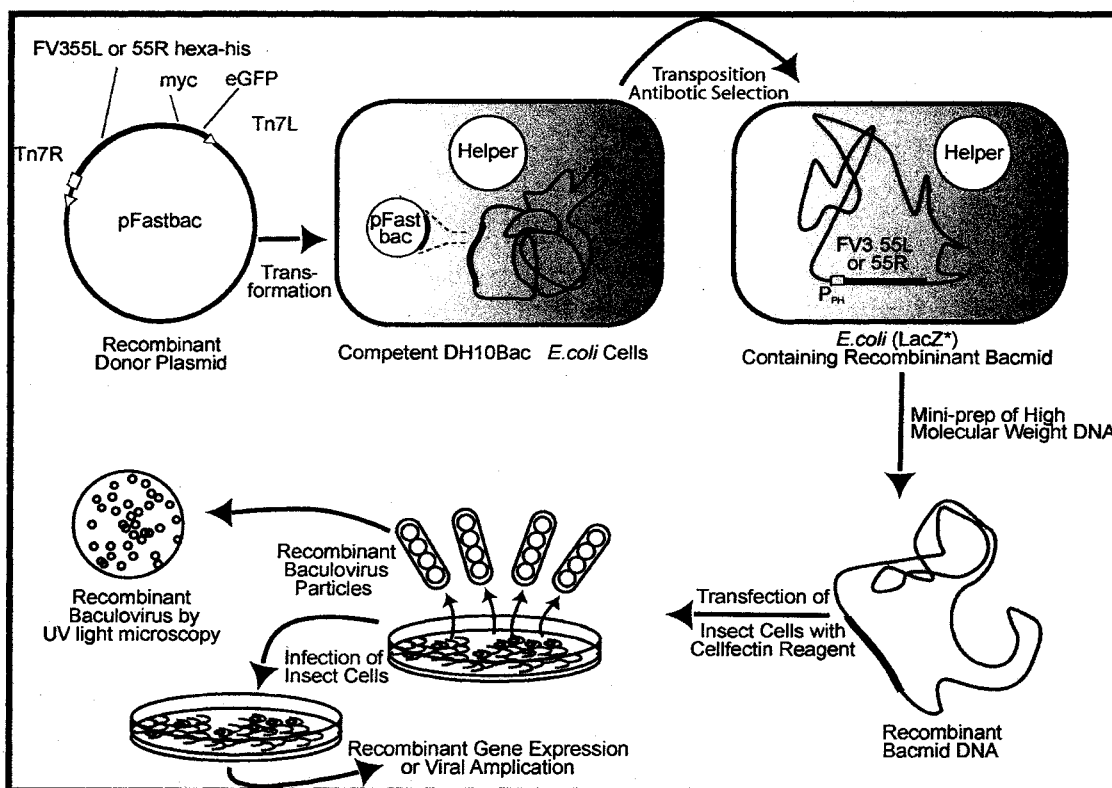


Figure 3.

Baculovirus expression system for producing the recombinant FV3 55L and 55R proteins. The donor plasmid pFastbac-dual-eGFP was constructed to contain a baculovirus polyhedrin promoter for over-expression of the cloned gene, a mini-transposon *Tn7*, a myc epitope, hexa-histidine tag for easy detection of recombinant protein in Western Blot and eGFP for expression of green fluorescent protein for easy detection of recombinant baculoviruses under UV microscope. The plasmid vector was transformed into DH10Bac *E. coli* cells which contain a helper plasmid and baculovirus DNA to facilitate transposition of the donor plasmid DNA into the baculovirus DNA. The recombinant bacmid DNA was isolated by alkaline-lysis method. The purified bacmid DNA was transfected into Sf-21 insect cells to produce recombinant baculovirus. Recombinant baculoviruses can be detected using UV microscope and large scale propagation of the viruses were produced for isolation and purification of the recombinant protein.

Western Blot of Recombinant 55L and 55R Proteins

To analyse the location of the FV3 recombinant protein in the infected cells, AcFV3-55RT and AcFV3-55LT recombinant baculovirus infected Sf-21 or Hi-5 cells were collected at 48, 72, 144 hpi and centrifuged at 5000 rpm (4100 x g) for 20 minutes to separate cell pellet and supernatant. Supernatant from AcFV3-55RT and AcFV3-55LT infected Sf-21 or Hi-5 cells were concentrated 1000 fold by using a Microcon concentrator (Pall). Both the concentrated supernatant and the infected cell pellets were mixed with an equal volume of SDS-gel loading and dissociation buffer (50 mM Tris-Cl, pH6.8, 100 mM DTT, 2% SDS, 0.1% bromophenol blue, 10% glycerol). The cell lysate was passed through a Hamilton micro-syringe several times to break up DNAs and other cellular debris. The samples were then boiled for 5 minutes followed by separation of the proteins on a 12% Tris-glycine polyacrylamide gel (Invitrogen) in Tris-glycine (25 mM Tris base, 0.192 M glycine w/v + 0.1% SDS) running buffer and ran at 125 volts constant for 1.5 hour under reducing condition. The proteins were then transferred to nitrocellulose membrane (Bio-Rad) by using a semi-dry Transblotter (Bio-Rad) and transfer buffer (running buffer without Tween 20 + 30% methanol, kept at 4°C). The transfer was performed at 12 volts constant for 1 hour.

Thereafter, the membrane was blocked in PBS (phosphate buffered saline, pH7.4) + 2% BSA for 1 hour at room temperature. A 1:10000 dilution of anti-penta-his (Qiagen) antibody in PBS + 2% BSA was applied to the membrane and incubated at 4°C overnight. The membrane was then washed 4 times for 10 minutes each on an orbital shaker with PBST (PBS + 0.05% Tween 20) followed by incubation with 1:5000 dilution of goat anti-

mouse IgG (G α M, Sigma) horseradish peroxidase (HRP) conjugate in PBST with 5% non-fat milk at room temperature on an orbital shaker for 1 hour. The membrane was washed 4 times for 10 minutes each with PBST and the recombinant proteins were detected by applying Luminol (Bio-Rad) and exposing the membrane to x-ray film (East-man Kodak) for 1 hour and then developed. Western blot for purified recombinant proteins were done in the same manner.

Purification of Recombinant Proteins

Sf-21 or Hi-5 cells infected with the recombinant baculovirus were collected at 72 hpi or 144 hpi and centrifuged at 5000 rpm (4100 x g) for 5 minutes at 4°C. The supernatant was removed and the cell pellet resuspended in deionized water (4°C) and homogenized on ice with a dounce homogenizer and then passed through a 26 gauge syringe several times to rupture the nuclear membrane. The cell lysate was transferred to a 15 ml conical centrifuge tube and 1 volume of 2X equilibration/wash buffer (100 mM Sodium Phosphate, 600 mM Sodium Chloride, pH7.0) was added and mixed gently. The cell lysate was then centrifuged at 12000 rpm (13,400 x g) at 4°C for 15 minutes and the clarified supernatant separated from the cell pellet. The supernatant was used for isolating the recombinant protein.

The protein purification process was performed at 4°C using BD TALONspin column by following manufacturer's protocol with some modifications. The column containing the IMAC resin was equilibrated 2-4 times by passing 1X equilibration buffer (50 mM Sodium Phosphate, 300 mM sodium chloride, pH 7.0) through the resin and then once with elution buffer

unannealed oligonucleotides were removed using the following procedure. After hybridization, a 6X DNA loading buffer (1% SDS, 0.1% xylene cyanol, 0.1% bromophenol blue and 50% glycerol) was added to a final concentration of 1X and the mixture was fractionated through an 8% native polyacrylamide gel for 1 hour at 100V in 0.5X TBE (45 mM Tris, 4.5 mM boric acid and 0.5 mM EDTA). The substrate was located by autoradiography, the product was excised from the gel and sliced into small pieces and eluted in 3 volumes of elution buffer (0.5 mM ammonium acetate, 10 mM magnesium acetate, 1 mM EDTA, pH 8.0) by incubating at 37°C for 2 hours. After centrifugation, the supernatant was collected, and the insoluble material was extracted once more with elution buffer. Following centrifugation, both supernatant fractions were combined, and the DNA was ethanol precipitated and dissolved in TE (10 mM Tris HCl, pH 7.5, 1 mM EDTA). Specific radio-activity of substrate was determined by liquid scintillation counting. The substrates thus prepared contain a 25 bp duplex DNA with a 5'-24mers single strand at one end and a 3'-25mers single strand at the other end.

DNA Helicase Assay

Helicase activity was assayed in reaction mixtures of 15 μ l each containing 20 mM Tris HCl pH 8.5, 10 mM MgCl₂, 2 mM DTT, 100 μ g/ml BSA, 5 mM NTP, 10 fmol of substrate and 1 μ l of cell extract as described in Figure 12 or 0.33, 1, and 3 μ l purified recombinant proteins as described in Figure 17 and incubated at 30°C for 30 minutes. After incubation, the reactions were stopped by adding 5 μ l of 5X loading buffer (100 mM EDTA, 1% SDS, 0.1% xylene cyanol, 0.1% bromophenol blue and 50% glycerol). Aliquots

were fractionated on a 8% native polyacrylamide gel in 0.5X TBE and electrophoresed for 1.5 hours at 150 V at 4°C. The helicase activity was visualized and quantitated by phosphorimaging.

DNase Assay

Preparation of Substrate

Plasmid pcDNA3.1myc-his/A DNA was isolated by using alkali-lysis method as above (Maniatis *et al.*, 1982). Ten micrograms of pcDNA3.1myc-his/A DNA was digested with *Xba*I and *Kpn*I and incubated at 37°C overnight and purified using QIAGEN PCR purification kit by following manufacturer's protocol. Restricted and unrestricted pcDNA3.1myc-his/A DNA was electrophoresed on 1% agarose gel to confirm proper restriction and molecular size of DNA. The gels were stained with ethidium bromide (10 mg/ml) and photographed on a UV-transilluminator.

Nuclease Assay

FV3 55L and 55R purified recombinant proteins were used to determine nuclease activity in reaction mixtures containing 100 ng of restricted or unrestricted pcDNA3.1myc-his/A DNA, 50 mM NaCl, 10 mM Tris HCl, 10 mM MgCl₂, 1 mM DTT, and 3 µl (10 fmol) each of 55L or 55R purified recombinant protein with or without 5 mM dATP, to a total volume of 10 µl or 15 µl and incubated at 30°C for 45 minutes. After incubation, the reaction was stopped by adding 2 µl of 6X loading buffer (1% SDS, 0.1% xylene cyanol, 0.1% bromophenol blue and 50% glycerol) and electrophoresed on a

1% agarose gel in TBE buffer. The agarose gels were stained with ethidium bromide (10 mg/ml) and imaged on an UV-transilluminator.

RESULTS

FV3 Genomic Organization

Cloned FV3 genomic DNA was sequenced using the primer walking method and transposon tagging system. FV3 genomic library clones were generated based on *KpnI* and *HindIII* restriction maps (Figure 4) previously published by Lee and Willis [1983]. Each cloned restriction fragment was linked by sequencing overlapping *KpnI* and *HindIII* fragments, or sequencing PCR products spanning the region between two non-overlapping fragments. Both strands of the entire FV3 genome were sequenced and each nucleotide was sequenced between 2 to 16 times. The results revealed that the FV3 genome contained a contiguous 105,903 bp nucleotide sequence, excluding the terminal redundancy. The G+C content of the FV3 genome was 55%, supporting earlier reports [Smith and MacAuslan, 1969; Houts *et al.*, 1970]. Upon alignment of all the sequences from each cloned restriction fragments, the FV3 genome was found to be circularly permuted and terminally redundant as described earlier [Goorha and Murti, 1982]. This feature was evident when the *HindIII* 'E' fragment could be aligned either next to *HindIII* 'D' fragment or joined at the other end of *HindIII* 'A' fragment. In circularly permuted genomes, the genes are not arranged in any particular order. As a result of the circular permutation and terminal redundancy [Goorha and

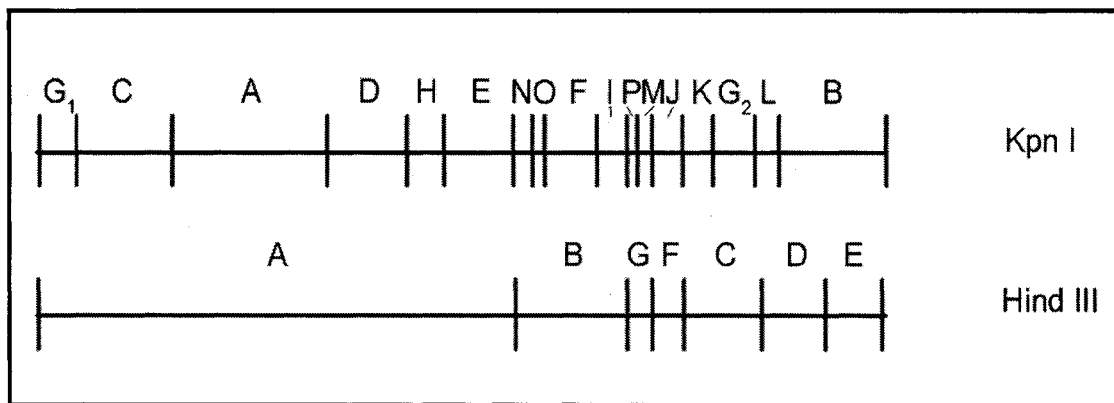


Figure 4.

KpnI and *HindIII* restriction maps of FV3 genomic DNA [Lee and Willis, 1983].

Murti, 1982] of its genome, FV3 replicates its genomic DNA in concatemeric manner so it will not risk losing a part of its genome during successive rounds of replication [Goorha, 1982]. The computer generated restriction maps of *EcoRI*, *HindIII*, *KpnI* and *Sall* based on the completely aligned FV3 genomic sequence is shown on Figure 5. The restriction maps for *EcoRI* and *Sall* from this sequence was found to be consistent with the restriction maps that were previously published [Lee and Willis, 1983, Tondre et al., 1988]. However, the *HindIII* and *KpnI* restriction maps from the sequence of the FV3 genome were found to differ slightly from the earlier *HindIII* and *KpnI* restriction maps (Figure 4) [Lee and Willis, 1983]. In the current *HindIII* map (Figure 5), 2 smaller fragments (*HindIII* 'H', 800 bp; *HindIII* 'I', 433 bp) were detected by computer analyses and 'G' and 'F' fragments were in reversed positions (Figure 5). In the *KpnI* map, an additional 3.75 kbp *KpnI* restriction fragment was found (Figure 5). This novel fragment was designated as *KpnI* 'Ia' (3.75 kbp, Figure 5) to distinguish it from previous *KpnI* 'I' (3.6 kbp, Figure 4).

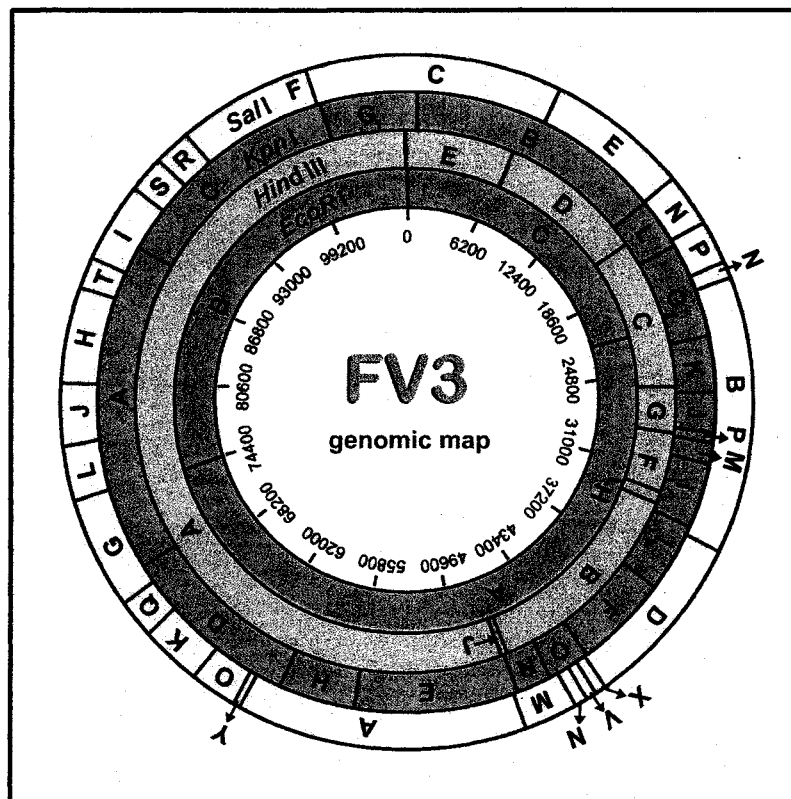


Figure 5.

Computer generated restriction map of FV3 genome from completely aligned genomic sequence. From inside circle to outside: *EcoRI*, *HindIII*, *KpnI* and *Sall* respectively. Note the extra fragments 'H' and 'J' in the *HindIII* map and 'la' in *KpnI* map. The restriction maps were generated using MacVector 7.0 (Oxford Molecular) from the aligned FV3 genomic sequence.

These may not have been detected earlier due to the fact that the smaller *HindIII* fragments may have ran out of the electrophoretic range, and also close migration of the two *KpnI* fragments of similar molecular size during electrophoretic separation [Lee and Willis, 1983]. Although FV3 has a relatively compact arrangement of ORFs, there are a few regions that do not appear to encode viral proteins. Most of these non-coding regions were short and contained TAAT and CAAT box-like regulatory sequences both upstream

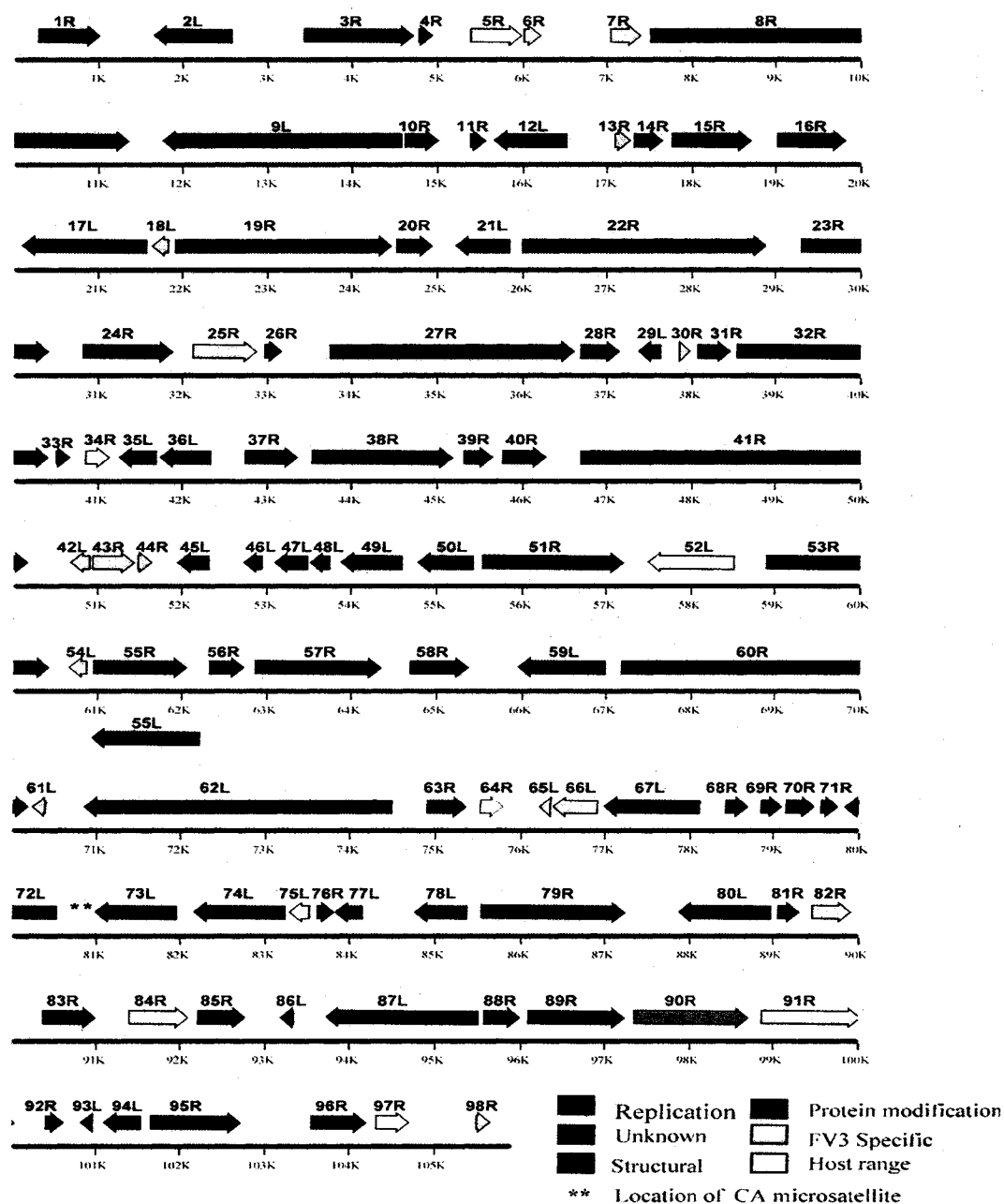


Figure 6.

Linear ORF map of FV3 genome. Predicted linear ORF map of FV3 genome excluding terminal redundancy. ORFs are numbered from left to right. Each ORF is represented by an arrow that indicates the approximate size and the direction of transcription based on the position of methionine initiation and termination codons. Potential function of each ORF is color-coded as indicated in the figure. The location of CA microsatellite is indicated by **.

and downstream of ORFs. These features are similar to that found in the TFV genome [He *et al.*, 2002]. Moreover, as expected, there was no evidence of introns.

A total of 98 non- overlapping putative ORFs containing 50 or more amino acids have been identified (Appendix A, Figure 6) by computer analysis using MacVector (Oxford Molecular). Eighty four of these putative ORFs have corresponding homologues in other iridoviruses infecting lower vertebrates [TFV (81 ORFs), LCDV1 (41 ORFs), ISKNV (23 ORFs)] or insects [CIV (31 ORFs)]. Eighteen (Appendix A, underlined) of the 84 ORFs were common to FV3, TFV, LCDV1, ISKNV and CIV. Fourteen potential ORFs unique to FV3 (6R, 7R, 13R, 18L, 30R, 42L, 43R, 44R, 54L, 61L, 64R, 65L, 66L and 98R) were either putative secretory proteins or possessed a transmembrane domain (Appendix A, marked with a k). Only two (54L, 64R) of these 14 ORFs share conserved domains with known proteins.

Microsatellite and Repeated Sequences

A unique feature of the FV3 genomic DNA was the existence of a microsatellite containing 34 tandemly repeated 'CA' dinucleotides. This sequence was located in the non-coding region between ORFs 72L and 73L and encompassed nucleotides 80839 to 80906 (Figure 6, marked with **). CA dinucleotide microsatellites are found most commonly in *Drosophila melanogaster* [England *et al.*, 1996; Schug *et al.*, 1998]. This is the first such sequence found in an animal virus. Microsatellites are tandemly repeated sequences that are made up of a single sequence motif not more than 6 bases long without any interruption by any other base or motif [Goldstein and

Schlötterer, 1999]. Microsatellites may serve as functional coding and/or regulatory elements. The presence of a microsatellite upstream of, or within, the promoter region can function as an enhancer [Kunzler *et al.*, 1995, Kashi *et al.*, 1997]. Microsatellites are mutational hotspots and produce polymorphisms that are useful as genetic markers for studies of quantitative genetic variation and evolutionary adaptation [Goldstein and Schlötterer, 1999]. The biological significance of this finding in FV3 still remains to be resolved. However, primers flanking this unique microsatellite region could be used to identify polymorphisms within frog virus isolates.

The FV3 genome also has many interspersed multiple tandem and inverted repeats, and also dyad symmetries which are commonly found in iridoviruses, ascoviruses, geminivirus, African swine fever virus and Epstein-Barr virus [Fischer *et al.*, 1988; Schnitzler and Darai, 1989; Dixon *et al.*, 1990; Fujiwara and Ono, 1995; Dry *et al.*, 1997; Müller *et al.*, 1999; Bigot *et al.*, 2000].

Regulatory Sequences - Putative Promoter Sequences, Transcriptional Start and Termination Sequences and RNA Polymerase II Binding Sites

FV3 genes are expressed in three temporal classes: immediate early, delayed early and late [Willis *et al.*, 1977; Elliot and Kelly, 1980]. Two of the immediate early genes have been previously sequenced and their promoters analyzed [Willis *et al.*, 1984b; Beckman *et al.*, 1988]. The promoters of the two genes have different structures, suggesting that FV3 does not employ a canonical promoter sequence for transcriptional regulation. Most of the analyzed FV3 ORFs have AT rich regions or GC motifs similar to those of eukaryotic genes upstream of the putative transcriptional start sites. The

sequences found upstream of the putative ORFs include CAAT, TATA and TATAAT boxes; however, some potential ORFs do not have any of these regulatory elements. Putative transcriptional start and termination sites [Willis and Granoff, 1985] were also found within an AT rich region preceding and at the end of most of the FV3 ORFs.

Transcriptional Regulation

FV3 tightly regulates viral gene expression using a variety of transcriptional control proteins. For example, early messages are synthesized in the nucleus and require host RNAP II and at least two viral proteins [Goorha, 1981a; Willis and Granoff, 1985; Thompson *et al.*, 1986]. A virion-associated protein is required for the synthesis of immediate-early (IE) messages, whereas a virus-induced factor is needed for delayed-early (DE) and late (L) transcription. Although neither protein has yet been identified, FV3 ORFs 37R and 81R encode proteins homologous to the NIF/NL1 interacting factor of LCDV1 and a transcriptional elongation factor that might be candidates for these transcriptional activators. Late viral transcription is thought to occur in the cytoplasm and is likely to be catalyzed by a virus-encoded or virus-modified polymerase. FV3 and other iridoviruses encode two proteins (ORFs 8R and 62L) with significant sequence homology to the two largest subunits of eukaryotic DNA-dependent RNAP II. Whether these form the core of a novel viral RNA polymerase or whether they modify an existing host RNA polymerase, has not yet been determined.

DNA Replication, Repair, Modification and Processing

The FV3 sequence has ORFs that could potentially encode several DNA replication, repair and modification enzymes. These include DNA polymerase (ORF 60R), ATPase (ORF 15R & ORF 22R), integrase (ORF 16R), replication factor (ORF 1R), a SAP DNA binding protein (ORF 49L), cytosine DNA methyltransferase (ORF 83R), RAD2 DNA repair protein (ORF 95R), NTPase/helicase-like protein (ORF 9L, ORF 55L and ORF 73L), and a 40 kDa protein of unknown function is also encoded by ORF 55 in the reverse direction of ORF 55L.

FV3 ORF 60R showed a high amino acid identity to the structural domain of DNA polymerase B family. The functions of this enzyme include elongation, DNA-binding, dNTP binding activities and a domain with 3' to 5' exonuclease activity. This protein also showed high identity (95-99%) to TFV and Regina ranavirus DNA polymerase genes but low identity (36-38%) to LCDV1, ISKNV, CIV. A putative replication factor and/or DNA packaging protein is encoded by FV3 ORF 1R and has a LCDV1 counterpart. A conserved C-terminal domain restricted to helicases of the DEXD/H helicase family is encoded by ORF 9L. Protein database (RPS-Blast) searches also showed that this ORF contains a conserved N-terminal domain of the SNF2 family, which is involved in a variety of processes including transcription regulation, DNA repair, DNA recombination and chromatin unwinding [Laurent *et al.*, 1991]. Both ORFs 22R and 73L encode putative NTPases. These ORFs also showed high identity to ORFs 9L and 78L of the TFV genome [He *et al.*, 2002] and also NTPases of *Regina ranavirus*, LCDV1 and ISKNV. FV3 ORF 95R encodes a homologue of the highly conserved N and I

region domain of xeroderma pigmentosum G, which functions in nucleotide excision repair and transcription coupled repair of oxidative DNA damage. In addition, protein database (RPS-Blast) searches suggested that this ORF may be a 5' to 3' exonuclease and could function in DNA excision and repair. This ORF also showed a high nucleotide and protein identity to TFV ORF 101R, but much lower identity to the homologues of LCDV1, ISKNV and CIV. A SAP DNA-binding domain was encoded by FV3 ORF 49L, suggesting that it is involved in chromosomal organization. Its counterpart in TFV is ORF 51L and ORF 110L in LCDV1, but it is not present or identified in ISKNV and CIV.

FV3 ORFs that encode for proteins involved in biosynthesis of nucleic acid precursors include FV3 ORF 63R, which has significant homology to deoxyuridine triphosphatase (dUTPase) the function of which is to hydrolyze dUTP to dUMP and pyrophosphate. This ORF has a high percentage of identity to TFV ORF 68R and low identity to CIV's homologue, but is not identified in LCDV1 and ISKNV. This ORF also showed a high identity to rat dUTPase. Other putative FV3 encoded enzymes involved in nucleic acid metabolism include deoxynucleoside kinase (ORF 85R), ribonucleoside diphosphate reductase alpha subunit (ORF 38R) and beta subunit (ORF 67L). These proteins also showed some degree of identity to TFV, LCDV1 and ISKNV ORFs.

Protein Modifications

An ATPase-like coding sequence homologous to its TFV counterpart ORF 16R is encoded by FV3 ORF 15R. Homologues of ORF 15R are identified in LCDV1 (ORF 54R), ISKNV (ORF 122R) and CIV (ORF 75L). This

protein has a conserved domain belonging to the AAA-ATPase family, which has chaperone-like functions that assist in the assembly or disassembly of protein complexes. Interestingly, this ORF also showed identity to vaccinia virus A32 protein, which is thought to be involved in viral DNA packaging [Koonin *et al.*, 1993; Cassetti *et al.*, 1998]. Another potential ORF involved in protein modification is encoded by ORF 79R, possibly an ATP-dependent protease which functions in post-translational modification, protein turn-over and as a chaperone [Ramachandran *et al.*, 2002]. Potential protein kinase ORFs include tyrosine kinase (ORF 27R), serine/threonine kinase (ORF 57R), phosphatidylinositol-specific phospholipase (ORF 32R) and protein kinase (ORF 19R).

Host-virus Interactions

In addition to the essential genes that are required for virus replication, FV3 also encodes a variety of putative genes involved in host-virus interactions. These include a protein similar to a herpesvirus secretory nuclear protein from the US22 protein family (ORF 5R) which may play a role in virus replication and pathogenesis, and a protein with homology to the vaccinia virus 3-beta-hydroxy-delta 5-C27 steroid oxidoreductase-like protein (ORF 52L), which has been suggested to suppress inflammatory responses and thus contribute to virulence [Reading *et al.*, 2003]. In addition, four proteins that may be involved in apoptotic signaling have also been identified: a protein containing CARD (caspase recruitment domain) and DEATH domain-like motifs (ORF 64R), a protein with homology to the LPS-induced tumor necrosis factor-alpha (LITAF, ORF 75L), a homologue of a LCDV1

protein similar to proliferating cell nuclear antigen (PCNA) (ORF 84R), and Bcl-2-like protein containing BH1 and BH2 regions (ORF 97R).

FV3 Specific Proteins

Other putative ORFs encode immediate early protein ICP-18 (ORF 82R) and ICP 46 (ORF 91R), delayed early p31K protein (ORF 25R) a late 40 kDa protein (ORF 55R) and/or a helicase-like protein (ORF55L) of which homologues are found in other iridoviruses (Appendix A). An interesting feature of the FV3 p31K protein encoded by ORF 25R was two stretches of 7 glutamic acid residues near the carboxyl terminal as previously reported by Schmitt *et al.*, [1990]. The function or significance of these 2 stretches of glutamic acid residues is not known.

A total of 14 ORFs are unique to FV3 and are not found in any other virus (Appendix A - marked with a k). Two of these unique ORFs include 54L and 64R. The 54L is a homologue of nuclear calmodulin-binding protein and 64R has a caspase recruitment domain. Interestingly, the anti-sense strand of ORF 55R (which encodes the FV3 40 kDa protein) encodes a potential ORF that translate into a helicase-like protein. This helicase-like protein shares a high degree of identity with TFV ORF 56L, a counterpart in epizootic haematopoietic necrosis virus (EHNV) and CIV ORF 161L. This protein is also similar to the T5 phage helicase. Protein database searches [RPS-Blast] showed that this putative protein has a highly conserved DEAD/DEAH-like domain of the helicase superfamily. This protein could function in the unwinding of duplexed nucleic acids, or could play a role in RNA transcription or nucleocytoplasmic transport and translation. However, additional studies

are required in order to ascertain the correct coding direction of ORF 55R or ORF 55L. Due to the high homology with conserved protein domain of a helicase-like protein, ORF 55L was assigned as the putative ORF for this region.

Structural and Other Genes

As expected, FV3 ORF 90R encodes the major capsid protein [Mao *et al.*, 1996], which is highly conserved among the iridoviruses. The sequence is frequently used for phylogenetic studies [Tidona *et al.*, 1998, He *et al.*, 2002, Jancovich *et al.*, 2003]. A delayed-early gene homologue of integrase is encoded by ORF 16R. This protein contains a conserved sequence of an active catalytic site and has the functions of an integrase-resolvase in recombination and religation via strand exchange [Parsons *et al.*, 1988]. The replication strategy of FV3 requires an integrase-resolvase, since viral DNA concatemers are thought to arise by recombination of smaller genomic DNA molecules [Goorha and Dixit, 1984]. Therefore, this enzyme may also be implicated in resolving concatemeric DNA complexes and facilitating the packaging of viral DNA [Rohozinski and Goorha, 1992].

Nucleotide Differences as Compared to Published Sequences

Several of FV3 specific genes have been sequenced previously. These include immediate early protein ICP-18 (ICR169) [Willis *et al.*, 1984, Accession #K02377] and ICP-46 (ICR489) [Beckman *et al.*, 1988, Accession #M19872], a cytosine DNA methyltransferase [Kaur *et al.*, 1995, Accession #U15575], the delayed early p31K protein [Schmitt *et al.*, 1990, Accession

#X52986], a putative integrase [Rohozinski and Goorha, 1992, Accession #M80548], late 40 kDa protein [Munnes *et al.*, 1995, Accession #X82828], major capsid protein [Mao *et al.*, 1996, Accession #U36913], ATPase [Accession #M80551] and eIF-2 α homologue [Essbauer *et al.*, 2001, Accession #AF131072]. For most of these genes, the sequence data matched the published sequence completely except for some minor discrepancies. However, in the case of the viral DNA methyltransferase gene in an aza-C^r mutant and a putative homolog of eIF-2 α , there were marked differences between the current sequences and those published earlier.

Kaur *et al.* (1995) reported that the viral DNA methyltransferase gene of FV3 differed from the corresponding gene in the aza-C^r mutant by a C→G substitution at position 1071. However, the aza-C^r mutant used in this experiment has a C→T transition at position 1072, which did not change the amino acid encoded in the wild-type protein. Additionally, it was found that the DNA methyltransferase gene of this aza-C^r mutant contained a 13 bp insertion between positions 1078-1090 (Figure 7). This 13-nucleotide insertion was a duplicated sequence from the wild type preceding the position of the insertion in the mutant (Figure 7). This leads to the truncation of the protein at its C-terminus and most likely rendered it non-functional in the mutant virus.

Surprisingly, a full-length copy of the ranavirus eIF-2 α gene in this FV3 isolate that was sequenced was not detected. Instead, a truncated ORF encoding only 195 bp from the 3' end of the gene was detected. This truncation conclusion was further supported by searching for rearrangement

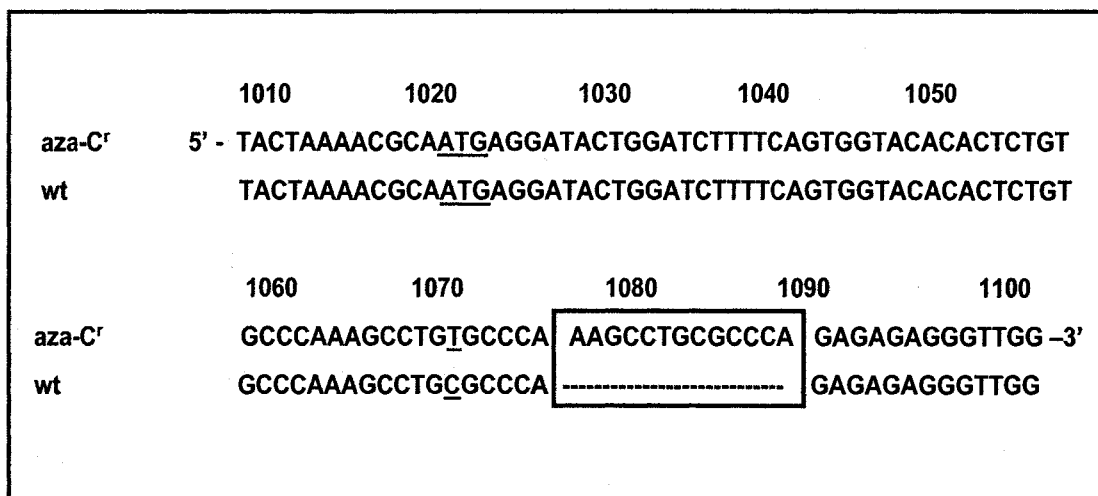


Figure 7.

Partial nucleotide sequence alignments of FV3 and aza-C^r DNA methyltransferase gene. The 5' end coding region of the DNA methyltransferase gene was aligned using CLUSTAL-X. Boxed area indicates the 13 bp insertion present in the aza-C^r mutant but not found in the wild type FV3 DNA methyltransferase gene. ATG indicates the start codon. Underlined nucleotide at position 1072 indicates a C→T transition between aza-C^r and wild-type FV3.

of this gene by transposition, insertion, or inversion elsewhere within the genome using Sequencher (GeneCodes) and MacVector (Oxford Molecular). Moreover, repeated attempts to obtain the full sequence by PCR analysis of wild type FV3 and aza-C^r mutant DNA as template using eIF-2 α specific primers from Essbauer *et al.*, [2001] and other primers flanking the region in question were unsuccessful. In all cases, only 195 bp at the 3' end of the eIF-2 α homologue were obtained. Apparently, this gene has undergone extensive rearrangements that have resulted in a truncated sequence compared to the eIF-2 α homologues of other iridoviruses. This result was unexpected, since the eIF-2 α gene is apparently highly conserved among eukaryotes, poxviruses, and other iridoviruses; particularly at the N-terminus [Essbauer *et al.*, 2001]. Interestingly, this FV3 isolate still shuts off host

protein synthesis and selectively synthesizes viral proteins, suggesting that FV3 eIF-2 α homologue alone is not responsible for this phenotype. It remains to be determined whether other FV3 encoded proteins play a role in maintaining protein synthesis in infected cells.

Relatedness of FV3 Genome to Other Iridoviruses

A comparison of FV3 ORFs with those of TFV, LCDV1, CIV and ISKNV revealed a number of homologues (Appendix A). Most of these encode DNA processing enzymes and DNA-binding proteins. However, FV3 also possesses ORFs that could encode proteins including a putative replication factor (ORF 1R, similar to LCDV1 ORF 162L), deoxynucleoside kinase (ORF 85R, similar to LCDV1 ORF 136R), and a protein that contains the BH1 and BH2 regions of B-cell lymphoma associated protein (ORF 97R). FV3 also has ORFs that could encode some secretory and transmembrane proteins of yet-to-be determined functions not found in other ranaviruses studied thus far (Appendix A, marked with a k).

DNA dot matrix (Pustell DNA matrix) analyses of FV3 genomic DNA with the TFV genome (Figure 8), LCDV1, ISKNV and CIV genomes (results not shown) revealed that LCDV1, ISKNV and CIV have little colinearity (i.e., conservation of gene order) or sequence similarity to FV3. In contrast, gene order between FV3 and TFV was markedly conserved, and sequence similarity was very high. Despite the generally conserved order of FV3 and TFV genes, several inversions, indicated by arrow heads in Figure 8 were observed in the latter half of the genome between ORFs 41R and 98R. Additionally, there are short regions of low sequence identity in the genomic

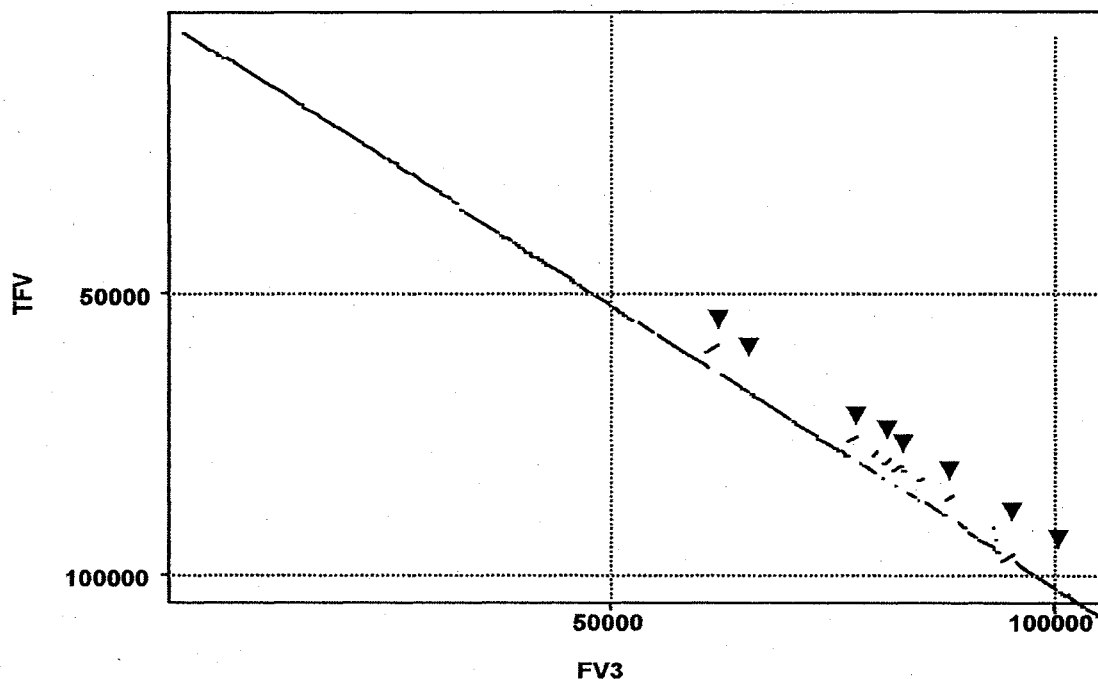


Figure 8.

DNA dot matrix plots comparing FV3 genome with TFV genome. Complete genomic sequences of FV3 and TFV were aligned using Pustell DNA dot matrix algorithm within the MacVector program. Solid lines indicate high level of sequence similarity. Arrowheads indicate inversions. DNA dot matrix parameters were set at 90% minimum score value with a hash value of 6 and Jump = 1. Both strands of DNA were aligned for the dot matrix plot.

sequences between nucleotides 2000-51000 (Figure 8, disjointed line). All of the 14 ORFs unique to FV3 (Appendix A, marked with a k) were found within these regions of DNA matrix incongruity between FV3 and TFV.

In an effort to determine the phylogenetic relationship of FV3 to other iridoviruses, the full-length major capsid protein sequences of 13 iridovirus (12 isolated from vertebrates and 1 from an invertebrate) were aligned using Clustal-X1.81 [Thompson *et al.*, 1997]. An unweighted parsimony bootstrap consensus tree was obtained by heuristic search with 100 bootstrap replicates using PAUP 4.0 [Swofford, 2003]. The bootstrap tree (Figure 9) showed that

FV3, TFV and Bohle iridovirus (BIV) are closely related and form a monophyletic group. This is supported by the bootstrap value of 74 as indicated on the branch in Figure 9. Fish (Flounder) Lymphocystis Disease Virus (FLDV) and LCDV1 appear to be closely related and were probably derived from a common ancestor, but were only distantly related to FV3, TFV and BIV. Additionally, piscine iridoviruses such as ISKNV, African lampeye (ALIV) and dwarf gurami iridovirus (DGIV) were closely related to each other but were not grouped with the ranaviruses as illustrated by the evolutionary relationships shown in Figure 9.

Six other highly conserved full length protein sequences have also been analyzed from FV3, TFV, LCDV1, ISKNV and CIV for phylogenetic inference using PAUP 4.0 [Swofford, 2003]. In all cases these analyses (Figure 10) provided additional evidence that TFV and FV3 are more closely related than any of the other iridoviruses. While these studies suggest that FV3 and TFV could be strains of the same viral species, the sequence inversions noted in Figure 8 indicated that the two isolates have undergone considerable genetic changes. It is unclear whether point mutations within key genes or alterations in the overall genetic organization of the viral genome are responsible for the enhanced lethality of TFV, or if the increase in pathogenicity is more a reflection of environmental factors (e.g., immune suppression following the stress of intensive farming practices). Taken together, the results from DNA dot matrix and phylogenetic analyses strongly suggest that frog iridoviruses (TFV, FV3 and BIV) are distinct from fish iridoviruses described here. Moreover, they support the current taxonomic view that Ranavirus (FV3, TFV), Lymphocystivirus (LCDV1), and

Megalocystivirus (ISKNV, RSBIV) comprise three distinct genera within the family Iridoviridae.

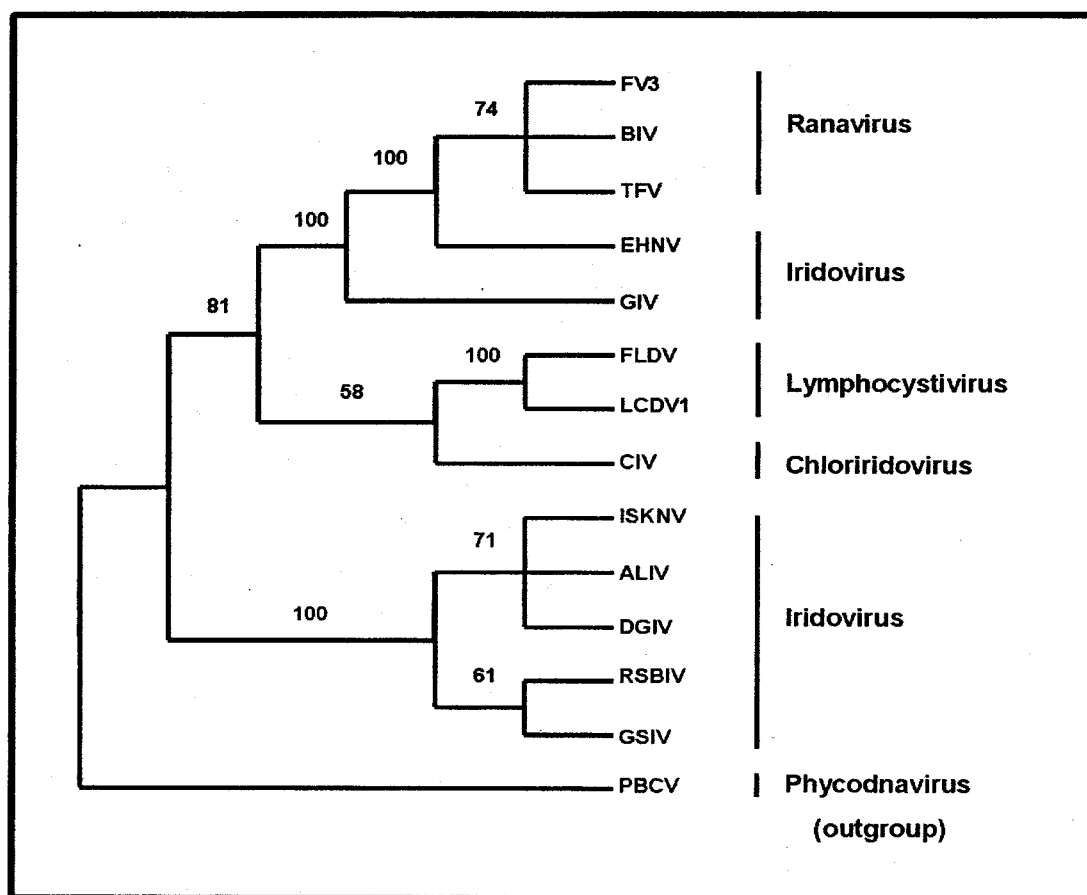


Figure 9.

Parsimony bootstrap tree of the major capsid protein of representative iridoviruses. Parsimony bootstrap consensus tree showing phylogenetic relationships between FV3 and other iridoviruses by alignment of the major capsid protein using Clustal-X and tree analysis by PAUP. Iridoviruses used for this analysis includes tiger frog virus (TFV), bohle iridoviruses (BIV), epizootic haemopoietic necrosis virus (EHN), grouper iridovirus (GIV), flounder lymphocystis disease virus (FLDV), lymphocystis disease virus 1 (LCDV1), chilo iridescent virus (CIV), infectious spleen and kidney necrosis virus (ISKNV), African lampeye iridovirus (ALIV), dwarf gurami iridovirus (DGIV), red seabeam iridovirus (RSBIV) and grouper sleepy disease iridovirus (GSDIV). *Paramecium bursaria* Chlorella Virus 1 (PBCV1, a phycodnavirus) is used as an outgroup. Numbers above the branches indicate bootstrap support values based on 100 replicates.

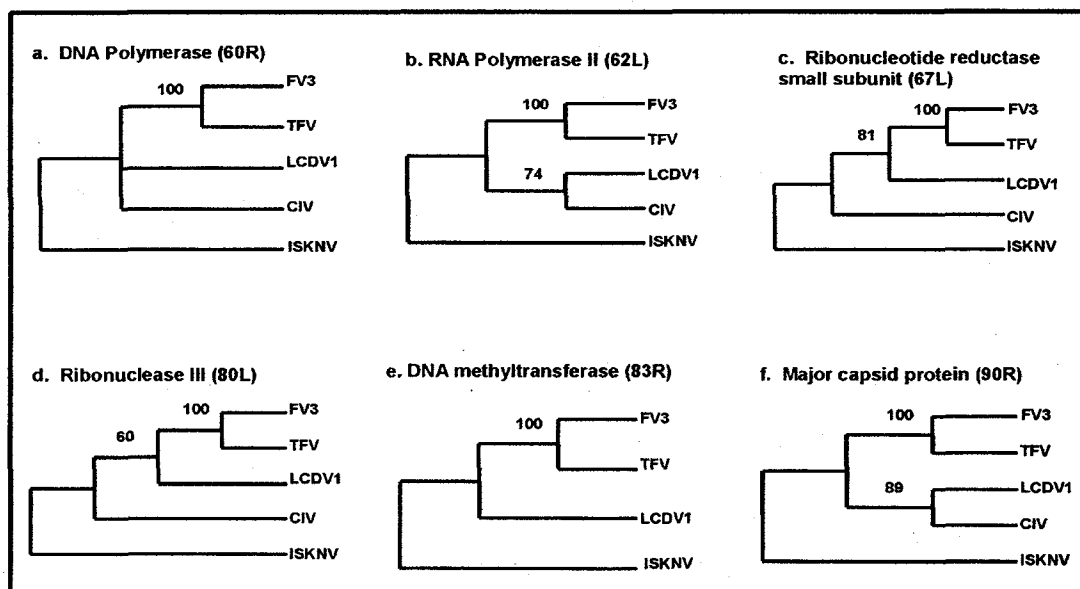


Figure 10.

Parsimony bootstrap trees of 6 conserved genes of FV3, TFV, LCDV1, ISKNV and CIV. Complete amino acid sequences of a) DNA polymerase (ORF 60R), b) RNA polymerase II (ORF 62L), c) Ribonucleotide reductase small subunit (ORF 67L), d) Ribonuclease III (ORF 80L), e) DNA methyltransferase (ORF 83R) and f) Major capsid protein (ORF 90R) of FV3, TFV, LCDV1, ISKNV and CIV were aligned using Clustal-X and parsimony bootstrap trees generated by PAUP. In all cases, high levels of support were obtained for the close relationship of FV3 and TFV. Numbers above branches indicate bootstrap support values based on 100 replicates. Note that CIV is not included in the DNA methyltransferase gene phylogenetic analysis as this gene is not present in this virus.

Analyses of ORFs 55L and 55R

Overlapping open reading frames have not been reported in Ranavirus genomes before. However, upon analysis of the genomic sequence of FV3, ORFs 55R and 55L were predicted to be in the same region covering nucleotides sequence 60937-62232 but the start codon of each ORF are in the opposite direction to each other (Appendix A, Figure 6).

In the sense direction of the nucleotide sequence, ORF 55R was previously shown to be expressed late in the replication cycle of FV3 and that

it encoded a 40 kDa protein of unknown function [Munnes *et al.*, 1995]. In contrast, blast results of the ORF 55L predicted amino acid sequence and nucleotide sequence showed that ORF 55L had domains that were homologous with conserved domains from DEAD/DEAH-like helicases (Figure 11). The DEAD/DEAH box helicases belong to a family of proteins from the superfamily 2 (SF2) DNA or RNA helicases involved in ATP-dependent RNA or DNA unwinding and are also suggested to play a role in DNA replication, repair and recombination, transcription and translation, and ribosomal structure and biogenesis. Among the class of DEAD/DEAH box proteins shown to have helicase activities are the human RecQ family, *E. coli* RecQ and yeast SGS1 [Gangloff *et al.*, 1994; Karow *et al.*, 2000; Nakayama *et al.*, 1985; Umezu *et al.*, 1993]. Most helicases in the superfamily 2 from various organisms contain all or a combination of the 7 known amino acids sequence motifs (Figure 11, top panel A) designated as I (Walker A), IA, IB, II (Walker B), III, V, and VI found in the core region of the molecule [Gorbalenya *et al.*, 1988, 1989; Tanner, 2003; Tanner *et al.*, 2003; reviewed in Tuteja and Tuteja, 2004]. Of the 3 classical groups of DEAD/DEAH box helicases, the DEAH* group (Figure 11, top panel A) displayed the most variation in motifs and all known helicases in this group characterized were found to be DNA helicases [reviewed in Tuteja and Tuteja, 2004]. These motifs are commonly used for prediction and detection of new helicases in genome sequences. However, the identification of these conserved fingerprints in a sequence cannot be used to definitively classify a protein as a helicase, as direct biochemical evidence of ATP-dependent helicase activity must also be demonstrated [Tuteja and Tuteja, 2004].

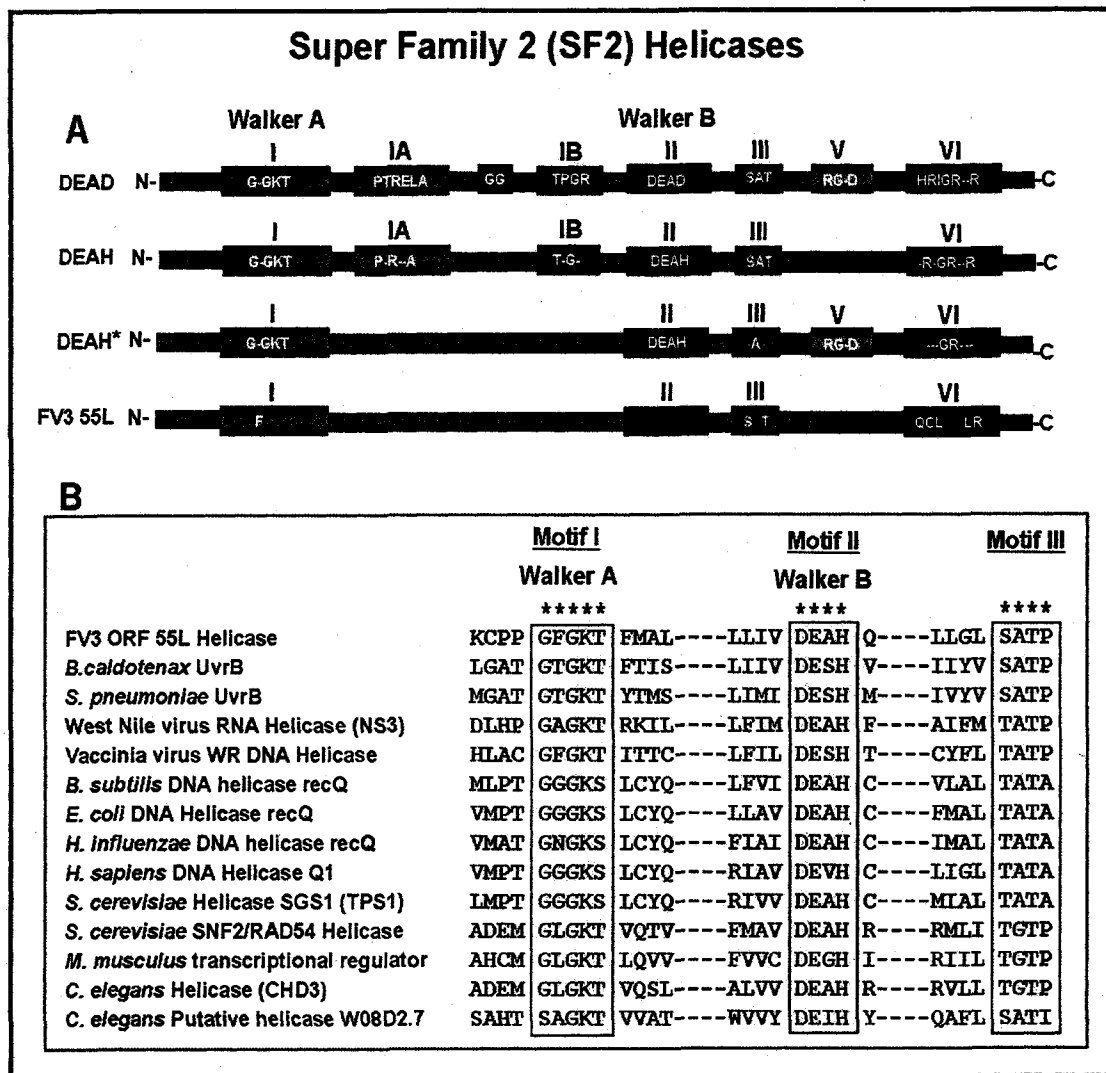


Figure 11.

Super family 2 (SF2) helicases conserved motifs and amino acids sequence alignment of ORF 55L with other known helicases. Top: Amino acid consensus motifs of DEAD/H-box helicases showing alignment of motifs Q, I (Walker A), IA, IB, II (Walker B), III, IV, V and VI [Tuteja and Tuteja, 2004]. Bottom: Amino acid sequence alignment of FV3 ORF 55L helicase-like protein with various organisms' helicase sequence using CDD database [Marchler-Bauer *et al.*, 2005]. Shown here are the 3 conserved domains of the FV3 helicase molecule aligned with respective organisms. Motif I or Walker A is the ATP-binding site; Motif II or Walker B is the DEAD/DEAH box and Motif III. *B. caldotenax*: 1D9ZA; *S. pneumoniae*: Q54986; West Nile virus: P06935; Vaccinia virus WR: P16712; *B. subtilis*: P50729; *E. coli*: P15043; *H. influenzae*: P71359; *H. sapiens*: P46063; *S. cerevisiae* SGS1: P35187; *S. cerevisiae* SNF2/RAD54: P32657; *M. musculus*: Q61687; *C. elegans* CHD3: Q22516; *C. elegans* W08D2.7: Q23223.

FV3 ORF 55L amino acid sequence was used to align with known helicases from other organisms as indicated in Figure 11 (Panel B), by using the conserved domain database (CDD) searches on the NCBI website. The results showed that FV3 ORF 55L has 4 of the 7 conserved motifs and resembled the most diverse DEAH* group of helicases. From these analyses, it is highly possible that both ORFs 55L and 55R are expressed during some time in the replication cycle of FV3, since a previous study has shown that ORF 55R was transcribed late in the infectious cycle and that ORF 55L predicted amino acid sequence showed homology with conserved domains of SF2 helicases (Figure 11).

Is there Helicase Activity in FV3 Infected Cells?

Infected Cells Helicase Assays

Because of the highly conserved helicase motifs found in ORF 55L amino acid sequence, it was interesting to assess if FV3 does possess helicase enzymatic activity. FV3 infected cells supernatant from cytoplasmic and nuclear extracts were used for helicase activity assays in conditions as described in materials and methods. The infected extracts were from 2, 4, 6, 12 and 24 hpi respectively. From the results shown in Figure 12, helicase activity was detected from 2 hpi onwards in both the nuclear and cytoplasmic extracts with peak activity at 12 hpi. Since second stage FV3 DNA replication occurs in the cytoplasm, the DNA helicase activity seen in the cytoplasmic extract is most likely of viral origin as cellular helicases are found

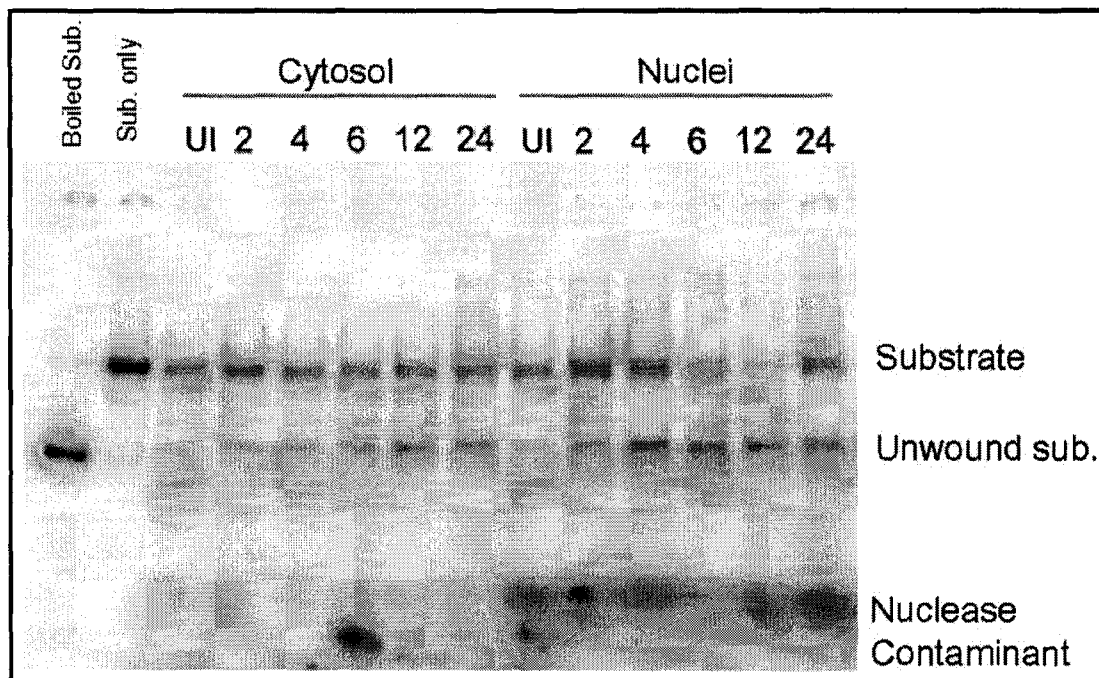


Figure 12.

Helicase assay of FV3 infected cells and uninfected cells. Cytoplasmic and nuclear infected cell extracts and uninfected cell extracts were used for helicase assay with hybridized oligonucleotides 49mers (labeled with γ - 32 P ATP) and 50mers with a region of 25 nucleotides duplex region. The substrates have a 5' 24mers and 3' 25mers single stranded ends. UI = uninfected cells,; 2, 4, 6, 12, 24 = hours post infection (hpi). The reactions were incubated at 30°C for 30 minutes and fractionated on a 8% native polyacrylamide gel in 0.5X TBE. Unwound substrate was observed at 2, 4, 6, 12 and 24 hpi in both cytoplasmic and nuclear extracts.

in the nucleoplasm for DNA unwinding, repair and recombination during DNA replication. The nuclear helicase activity is also evident in Figure 12 with increased helicase activity in the nuclear extract as compared with activity shown in the cytoplasmic extract. This could be a combination of both cellular and viral helicase activities. Also, the nuclease activity as seen in Figure 12 might be cellular nuclease as this activity was not seen in the cytoplasmic extract. This experiment confirms that helicase activity is indeed present in

FV3 infected cells and that it is most likely from FV3, especially since activity is also seen in the cytoplasmic extract. However, this information does not confirm if ORF 55L protein product is directly involved in this reaction, since there are at least three ORFs in the FV3 genome that may have potential helicase activity (ORFs 9L, 55L and 73L; Appendix A). Therefore, more specific studies are required to indentify the gene(s) that encode the viral helicase activity.

Are Both FV3 ORFs 55L and 55R Expressed at the RNA Level?

2-Step RT PCR

To answer this question, total RNAs were extracted from FV3 infected cells and used for cDNA synthesis. Since both genes lie in the same DNA region and are complementary to each other (Figure 6), a single step reverse transcription PCR (RT-PCR) reaction would not be able to differentiate which specific gene is expressed, as both 5' and 3' primers would be present during reverse transcription and therefore both transcripts would be used for cDNA synthesis. Therefore, 2-step RT-PCR reactions (cDNA synthesis with only one primer followed by PCR with both) were used to differentiate transcripts of ORFs 55L and 55R. The cDNAs were then used for PCR reactions. The results as shown in Figure 13 demonstrated that at 6 hpi and 24 hpi, both ORFs are expressed with the expected fragment size from both pairs of primers (*EcoRI*-3L/*Bam*HI-5L and *EcoRI*-3R/*Bam*HI-5R) used. In Figure 13A Lanes (a), 55L transcript was amplified with *EcoRI*-3L primer at 6 and 24 hpi whereas in the same figure in Lanes (c), *Bam*HI-5L primer amplified 55R transcript at 6 and 24 hpi with the expected fragment size of 1300 bp from

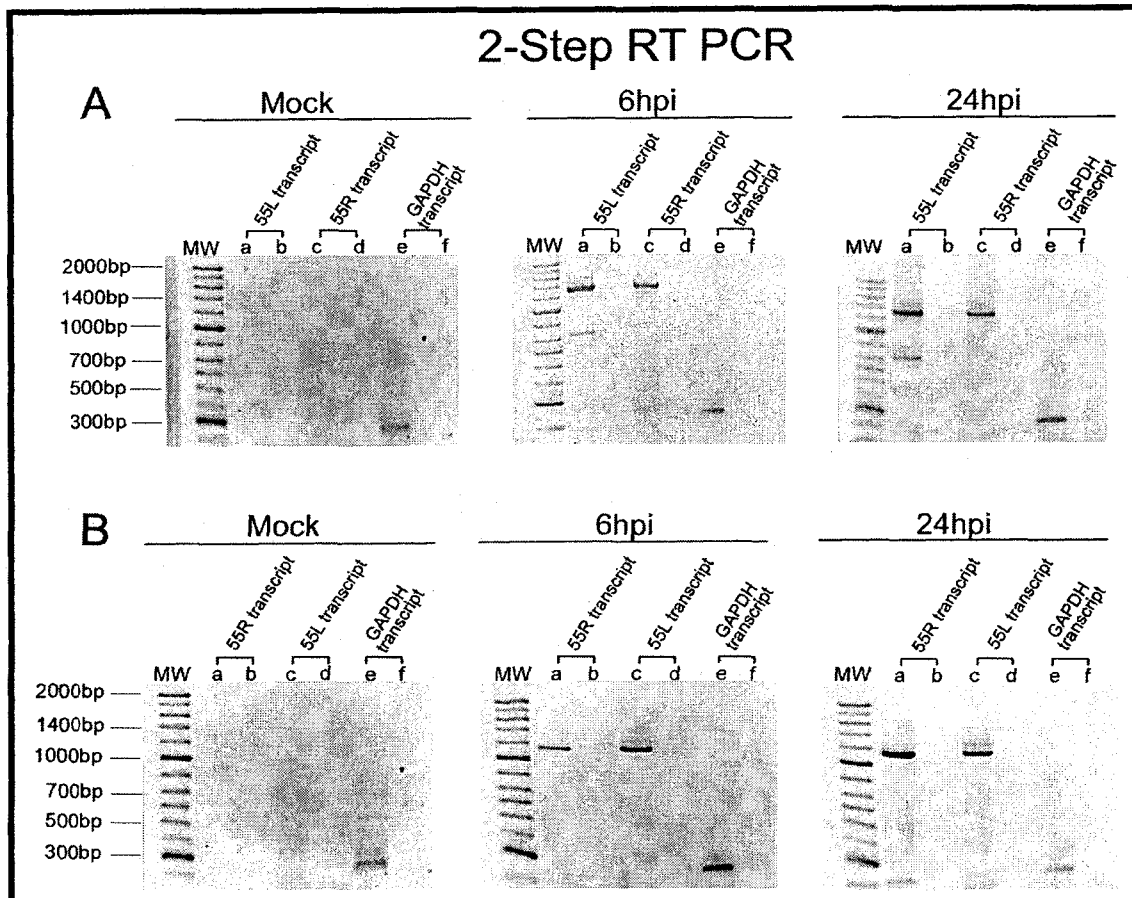


Figure 13.

Agarose gel electrophoretic analysis of 2-Step RT-PCR amplifications of total RNAs extracted from FV3-infected FHM cells. Cells were infected with heat-inactivated FV3 at 50 pfu/ml for 4 hours and then superinfected with active FV3 at 100 pfu/ml for 6 hours. In both A and B gels, MW indicates DNA size ladder; e. GAP3 primer with reverse transcriptase. f. GAP3 primer without reverse transcriptase. A: a. *EcoRI*-3L primer with reverse transcriptase. b. *EcoRI*-3L without reverse transcriptase. c. *BamHI*-5L primer with reverse transcriptase. d. *BamHI*-5L without reverse transcriptase. B: a. *EcoRI*-3R primer with reverse transcriptase. b. *EcoRI*-3R primer without reverse transcriptase. c. *BamHI*-5R primer with reverse transcriptase. d. *BamHI*-5R primer without reverse transcriptase. 5 μ l of each PCR reaction was loaded on each well. Mock = Mock-infected cells. 6hpi = 6 hours post-infection. 24hpi = 24 hours post-infection. In A gels: *EcoRI*-3L primer RT-PCR resulted in amplification of 55L transcript in all lanes (a), while *BamHI*-5L resulted in amplification of 55R transcript in all lanes (c) with the expected 1300 bp fragment size. In B gels: *EcoRI*-3R primer RT-PCR resulted in amplification of 55R transcript in all lanes (a), while *BamHI*-5R resulted in amplification of 55L transcript in all lanes (c) with the expected 1200 bp fragment size. All lanes (e) showed amplification of 276 bp for GAPDH. All lanes (b), (d) and (f) showed no amplifications, confirming no DNA contamination.

this primer pair. This was also confirmed by Figure 13B using *EcoRI*-3R and *BamHI*-5R primer pairs, which amplified both 55R (Lanes a) and 55L (Lanes c) transcripts at 6 and 24 hpi with an expected 1200 bp fragment size respectively.

Temporal Classification of ORFs 55L and 55R Transcripts

In order to differentiate the temporal classes of these two ORFs, cycloheximide (CHX) or fluorophenylalanine (FPA) were added during FV3 infection. CHX is a protein synthesis inhibitor and will allow only immediate-early transcription of FV3 ORFs. CHX inhibits protein elongation, preventing viral protein synthesis and DNA replication that are essential for other temporal classes of viral transcripts to be produced [Willis *et al.*, 1977; Willis and Granoff, 1978]. FPA is a phenylalanine analogue that can inhibit protein function of those that contain phenylalanine at critical sites. This inhibitor will allow classification of delayed-early transcription of FV3 ORFs [Willis *et al.*, 1977]. As shown in Figure 14A and C, both ORFs were suggested to be immediate-early genes, since they were both amplified from cDNA obtained from CHX treated total RNAs. In ORF 55R CHX- treated transcript amplification, a 1300 bp expected fragment was shown in Figure 14A Lane (c) with *BamHI*-5L primer and a 1200 bp expected fragment in Figure 14C Lane (a) with *EcoRI*-3R primer. ORF 55L transcript was amplified as shown in Figure 14A Lane (a) using *EcoRI*-3L primer and Figure 14C Lane (c) using *BamHI*-5R primer with an expected fragment size of 1300 bp and 1200 bp respectively.

In FPA treated transcript amplifications, ORF 55L transcript was amplified with primer *EcoRI*-3L (Figure 14B, Lane a) and primer *BamHI*-5R (Figure 14D, Lane c) with the expected fragment size of 1300 bp and 1200 bp respectively. Additionally, there is also some non-specific primer bindings that resulted in non-specific amplification in Figure 14B, Lane (a). In FPA treated ORF 55R transcript amplifications, primer *BamHI*-5L (Figure 14B, Lane c) amplification did not show any result. It is not clear why this is not amplified, as this primer seems to work well in other amplifications. However, amplification using primer *EcoRI*-3R (Figure 14D, Lane a) did show an expected 1200 bp product. ORF 55L transcript was also amplified with *BamHI*-5R primer with the expected 1200 bp product (Figure 14D, Lane c).

Since FPA treatment classifies delayed-early transcripts in FV3 mRNA synthesis, it seems that these transcripts are more abundantly expressed later in the infectious cycle. This is evident by the stronger amplifications of the transcripts shown in Figure 14B and D. Taken together, these results confirmed that both genes are expressed at the RNA level and are immediate-early genes. The product size was limited by the primer pairs' annealing sites (*EcoRI*-3L and *BamHI*-5L - 1300 bp; *EcoRI*-3R and *BamHI*-5R - 1200 bp) relative to the DNA sequences of the 2 ORFs.

Are Both ORFs 55L and 55R Expressed at the Protein Level?

Expression of FV3 ORFs 55L and 55R Proteins

Since RT-PCR results revealed that both ORFs were transcribed, the next step was to assess if the proteins of these ORFs were also expressed, and to assay the potential protein functions of ORF 55L and ORF 55R. Both

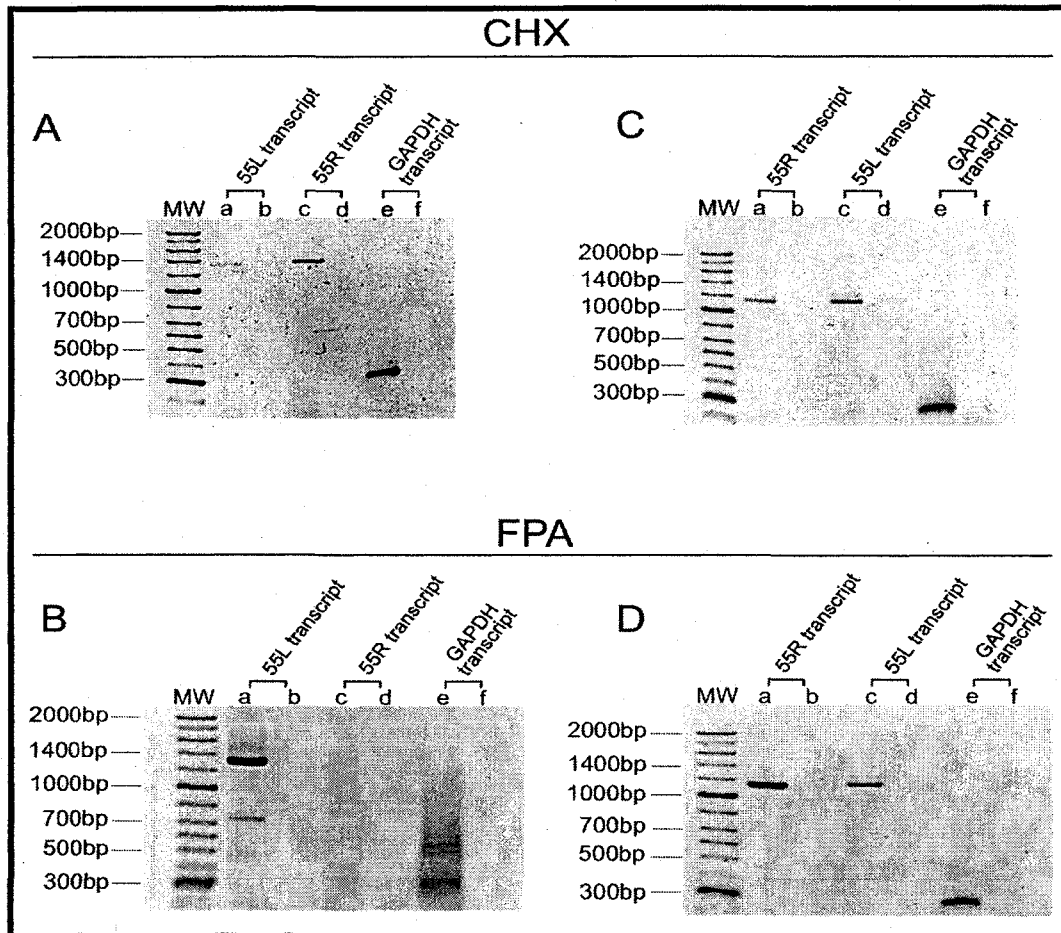


Figure 14.

Agarose gel electrophoretic analysis of RT-PCR amplifications of total RNAs extracted from FV3-infected FHM cells treated with cycloheximide (CHX, 10 $\mu\text{g/ml}$) and fluorophenylalanine (FPA, 100 $\mu\text{g/ml}$). In all gels, MW indicates DNA size ladder; e. GAP3 primer with reverse transcriptase. f. GAP3 primer without reverse transcriptase. A and B: a. RT-PCR product of *EcoRI*-3L primer cDNA with reverse transcriptase. b. RT-PCR with *EcoRI*-3L primer without reverse transcriptase. c. RT-PCR product of *Bam*HI-5L primer cDNA with reverse transcriptase. d. RT-PCR with *Bam*HI-5L primer without reverse transcriptase. C and D: a. RT-PCR product of *EcoRI*-3R primer cDNA with reverse transcriptase. b. RT-PCR with *EcoRI*-3R primer without reverse transcriptase. c. RT-PCR product of *Bam*HI-5R primer cDNA with reverse transcriptase. d. RT-PCR with *Bam*HI-5R primer without reverse transcriptase. 5 μl of each PCR reaction was loaded on each well. In both A and B gels: All lanes (a) resulted in 55L transcript (1300 bp) amplification with *EcoRI*-3L primer while in all lanes (c), 55R transcript was amplified with *Bam*HI-5L primer. In C and D gels: All lanes (a) resulted in 55R transcript (1200 bp) amplification with *EcoRI*-3R primer while in all lanes (c), 55L transcript was amplified with *Bam*HI-5R primer. All lanes (e) are amplifications of the GAPDH (276 bp) positive control and all lanes (b), (d) and (f) are negative controls without reverse transcriptase PCR.

genes were cloned into pFastBac baculovirus vector for protein expression in Sf-21 or Hi-5 cells. The recombinant proteins were cloned with a myc epitope and hexa-histidine tag, and a eGFP cassette for direct detection of recombinant virus with UV light microscopy, and protein via Western blot respectively. Recombinant baculovirus containing the cloned FV3-55L or FV3-55R genes can be easily identified under UV microscope for glowing green plaques (expression of eGFP), as seen in Figure 15.

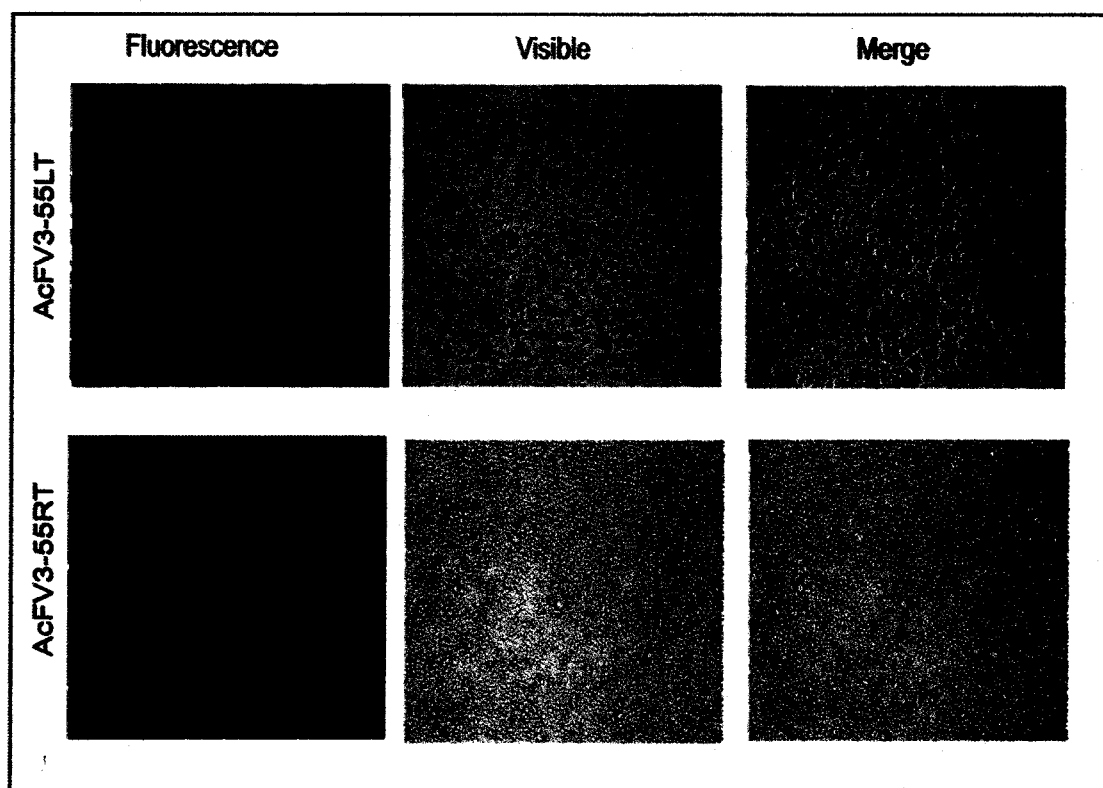


Figure 15.

UV fluorescent microscopy of recombinant baculovirus infected Sf-21 cells. Virus particles expressing eGFP and the cloned FV3-55L and 55R can be visualized under UV microscope. Left panels showed recombinant virus particles under UV fluorescence. Middle panels showed the same under visible light and the right panels are a composite of both UV and visible light microscopic images.

A time course assay of the expression of the recombinant proteins was assessed by lysing the infected cells and performing Western blot analysis (Figure 16). The recombinant proteins were detected by using Western blot with penta anti-penta-his antibody against the hexa-histidine tag of the recombinant proteins and goat-anti-mouse IgG ($G\alpha M$ -HRP) horseradish conjugate. As shown in Figure 16, AcFV3-55L seems to be expressed better in Hi-5 cells than Sf-21. At 48-72 hpi, AcFV3-55L protein was detected at 47 kDa, which is the expected molecular weight of the protein. AcFV3-55R was better expressed in Sf-21 cells at 72-144 hpi, a 50 kDa and 45 kDa protein were detected. This protein was larger than the expected 40 kDa. However,

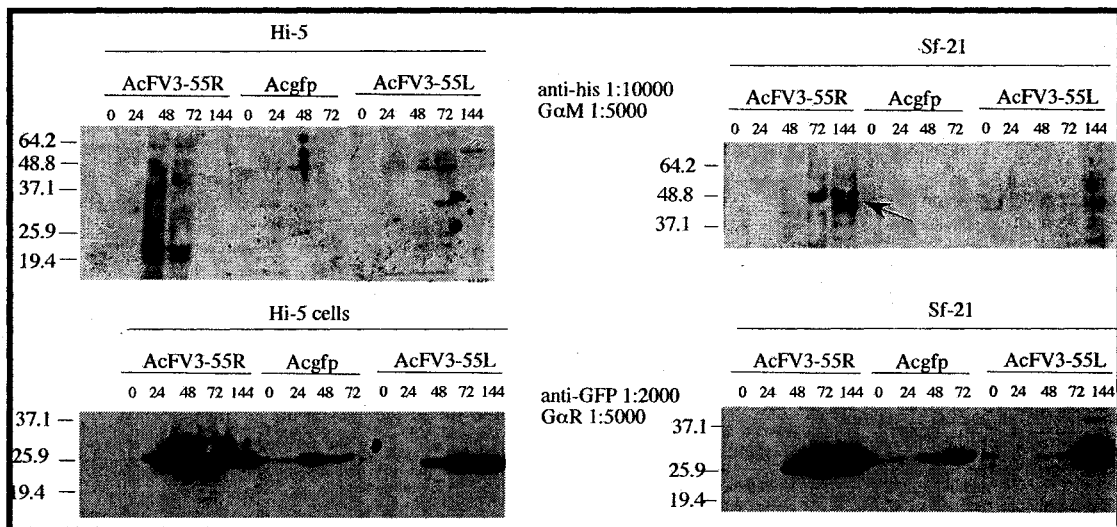


Figure 16.

Western Blot of AcFV3-55L and AcFV3-55R recombinant proteins. Anti-his 1:10000 antibody was used to detect recombinant AcFV3 55L and 55R proteins from Sf-21 and Hi-5 cells. AcFV3 55L was easily detected when expressed in Hi-5 cells whereas FV3 55R was detected in Sf-21 cells. AcFV3 55L showed a band of 47 kDa protein at 48 and 72 hpi, while AcFV3 55R was detected at 50 kDa and 45 kDa at 72 and 144 hpi. Acgfp was used as a negative control for penta anti-his antibody. Anti-gfp antibody was used to detect GFP protein as a positive control for detection of all expressed GFP proteins on the Western Blot.

the molecular size estimations were based on the protein molecular weight marker ran along with the samples. Expressed recombinant proteins were purified using a magnesium resin TALONspin column (Clontech) that has an affinity for the hexa-histidine tag and was also detected using Western Blot analysis.

P
=

Helicase Assays of Recombinant ORFs 55L and 55R proteins

Purified recombinant 55L and 55R proteins were used for helicase assays using the same materials and methods used in the infected cell extracts helicase assays. In each 20 μ l reaction, 0.33, 1, and 3 μ l (10 fmol/ μ l) each of purified 55L and 55R recombinant proteins were used in separate reactions to detect unwinding activity of the single stranded ends duplex DNA. The assay was conducted with eluted 55L and 55R recombinant proteins and additionally, a 10-fold concentrated 55L purified recombinant protein was also used. Surprisingly, no helicase activity was detected in either protein assay. Instead, there was marked DNase activity as seen in Figure 17. It is not clear whether both proteins did possess nuclease activity or that they might have other helicase related functions, but require a co-factor or other viral encoded protein(s) to work in concert. Since the substrates had very long single stranded ends (5'-24mers; 3'-25mers), the residual bands near the area of the expected product band may be DNase digested double-stranded or digested, unwound single stranded DNA from the substrates.

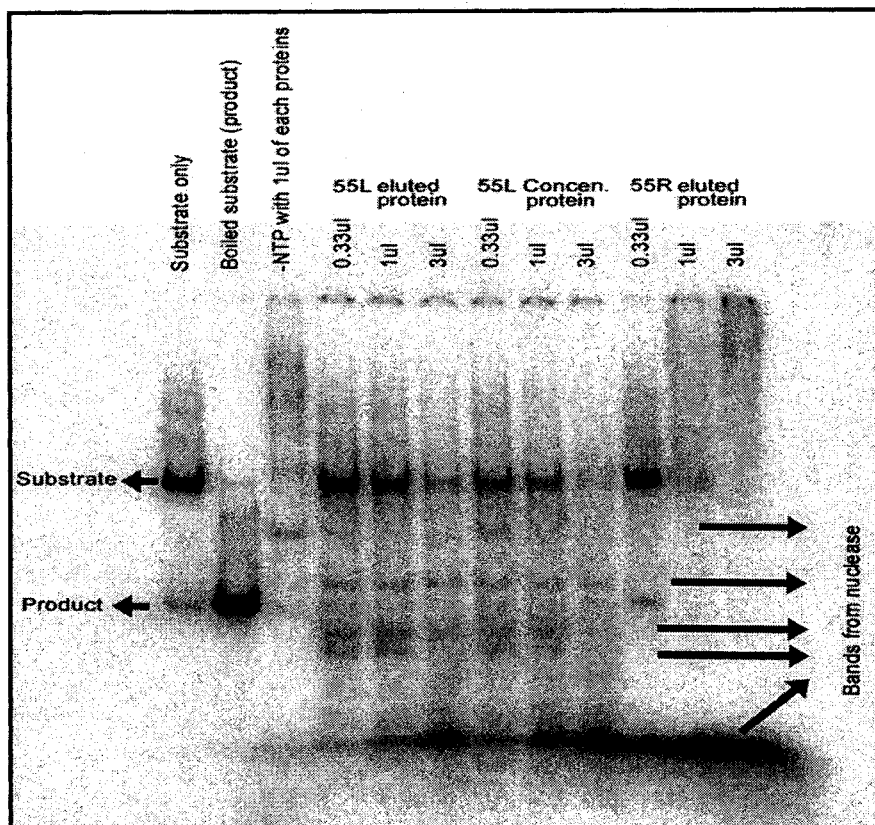


Figure 17

Helicase assay of purified recombinant FV3 55L and 55R proteins. Oligonucleotide substrates containing a stretch of 25 nucleotide duplex region and a 5'- 24mers single stranded (labeled with γ -32P) and 3'-25mers single stranded ends were incubated with 0.33, 1, and 3 μ l (10 fmol/ μ l) of each protein as indicated and measured for helicase activity. No helicase activity was detected. Instead, nuclease activities were detected from both FV3 55L and 55R purified recombinant proteins.

DNase Assay

To further determine the DNase activity of 55L and 55R proteins, circular plasmid pcDNA3.1myc-hisA (Invitrogen) DNAs were used for DNase activity assays for both proteins. The plasmid pcDNA3.1myc-hisA DNA was digested with XbaI and KpnI restriction enzymes to produce linearized DNA with single stranded ends. In each reaction, 100 ng of restriction enzyme

digested or undigested pcDNA3.1Amc-hisA DNAs was used with 3 μ l (10 fmol/ μ l) of 55L or 55R purified recombinant protein in reaction buffer with or without 5 mM dATP, and incubated at 30°C for 45 minutes. The reaction was stopped by adding 2 μ l of 5X loading buffer (1% SDS, 0.1% xylene cyanol, 0.1% bromophenol blue and 50% glycerol) and electrophoresed on a 1% agarose gel in TBE buffer.

The results showed that 55L protein has high DNase activity as both restriction enzyme digested and undigested plasmid DNAs were totally (lanes 5 & 6, cut plasmids) or partially (Lane 4, uncut plasmids) degraded with or without dATP (Figure 18) respectively. As for the 55R protein DNase assay, only the uncut plasmid (Lane 4, Figure 18) showed a small amount of degradation. Interestingly, the supercoiled plasmid DNA (Lane 4 band at 6000 bp, Figure 18) was converted to open circle plasmid DNA (Lane 4 band at 10000bp, Figure 18) with some degradation when compared to control uncut plasmid DNA (Lane 2). Whether this protein possessed an activity that can relax supercoiled DNA cannot be determined in this experimental condition. However, the linearized DNA (Lanes 5 & 6) was not totally degraded by the protein. It is not clear if there were any small amounts of cleavage as this experimental condition was not able to detect single nucleotide degradation. In this assay, it seems that 55R protein does not show any clear nuclease activity. This is contradictory to the pronounced nuclease activity shown in the helicase activity assay using oligonucleotide substrates (Figure 17). The difference between these two experiments is the substrates used. In the helicase activity assay (Figure 17), the oligonucleotide substrates have much longer single stranded ends (5'-24mers; 3'-25mers) and only a short duplex

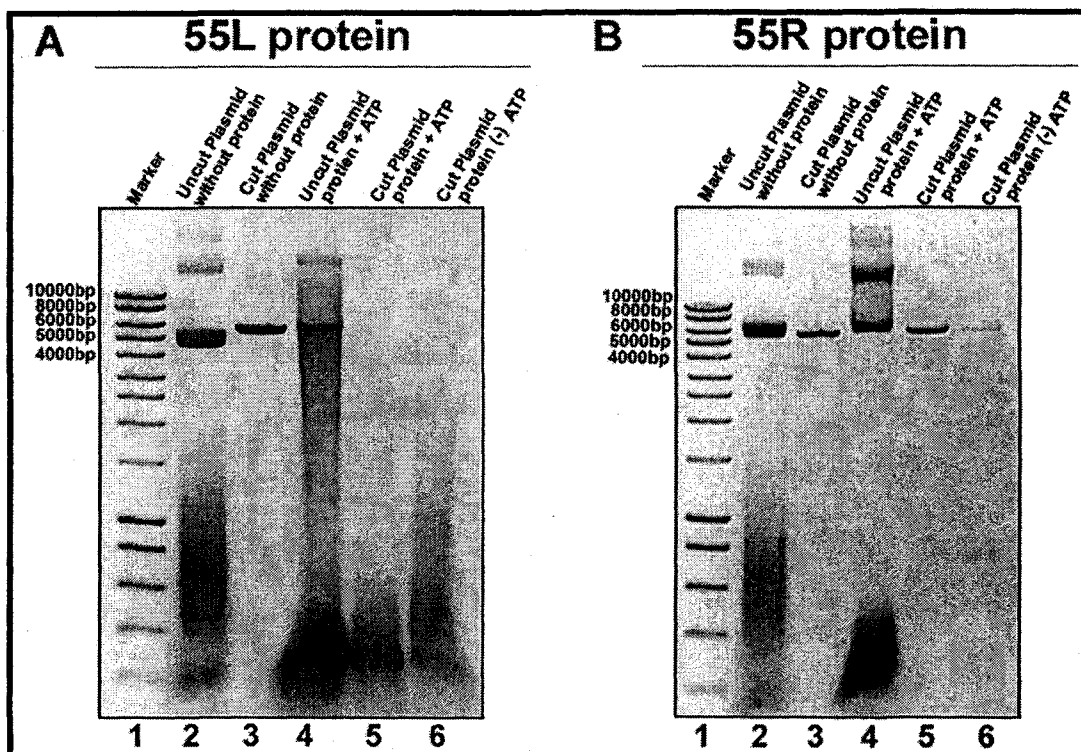


Figure 18

DNA nuclease activity assays of FV3 55L and 55R purified recombinant proteins with pCDNA3.1myc-hisA plasmid DNAs. 100ng of DNA was used for each reaction except Lane 6 on 55R was 50ng. Lane 1 on both gels are DNA molecular size markers. Lane 2 = undigested plasmid DNA in buffer; Lane 3 = XbaI and KpnI digested plasmid DNA in buffer; Lane 4 = undigested plasmid DNA with 5mM ATP and protein ; Lane 5 = XbaI and KpnI digested plasmid with 5mM ATP and protein; Lane 6 = XbaI and KpnI digested plasmid without ATP and protein. The nuclease activity was demonstrated on gel on the left for 55L protein.

region of 25mers in a 49mers or 50mers strand of hybridized DNAs. Whereas, the substrates used in the nuclease activity assay (Figure 18) were circularized plasmid DNAs of about 6 kbp and digested plasmid DNAs with only 4 nucleotides hanging ends, therefore they were not totally degraded.

From the results in the helicase assay with oligonucleotides and nuclease assay with plasmid DNA, there is a possibility that 55R protein may be an exonuclease which cleaves only single stranded ends of DNA.

Exonucleases are enzymatic proteins that function in proof-reading and excision repair, which cleaves single-stranded DNA during DNA replication. In vivo, nucleases cut the backbone of DNA, unless DNA is protected by bound proteins. It is possible that 55R may possess one of these functions, but because in this experimental system, other co-factors of DNA binding proteins such as single strand binding protein, DNA polymerase and free nucleotides are not present to play a concerted role in the DNA repair process, thereby causing a high degradation of the short oligonucleotide substrates in the helicase assay system (Figure 17).

Similar situations can be inferred about 55L protein. It seems that 55L protein possess both endonucleolytic and exonucleolytic activities. Although no clear helicase activity can be detected in these assays for 55L, there is a possibility that the nucleolytic activity may not be its only function. Helicases such as the human RecQ family are known to interact with a number of proteins such as replication protein A (RPA) [Cui *et al.*, 2004], EXO I [Doherty *et al.*, 2005], topoisomerase III α [Johnson *et al.*, 2000], and importin- α homologs [Seki *et al.*, 1997] involved in DNA metabolism. The human replication protein A - a single stranded binding protein was also shown to increase the processivity of human RecQ1 to unwind substrates greater than 100bp [Shen *et al.*, 1998b; Huang *et al.*, 1998; Suzuki *et al.*, 1999]. The RecQ group of proteins is commonly characterized by DNA helicases although an exception is the human RecQ4 [Yin *et al.*, 2004] which does not have any helicase activity. Also, the human helicase WRN which causes Werner syndrome characterized by premature aging was found to be both a helicase and an exonuclease residing on the same polypeptide [Shen *et*

al.,1998a; Huang *et al.*, 1998; Suzuki *et al.*, 1999]. WRN's exonuclease activity was also shown to be stimulated by Ku 70/80 heterodimers [Li and Comai, 2001; Li *et al.*, 2004]. Therefore, the lack of helicase activity in 55L protein could be due to the absence of some of these DNA binding proteins in the *in vitro* system to enhance its unwinding activity.

Additionally, different helicases from different organisms have been shown to have certain specificity for substrates. For example human RecQ1 was shown to fully unwind substrates with a 17 nucleotide duplex region regardless of hanging tails at the 3' or 5' ends [Cui *et al.* [2003]. These researchers also demonstrated that when the substrate was increased to 33bp duplex region, it could not be unwound by RecQ1. However, RecQ1 was also able to unwind blunt-ended substrate with a 25 nucleotide 'bubble' in the middle. Human RecQ1 was also shown to only unwind substrates that have a single stranded 3' end longer than 10 nucleotides [Cui *et al.*, 2003]. Therefore, another reason for the lack of helicase activity in 55L protein could be also due to substrate specificity.

For future experiments, one factor to consider is to test for substrate specificity of ORF 55L protein for possible helicase activity with various constructs of substrates. Other studies could be done with protein co-factors involved in DNA metabolism with the purified 55L protein to better characterize its function and whether it works in concert with other viral encoded or cellular protein co-factors in DNA metabolism. In addition, the nucleolytic activity of 55L could also play a role in viral defense mechanisms via restriction modification and to restrict foreign or cellular DNA in order to inhibit cellular DNA, RNA and protein syntheses by destroying cellular DNAs.

DISCUSSION

Although iridoviruses have not yet been studied as intensively as other large DNA viruses, results obtained with FV3 have led to a better understanding of transcription and translational control mechanisms in eukaryotes. For example, FV3 is a particularly good model in which to examine the impact of methylation on gene transcription since host RNA polymerase II, in association with one or more virus-induced proteins, has been shown to transcribe the highly methylated viral genome. The molecular mechanisms involved in this process are of significant biological and medical importance since one of the first steps along the neoplastic pathway involves transcription of oncogenes silenced by methylation. Thus, determination of the genomic sequence of FV3 provides the blueprint needed to elucidate these and other important steps in eukaryotic biology. The sequential expression and regulation of FV3 genes is a great example of gene expression and regulation in eukaryotic systems. Since many of the ORFs were conceptionally translated using computer aided analyses in this study, many more molecular based studies can be conducted based on the results of this research. The discovery of overlapping reading frames in Ranavirus is a novel one from this research. With more cloning and protein function assays, it is very likely that more overlapping reading frames will be found in FV3 genome or other iridovirus genomes. Although protein functions of FV3 55R cannot be clearly demonstrated under these experimental conditions, the DNase activity exhibited by FV3 55L was demonstrated. It is possible that

this protein might have some DNA unwinding helicase-like and exonucleolytic activities, but that the helicase-like activity may require one or more viral encoded or cellular co-factors to stimulate its reaction or that this protein requires specific substrates for its helicase activity.

In summary, the genomic sequence of FV3 elucidated in this study provides the basis for more important studies in the future, especially to elucidate protein functions that might have some implications with host-virus immuno-modulatory functions, or studies of proteins that might have similar activities with human proteins that cause debilitating and degenerating diseases.

Appendix A
List of FV3 ORFs

List of FV3 ORFs

FV3 ORF ^a	Start/Stop	AA ^b	kDa ^c	IP ^d	Predicted functions/ conserved domain	Best match					TFV	LCDV1	ISKNV	CIV
						Species	Accession no. ^e	BLASTP score	% Id ^f	Length (AA)	ORF ^g	ORF ^h	ORF ⁱ	ORF ^j
1R	272-1042	256	29.7	9.42	Replication factor and/or DNA packing protein; SP	LCDV1	NP078747	147	42	162	-	162L	061L	282R
2L	2611-1649	320	34.6	8.81	Myristylated membrane protein, DUF230 poxvirus protein of unknown function; TM	LCDV1	NP078745	191	37	21	2L	160L	-	337L
3R	3418-4734	438	48.3	6.40	IIV6 ORF229L; SP	IIV6	NP149692	51	22	256	4R	-	-	229L
4R	4775-4957	60	6.5	9.15	TM						5R	-	-	-
5R	5390-6004	204	23.4	4.28	FPV ORF250; US22 herpesvirus early nuclear protein; SP	FPV	Pfam02393	73	34	122	6R	-	-	-
6R ^k	6007-6234	75	8.8	5.39	SP						-	-	-	-
7R ^k	7025-7411	128	13.7	11.97	SP						-	-	-	-
8R	7503-11,384	1293	140.8	6.18	DNA-dependent RNA polymerase largest subunit; SP	TFV	AAL77794 Pfam04997	2,609	99	1,293	8R	016L	028L	176R
9L	14,599-11,753	948	106.4	8.99	NTPase, SNF2 family, N- terminal, Helicases C- terminal, DEAD/H Helicases; SP	TFV	AF389451 Pfam00176 Pfam00271	4,747	98	948	9L	132L	63L	022L
10R	14,615-15,028	137	14.9	9.56	TM						10R	-	-	-
11R	15,378-15,590	70	7.9	4.61	TM						11R	-	-	-
12L	16,549-15,656	297	32.7	8.02	Unknown protein; SP	LCDV1	NP078701	112	31	236	12L	108L	096L	287R
13R ^k	17,090-17,296	68	7.5	5.21	SP						-	-	-	-
14R	17,311-17,670	119	13.4	4.83	Unknown protein; SP	LCDV1	NP078646	38	27	95	15R	042L	-	-
15R	17,766-18,734	322	36.1	5.03	AAA-ATPase, poxvirus A32 Protein; SP	TFV	AF389451 Pfam04665	630	97	322	16R	054R	122R	075L
16R	19,014-19,841	275	30.0	11.59	Integrase homologue; SP	FV3	P29164	568	100	275	17R	-	-	-
17L	21,590-20,082	502	53.5	6.09	SP						18L	-	-	-
18L ^k	21,864-21,628	78	8.3	5.49	TM						-	-	-	-
19R	21,916-24,471	851	92.9	9.89	Conserved uncharacterized Protein; SP	LCDV1	NP078619	186	28	538	20R	10L	-	380R
20R	24,519-24,965	148	16.0	9.11	Unknown protein; TM	LCDV1	NP078769	58	44	75	21L	194R	-	117L
21L	25,861-25,202	219	25.4	4.62	ORF56L; SP	ISKNV	AF371960	118	42	131	-	-	056R	067R
22R	25,991-28,913	973	108.7	6.80	D5 family NTPase, ATPase; SP	LCDV1	NP078717 COG3378	577	36	975	22R	128L	109L	184R
23R	29,290-30,438	382	42.5	6.45	SP						23R	-	-	-
24R	30,821-31,918	365	41.0	6.44	SP						24R	-	-	-
25R	32,112-32,900	262	29.6	5.34	P31K protein; SP	FV3	CAA37177	515	99	262	25R	122R	-	-
26R	32,967-33,197	78	8.0	9.16	eIF-2 α homologue; SP	FV3	AF131072	127	86	71	26R	-	-	-

List of FV3 ORFs (Continued)

FV3 ORF ^a	Start/Stop	AA ^b	kDa ^c	IP ^d	Predicted functions/ conserved domain	Best match					TFV	LCDV1	ISKNV	CIV
						Species	Accession no. ^e	BLASTP score	% Id ^f	Length (AA)	ORF ^g	ORF ^h	ORF ⁱ	ORF ^j
27R	33,728-36,640	970	107.2	8.82	Tyrosine kinase, CAP 10, putative lypopolysaccharide modifying enzyme; SP	TFV	AAL77799 Smart0672	1,972	97	970	29R	195R	-	179R
28R	36,689-37,177	162	18.2	9.00	Unknown protein; SP	LCDV1	NP078685	61	33	84	30R	90R	-	-
29L	37,652-37,356	98	11.3	11.50	SP						31L	-	-	-
30R ^k	37,854-38,006	50	6.0	11.32	TM						-	-	-	-
31R	38,068-38,487	139	15.2	6.76	SP						32R	-	-	-
32R	38,537-40,426	629	70.0	9.96	Neurofilament triplet H1 Protein; SP	Rabbit	A43427	102	25	474	33R	-	-	-
33R	40,509-40,700	63	6.6	9.22	Unknown protein; TM	LCDV1	NP078706	40	39	41	34R	113L	-	308L
34R	40,844-41,164	106	11.4	6.68	Human parainfluenza virus 1 L protein; TM		AF117818	38	34	80	36R	-	-	-
35L	41,717-41,256	153	17.3	12.15	SP						37L	-	-	-
36L	42,353-41,370	207	22.7	10.80	SP						38L	-	-	-
37R	42,749-43,378	209	23.3	10.24	NIF/NLI interacting factor, p	LCDV1	NP078678	95	38	199	40R	082L	005L	355R
38R	43,519-45,216	565	62.4	8.77	Ribonucleoside diphosphate reductase alpha subunit; ribonucleoside reductase, barrel Domain; SP	TFV	AAL77800 Pfam02867	1,132	98	555	41R	176R	-	85L
39R	45,322-45,672	116	12.7	9.80	Hydrolase of the metallo-beta-lactamase superfamily; SP	Archea	NP614059	34	38	58	42R	-	-	-
40R	45,761-46,309	182	19.6	9.69	TM						43R	-	-	-
41R	46,691-50,188	1165	129.0	9.02	RRV orf-2 like protein; SP	RRV	AAK37740	2,303	97	1,165	45R	163R	076L	295L
42L ^k	50,941-50,864	85	9.4	9.74	SP						-	-	-	-
43R ^k	50,940-51,455	171	19.3	6.09	TM						-	-	-	-
44R ^k	51,476-51,661	61	7.0	12.31	SP						-	-	-	-
45L	52,348-51,938	136	15.6	5.63	LCDV1 Orf-88 like protein; SP	RRV	AAK54494	254	98	128	47L	36R	-	-
46L	52,968-52,723	114	8.6	12.78	Neurofilament triplet H1-like Protein; SP	RRV	AAK54495	119	81	78	48L	-	-	-
47L	53,509-53,093	138	15.5	7.24	SP						49L	-	-	-
48L	53,763-53,512	83	9.6	7.16	SP						50L	-	-	-
49L	54,621-53,872	249	27.4	6.16	LCDV1 Orf58-like protein, SAP DNA binding domain; SP	RRV	AAK54496 Pfam02037	324	86	194	51L	110L	-	-
50L	55,459-54,770	229	22.4	4.76	SP						52L	-	-	-
51R	55,539-57,224	561	61.7	5.41	Unknown; SP	LCDV1	NP078649	75	24	487	53R	48R	-	-
52L	58,548-57,481	355	39.3	8.95	3-beta-hydroxy-delta 5-C27 steroid oxidoreductase-like protein; TM	TFV	AAI77802	727	99	355	54L	153L	-	-

List of FV3 ORFs (Continued)

FV3 ORF ^a	Start/Stop	AA ^b	kDa ^c	IP ^d	Predicted functions/ conserved domain	Best match					TFV	LCDV1	ISKNV	CIV
						Species	Accession no. ^e	BLASTP score	% Id ^f	Length (AA)	ORF ^g	ORF ^h	ORF ⁱ	ORF ^j
53R	58,886-60,454	522	54.7	6.38	LCDV1 orf-20 like protein; SP	RRV	AAk54492	1,010	97	523	55R	67L	007L	118L
54L ^k	60,899-60,669	76	8.8	11.06	Nuclear calmodulin-binding Protein; SP	Gallus gallus	AAC69888	31	34	56	-	-	-	-
55L	62,232-60,937	431	47.6	6.82	Helicase-like protein; SP	TFV	AAL77803	869	98	431	56L	-	-	161L
55R	61,082-62,221	379	40.1	10.30	FV3 40 kDa protein; SP	FV3	X82828	794	100	379	56L	-	-	-
56R	62,320-62,757	145	17.0	11.51	SP						58R	-	-	-
57R	62,871-64,367	498	53.6	6.35	Phosphotransferase, S_TKc, Serine/Threonine protein Kinases; SP	LCDV1	NP078729 Smart00220	128	23	473	59R	143L	013R	-
58R	64,692-65,405	237	26.3	11.86	SP						61R	-	-	-
59L	67,014-65,956	352	39.8	9.25	RGV 9807 unknown protein; SP	RGV	AAL13097	721	99	352	62L	-	-	-
60R	67176-70217	1013	115.0	8.66	DNA polymerase like protein; DNA Polymerase, family B exonuclease; SP	TFV	AAL77804 Pfam03104	2,028	99	1,013	63R	135R	019R	037L
61L ^k	70408-70226	60	7.0	9.40	SP						-	-	-	-
62L	74516-70851	1221	133.0	8.88	DNA-directed RNA polymerase II second largest subunit-like protein, RNA polymerase domain 6, 7, 3, 2 beta subunit; SP	TFV	AAL77805 Pfam00562 Pfam04563 Pfam04560	2,443	98	1,227	65L	025L	034R	428L
63R	74895-75389	164	17.4	6.49	dUTPase-like protein; SP	TFV	AAL77806	322	98	164	68R	-	-	438L
64R ^k	75529-75816	95	10.4	6.57	Interleukin-1 beta convertase precursor; CARD, Caspase-recruitment domain/DEATH; SP	Horse	Q9TV13 Pfam00619	59	36	85	-	-	-	-
65L ^k	76373-76209	54	4.9	4.01	SP						-	-	-	-
66L ^k	76921-76370	183	20.3	9.08	SP						-	-	-	-
67L	78139-76976	387	43.9	4.99	Ribonucleoside- reductase diphosphate beta subunit- like protein; SP	TFV	AAL77807 Pfam00268 COG0208	785	98	387	71L	027R	024R	376L
68R	78422-78709	95	10.3	6.54	SP						72R	-	-	-
69R	78845-79111	88	9.3	8.56	Unknown protein; TM	LCDV1	NP078755	33	26	69	74R	172L	-	-
70R	79129-79503	124	13.4	10.80	SP						75R	-	-	-
71R	79543-79776	77	8.3	4.29	SP						76R	-	-	-
72L	80549-79833	238	26.0	10.30	SP						77L	-	-	-
73L	81971-80997	212	24.0	6.35	NTPase/helicase-like protein; SP	TFV	AAL77808	650	95	324	78L	107R	-	-
74L	83258-82146	370	39.2	11.50	SP						79L	-	-	-

List of FV3 ORFs (Continued)

FV3 ORF ^a	Start/Stop	AA ^b	kDa ^c	IP ^d	Predicted functions/ conserved domain	Best match					TFV	LCDV1	ISKNV	CIV
						Species	Accession no. ^e	BLASTP score	% Id ^f	Length (AA)	ORF ^g	ORF ^h	ORF ⁱ	ORF ^j
75L	83544-83290	84	9.2	7.24	LITAF, PIG7, possible membrane associated motif in LPS- induced tumor necrosis alpha factor; TM		Smart00714				80L	-	-	-
76R	83607-83828	73	8.0	11.17	SP						81R	-	-	-
77L	84172-83825	115	12.8	10.01	LCDV Orf2-like protein; SP	RRV	AAK84402	237	96	115	82L	32R	-	-
78L	85395-84757	212	24.0	6.35	SP						83L	-	-	-
79R	85531-87249	572	63.6	9.29	ATPase-dependent protease; SP		COG1220				84R	-	-	-
80L	88987-87872	371	40.4	8.36	Ribonuclease-like protein; Ribonuclease III; SP	TFV	AAL77809 pfam00636	725	99	371	85L	137R	087R	142R
81R	89043-89321	92	10.5	9.26	Transcription elongation Factor SII; C2C2 zinc finger; SP	TFV	AAL77810	195	98	92	86R	171R	029L	349L
82R	89450-89923	157	17.7	5.23	Immediate early protein ICP-18; SP	FV3	AAA43825	325	100	157	87R	-	-	-
83R	90373-91017	214	24.7	9.41	Cytosine DNA methyl-Transferase; SP	FV3	AAA86859	455	100	214	89R	005L	046L	-
84R	91389-92126	245	26.0	8.60	Proliferating cell nuclear antigen; SP	LCDV1	NP078615	77	24	246	090R	003L	112R	436L
85R	92201-92788	195	22.1	5.21	Deoxynucleoside kinase; SP	LCDV1	NP078725	119	41	168	-	136R	032R	143R
86L	93363-93178	61	6.80	8.50	SP						092L	-	-	-
87L	95533-93716	605	65.4	10.21	Unknown protein; SP	LCDV1	NP078643	69	28	200	93L	39R	-	-
88R	95566-96018	150	16.5	9.91	Evr1_Air-augmenter of liver regeneration; SP	ISKNV	AAL98767 pfam04777	88	43	113	94R	081R	043L	347L
89R	96086-97252	388	44.2	9.74	SP						95R	-	-	-
90R	97345-98736	463	49.9	5.68	Major capsid protein; SP	FV3	Q67473	927	100	463	96R	147L	006L	274L
91R	98860-10047	395	45.5	5.47	Immediate early protein ICP-46; SP	FV3	P14358	765	94	401	97R	047L	-	393L
92R	100398-100637	79	8.90	9.97	SP						98R	-	-	-
93L	100986-100819	55	5.7	3.78	SP						99L	-	-	-
94L	101563-101096	155	17.8	9.62	P8.141C; TM	RRV	AAK53746	304	94	155	100R	019R	086L	307L
95R	101656-102747	363	40.6	7.43	DNA repair protein RAD2, Xeroderma pigmentosum G N-region; Helix-hairpin- Helix, Class 2 (Pol I) family; SP	TFV	AAL77816 Smart00485 Smart00279	724	96	363	101R	191R	027L	369L
96R	103549-104220	223	24.3	4.84	Unknown protein; SP	LCDV1	NP078768	57	25	229	103R	193L	-	-
97R	104303-104716	137	15.3	4.94	Myeloid cell leukemia protein, MCL-1; TM	Gallus gallus	AAD31644	33	31	59	104R	-	-	-
98R ^k	105482-105682	67	7.8	12.49	SP						-	-	-	-

List of FV3 ORFs (*Continued*)

Legends

Note: SP, secretory protein; TM, Transmembrane domain; LCDV-1, lymphocystis disease virus 1; ISKNV, infectious spleen and kidney necrosis virus; FPV, fowlpox virus; EHNV, epizootic haematopoietic necrosis virus. Dash (-) mark denotes no corresponding homologous ORF in the genome.

a denotes common ORFs among FV3, TFV, LCDV-1, ISKNV and CIV

ORFs are numbered and begin from the left end (from *Hind*III "E") of the genome. Direction of transcription is indicated by left "L" for anti-sense strand and right "R" for sense strand of the DNA.

b AA - Number of amino acids of each FV3 putative protein.

c kDa - Molecular mass of each protein as predicted by MacVector 7.0.

d IP - Isoelectric points of each protein calculated by MacVector 7.0.

e Accession numbers, NCBI RPS-BLAST protein database reference numbers.

f Percentage of amino acid identity based on BLASTP analysis

g Best matched ORF from the tiger frog virus (TFV) genome

h Best matched ORF from the lymphocystis disease virus 1 (LCDV-1) genome, indicated ORF numbers are from Tidona and Darai (1997).

i Best matched ORF from the infectious spleen and kidney necrosis virus (ISKNV) genome

j Best matched ORF from the Chilo iridescent virus (CIV) genome

k FV3 unique ORFs not present in other iridoviruses

Appendix B
Radiation Safety Compliance

Radiation Safety Committee



Kalamazoo, Michigan 49008-5116
616 387-5933 or 616 387-6298
FAX: 616 387-5888

WESTERN MICHIGAN UNIVERSITY

February 23, 2006

To whom it may concern:

This letter is to inform you that Ms. Wendy Guat Hoon Tan, while completing her doctoral program, was fully qualified in accordance with Western Michigan University's policies and procedures for use of radioactive material. Ms. Tan's conduct during her use of radioactive material was above reproach.

If you have any questions concerning her use of radioactive materials or require specific examples of the isotopes and how she used them, please feel free to contact me at 269-387-5933

Respectfully,

A handwritten signature in black ink, appearing to read "J. F. Center".

J. F. Center
Radiation Safety Officer
Western Michigan University

Appendix C
Recombinant DNA Biosafety Approval

Recombinant DNA Biosafety Committee**Project Approval Certification****For rDNA Biosafety Committee Use Only**

Project Title: Expression of Tanapox Virus and Frog Virus 3 proteins

Principal Investigator: Karim Essani

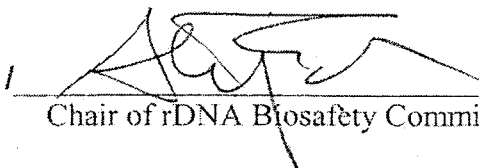
IBC Project Number: 05-KEa

Date Received by the rDNA Biosafety Committee: 10/1/05

Reviewed by the rDNA Biosafety Committee

Approved

Approval not required



Chair of rDNA Biosafety Committee Signature

12/1/05

Date

Revised 5/02 WMU RDBC
All other copies obsolete

BIBLIOGRAPHY

- Adesnik, M., and Darnell, J. E. (1972). Biogenesis and characterization of histone messenger RNA in HeLa cells. *J. Mol. Biol.* 67, 397-406.
- Ahne, W., Sckitfekdt, H. J., and Thomsen, I. (1989). Fish viruses: Isolation of an icosahedral cytoplasmic deoxyribovirus from sheatfish (*Silurus glanis*). *J. Vet. Med. B.* 36, 333-336.
- Altschul, S. F., Madden, T. L., Schäffer, A. A., Zhang, J., Zhang, Z., Miller, W., and Lipman, D. J. (1997). Gapped BLAST and PSI-BLAST: a new generation of protein database search programs. *Nucleic Acids Res.* 25, 3389-3402.
- Aubertin, A. M., Hirth, C., Travo, C., Nonnenmacha, H., and Kirn, A. (1973). Preparation and properties of an inhibitory extract from frog virus 3 particles. *J. Virol.* 11, 694-701.
- Aubertin, A. M., Travo, C., and Kirn, A. (1976). Proteins solubilized from frog virus 3 particles: effect on transcription. *J. Virol.* 18, 34-41.
- Aubertin, A. M., Tondre, L., Lopez, C., Obert, G., and Kirn, A. (1983). Sodium dodecyl sulfate-mediated transfer of electrophoretically separated DNA-binding proteins. *Analytical Biochemistry.* 131, 127-134.
- Becker, A., and Murialdo, H. (1978). Head morphogenesis of complex double-stranded DNA bacteriophages. *Microbiology.* 42, 529-576.
- Beckman, W., Tham, T. N., Aubertin, A. M., and Willis, D. B. (1988). Structure and regulation of the immediate-early frog virus 3 gene that encodes ICR489. *J. Virol.* 62, 1271-1277.
- Berry, E. S., Shea, T. B., and Gablik, J. (1983). Two iridovirus isolates from *Carassium auratus*. *J. Fish Dis.* 6, 501-510.
- Bigot, Y., Stasiak, K., Rouleux-Bonnin, F., and Federici, B. A. (2000). Characterization of repetitive DNA regions and methylated DNA in ascovirus genomes. *J. Gen. Virol.* 81, 3073-3082.
- Braunwald, J., Tripier, F., and Kirn, A. (1979). Comparison of the properties of enveloped and naked frog virus 3 (FV3) particles. *J. Gen. Virol.* 45, 673-682.

- Braunwald, J., Nonnenmacher, H., and Tripier-Darcy, F. (1985). Ultrastructural and biochemical study of frog Virus 3 uptake by BHK-21 cells. *J. Gen. Virol.* 66, 283-293.
- Campadelli-Fuime, G., Costanzo, F., Fao-Tomasi, L., and LaPlaca, M. (1975). Modification of cellular RNA polymerase II after infection with frog virus 3. *J. Gen. Virol.* 27, 341-394.
- Cassetti, M. C., Merchlinsky, M., Wolffe, E. J., Weisberg, A. S., and Moss, B. (1998). DNA packaging mutant: repression of the vaccinia virus A32 gene results in noninfectious, DNA-deficient, spherical, enveloped particles. *J. Virol.* 72, 5769-5780.
- Chinchar, V. G. (2002). Ranaviruses (family Iridoviridae): emerging cold-blooded killers. *Arch. Virol.* 147, 447-470.
- Cordier, O., Aubertin, A. M., Lopez, C., and Tondre, L. (1981). Inhibition de la transduction par le FV3: Action des proteines virales de structure solubilisees sur la synthesis proteique in vivo et in vitro. *Ann. Virol. Inst. Pasteur.* 132E, 25-39.
- Cui, S., Klima, R., Ochem, A., Arosio, D., and Falaschi, A. (2003). Characterization of the DNA-unwinding activity of human RecQ1, a helicase specifically stimulated by human replication protein A. *J. Biol. Chem.* 278, 1424-1432.
- Cui, S., Arosio, D., Doherty, K. M., Brosh, R. M. Jr., Falaschi, A., and Vindigni, A. (2004). Analysis of the unwinding activity of the dimeric RECQ1 helicase in the presence of human replication protein A. *Nucleic Acids Res.* 32, 2158-2170.
- Darai, G., Anders, K., Koch, H.G., Delius, H., Gelderblom, H., Samalecos, C., and Flugel, R.M. (1983). Analysis of the genome of fish lymphocystis disease virus isolated directly from epidermal tumors of pleuronectes. *Virology.* 126, 466-479.
- Darai, G., Delius, H., Clarke, J., Apfel, H., Schnitzler, P., and Flugel, R. M. (1985). Molecular cloning and physical mapping of the genome of fish lymphocystis disease virus. *Virology.* 146, 292-301.
- Darcy-Tripier, F., Nermut, M. V., Braunwald, J., and William, L. D. (1984). The organization of frog virus 3 as revealed by freeze-etching. *Virology.* 138, 287-299.

- Delius, H., Darai, G., and Flugel, R.M. (1984). DNA analysis of insect iridescent virus 6: Evidence for circular permutation and terminal redundancy. *J. Virol.* 49, 609-614.
- Devauchelle, G. (1977). Ultrastructural characterization of an iridovirus from the marine worm *Nereis Diversicolor* (O. F. Müller). *Virology.* 81, 237-246.
- Dixon, L. K., Bristow, C., Wilkinson, P. J., and Sumption, K. J. (1990). Identification of a variable region of the African swine fever virus genome that has undergone separate DNA rearrangements leading to expansion of minisatellite-like sequences. *J. Mol. Biol.* 216, 677-688.
- Doherty, K. M., Sharma, S., Uzdilla, L. A., Wilson, T. M., Cui, S., Vindigni, A., and Brosh, R. M., Jr. (2005). RECQ1 helicase interacts with human mismatch repair factors that regulate genetic recombination. *J. Biol. Chem.* 280, 28085-28094.
- Drillien, R., Spehner, D., and Kirn, A. (1980). Inactivation of the toxicity of frog virus 3 proteins by UV irradiation. *FEMS Lett.* 7, 87-90.
- Dry, I. B., Krake, L. R., Rigden, J. E., and Rezaian, M. A. (1997). A novel subviral agent associated with a geminivirus: The first report of a DNA satellite. *Proc. Natl. Acad. Sci. USA.* 94, 7088-7093.
- Elliot, R. M., and Kelly, D. C. (1980). Frog virus 3 replication: Induction and Intracellular distribution of polypeptides in infected cells. *J. Virol.* 33, 28-51.
- England, P. R., Briscoe, D. A., and Frankham, R. (1996). Microsatellite polymorphisms in a wild population of *Drosophila melanogaster*. *Genet. Res.* 67, 285-290.
- Eisen, H., Pereira, Da Silva L. H., and Jacob, F. (1968). The regulation and mechanism of DNA synthesis in bacteriophage lambda. *Cold Spring Harbor Symp. Quant. Biol.* 33, 755-764.
- Essbauer, S., Bremont, M., and Ahne, W. (2001). Comparison of the eIF-2 α homologous proteins of seven Ranaviruses (Iridoviridae). *Virus Genes.* 347, 347-359.
- Fenner, F., and Woodroffe, G. M. (1960). The reactivation of poxviruses II. The range of reactivating viruses. *Virology.* 11, 185-201.
- Fischer, M., Schnitzler, P., Scholz, J., Rösen-Wolff, A., Delius, H., and Darai, G. (1988). DNA nucleotide sequence analysis of the PvuII DNA

- fragment L of the genome of insect iridescent virus type 6 reveals a complex cluster of multiple tandem, overlapping, and interdigitated repetitive DNA elements. *Virology*. 167, 497-506.
- Fujiwara, S., and Ono, Y. (1995). Repetitive sequence in the Epstein-barr Virus EBNA-3C gene is related to a family of minisatellite arrays in the human genome. (1995). *Virus Genes*. 11, 31-35.
- Gangloff, S., McDonald, J. P., Bendixen, C., Arthur, L., and Rothstein, R. (1994). The yeast type I topoisomerase Top3 interacts with Sgs1, a DNA helicase homolog: a potential eukaryotic reverse gyrase. *Molecular and Cellular Biology*. 14, 8391-8398.
- Gendrault, T. J., Steffan, A. M., Bingen, A. and Kirn, A. (1981). Penetration and uncoating of frog virus 3 (FV3) in cultured rat Kupffer cells. *Virology*. 112, 375-384.
- Gilbert, W., and Dressler, D. (1968). DNA replication: The rolling circle model. *Cold Spring Harbor Symp. Quant. Biol.* 33, 473-484.
- Goldstein, D. B., and Schlötterer, C. (1999). *Microsatellites. Evolution and applications.* Oxford University Press, Inc, New York.
- Goorha, R. (1981a). Frog virus 3 requires RNA polymerase II for its replication. *J. Virol.* 37, 496-499.
- Goorha, R. (1981b). DNA binding proteins in frog virus 3-infected cells. *J. Gen. Virol.* 56, 131-140
- Goorha, R. (1982). Frog virus 3 DNA replication occurs in two stages. *J. Virology*. 43, 519-528.
- Goorha, R., and Dixit, P. (1984). A temperature-sensitive (ts) mutant of frog virus 3 (FV3) is defective in second-stage DNA replication. *Virology*. 136, 186-195.
- Goorha, R., and Granoff, A. (1974a). Macromolecular synthesis in cells infected by frog virus 3. I. Virus-specific protein synthesis and its regulation. *Virology*. 60, 237-250.
- Goorha, R., and Granoff, A. (1974b). Macromolecular synthesis in cells infected by frog virus 3. II. Evidence for post-transcriptional control of a viral structural protein. *Virology*. 60, 251-259.

- Goorha, R., Granoff, A., Willis, D. B., and Murti, K. G. (1984). The role of DNA methylation in virus replication: Inhibition of frog virus 3 replication by 5-azacytidine. *Virology*. 138, 94-102.
- Goorha, R., Murti, G., Granoff, A., and Tirey, R. (1978). Macromolecular synthesis in cells infected by frog virus 3. VIII. The nucleus is a site of frog virus 3 DNA and RNA synthesis. *Virology*. 84, 32-50.
- Goorha, R., and Murti, K. G. (1982). The genome of frog virus 3, an animal DNA virus, is circularly permuted and terminally redundant. *Proc. Natl. Acad. Sci. USA*. 79, 248-262.
- Goorha, R., Willis, D. B., and Granoff, A. (1977). Macromolecular synthesis in cells infected by frog virus 3. VI. Frog virus 3 replication is dependent on the cell nucleus. *J. Virol.* 21, 802-805.
- Goorha, R., Willis, D. B., and Granoff, A. (1979). Macromolecular synthesis in cells infected by frog virus 3. XII. Viral regulating proteins in transcriptional and post-transcriptional controls. *J. Virol.* 32, 442-448.
- Gorbalenya, A. E., Koonin, E.V., Donchenko, A. P., and Blinov, V. M. (1988). A novel superfamily of nucleoside triphosphate-binding motif containing proteins which are probably involved in duplex unwinding in DNA and RNA replication and recombination. *FEBS Lett.* 235, 16-24.
- Gorbalenya, A. E., Koonin, E. V., Donchenko, A. P., and Blinov, V. M. (1989). Two related superfamilies of putative helicases involved in replication, recombination, repair and expression of DNA and RNA genomes. *Nucleic Acids Res.* 17, 4713-4730.
- Granoff, A. (1969). Viruses of amphibia. *Curr. Top. Microbiol. Immunol.* 50, 107-137.
- Granoff, A., Came, P. E., and Breeze, D. C. (1966). Viruses and renal carcinoma of *Rana pipiens*. *Virology*. 29, 133-148.
- Gravell, M., and Granoff, A. (1970). Viruses and renal adenocarcinoma of *Rana pipiens*. IX. The influence of temperature and host cell on replication of frog polyhedral cytoplasmic deoxyribovirus (PCDV). *Virology*. 41, 596-602.
- Gravell, M., and Naegele, R. F. (1970). Nongenetic reactivation of frog polyhedral cytoplasmic deoxyribovirus (PCDV). *Virology*. 40, 170-174.

- Gravell, M., and Cromeans, T. (1971). Mechanisms involved in the nongenetic reactivation of frog polyhedral cytoplasmic deoxyribovirus: Evidence for RNA polymerase in the virion. *Virology*. 46, 39-49.
- Guir, M., Braunwald, J., and Kirn, A. (1970). Inhibition de la synthèse du DNA et des RNA cellulaires dans les cellules KB infectées avec le virus 3 de la grenouille (FV3). *CR. Hebd. Acad. Ser Paris*. 270, 2605-2608.
- He, J. G., Zeng, K., Weng, S. P., and Chan, S. M. (2000). Systemic disease caused by iridovirus-like agent in cultured mandarin fish, *Siniperca chuatsi* (Basillewsky), in China. *J. Fish Dis*. 23, 219-222.
- He, J. G., Deng, M., Weng, S. P., Li, Z., Zhou, S. Y., Long, Q. X., Wang, X. Z. and Chan, S. M. (2001). Complete genome analysis of the mandarin fish infectious spleen and kidney necrosis iridovirus. *Virology*. 291, 126-139.
- He, J. G., Lu, L., Deng, M., He, H. H., Weng S. P., Wang, X. H., Zhou, S. Y., Long, Q. X., Wang, X. Z. and Chan, S. M. (2002). Sequence analysis of the complete genome of an iridovirus isolated from the tiger frog. *Virology*. 132, 185-197.
- Hedrick, R. P., McDowell, T. S., Anhe, W., Torhy, C., and de Kinkelin, P. (1992). Properties of three iridovirus-like agents associated with systemic infections of fish. *Dis. Aquat. Org*. 13, 203-209.
- Hengstberger, S. G., Hyatt, A. D., Speare, R., and Coupar, B. E. H. (1993). Comparison of Epizootic haematopoietic necrosis and Bohle iridoviruses, recently isolated Australian iridoviruses. *Dis. Aquat. Org*. 15, 93-107.
- Hofmann, K., and Stoffel, W. (1993). Tmbase – A database of membrane spanning protein segments. *Biol. Chem. Hoppe-Seyler*. 374, 166.
- Houts, G. E., Gravell, M., Darlington, R. W. (1970). Base composition and molecular weight of DNA from a frog polyhedral cytoplasmic deoxyribovirus. *Proc. Soc. Exp. Biol. Med*. 135, 232-236.
- Houts, G. E., Gravell, M., and Darlington, R. W. (1974). Electron microscopic observation of early events of frog virus 3 replication. *Virology*. 58, 587-594.
- Huang, S., Li, B., Gray, M.D., Oshima, J., Mian, I.S., and Campisi, J. (1998). The premature ageing syndrome protein, WRN, is a 3'→5' exonuclease. *Nature Genetics*. 20, 114-116.

- Jancovich, J. K., Mao, J., Chinchar, V. G., Wyatt, C., Case, S. T., Kumar, S., Valente, G., Subrmanian, S., Davidson, E. W., Collins, J. P., and Jacobs, B. L. (2003). Genomic sequence of a ranavirus (family Iridoviridae) associated with salamander mortalities in North America. *Virology*. 316, 90-103.
- Johnson, F. B., Lombard, D. B., Neff, N. F., Mastrangelo, M. A., Dewolf, W., Ellis, N. A., Marciniak, R. A., Yin, Y., Jaenisch, R., and Guarente, L. (2000). Association of the Bloom syndrome protein with topoisomerase IIIalpha in somatic and meiotic cells. *Cancer Res.* 60, 1162-1167.
- Karow, J. K., Wu, L., and Hickson, I. D. (2000). RecQ family helicases: roles in cancer and aging. *Curr. Opin. Genet. Dev.* 10, 32-38.
- Kashi, Y., King, D., and Soller, M. (1997). Simple sequence repeats as a source of quantitative genetic variation. *Trends Genet.* 13, 74-78.
- Kaur, K., Rohozinski, J., and Goorha, R. (1995). Identification and characterization of the frog virus 3 DNA methyltransferase gene. *J. Virol.* 76, 1937-1943.
- Kelly, D. C., Atkinson, M. A. (1975). Frog virus 3 replication: electron microscope observations on the terminal stages of infection in chronically infected cell cultures. *J. Gen. Virol.* 28, 391-407.
- Koonin, E. V., Senkevich, T. G., and Chernos, V. I. (1993). Gene A32 product of vaccinia virus may be an ATPase involved in viral DNA packaging as indicated by sequence comparisons with other putative viral ATPases. *Virus Genes.* 7, 89-94.
- Kucera, L. (1970). Effects of temperature on frog polyhedral cytoplasmic deoxyribovirus multiplication: Thermosensitivity of initiation, replication, encapsidation of viral DNA. *Virology.* 42, 576-581.
- Kunzler, P., Matsuo, K., and Schaffner, W. (1995). Pathological, physiological, and evolutionary aspects of short unstable DNA repeats in the human genome. *Biol. Chem. Hoppe Seyler.* 376, 201-211.
- Laurent, B. C., Treitel, M. A., and Carlson, M. (1991). Functional interdependence of the yeast SNF2, SNF5, and SNF6 proteins in transcriptional activation. *Proc. Natl. Acad. Sci. USA.* 1, 88:2687-2691.
- Lee, M. H., and Willis, D. B. (1983). Restriction endonuclease mapping of the frog virus 3 genome. *Virology.* 126, 317-327.

- Li, B., and Comai, L. (2001). Requirements for the nucleolytic processing of DNA ends by the Werner Syndrome protein-Ku70/80 complex. *J. Biol. Chem.* 276, 9896-9902.
- Li, B., Navarro, S., Kasahara, N., and Comai, L. (2004). Identification and biochemical characterization of a Werner's Syndrome protein complex with Ku70/80 and poly(ADP-ribose) polymerase-1. *J. Biol. Chem.* 279, 13659-13667.
- Luder, A., and Mosig, G. (1982). Alternate mechanism for initiation of DNA replication forks in bacteriophage T4-priming by RNA polymerase and by recombination. *Proc. Natl. Acad. Sci. USA.* 79, 101-1105.
- Maes, R., and Granoff, A. (1967). Viruses and renal carcinoma of *Rana pipiens*. IV. Nucleic acid synthesis in frog virus 3-infected BHK 21/13 cells. *Virology.* 33, 491-502.
- Maniatis, T., Fritsch, E. F., and Sambrook, J. (1982). *Molecular cloning. A Laboratory Manual.* Cold Spring Harbor Laboratory.
- Mao, J., Tham, T. N., Gentry, G. A., Aubertin, A., and Chinchar, V. G. (1996). Cloning, sequence analysis, and expression of the major capsid protein of the iridovirus frog virus 3. *Virology.* 216, 431-436.
- Marchler-Bauer, A., Anderson J. B., Cherukuri, P. F., DeWeese-Scott, C., Geer, L. Y., Gwadz, M., He, S., Hurwitz, D. I., Jackson, J. D., Ke, Z., Lanczycki, C.J., Liebert, C.A., Liu, C., Lu, F., Marchler, G. H., Mullokandov, M., Shoemaker, B. A., Simonyan, V., Song, J. S., Thiessen, P. A., Yamashita, R. A., Yin, J. J., Zhang, D., and Bryant, S. H. (2005). CDD: a Conserved Domain Database for protein classification. *Nucleic Acids Res.* 33, D192-196.
- Marschang, R. E., Becher, P., Postaus, H., Wild, P., and Thiel, H. J. (1999). Isolation and characterization of an iridovirus from Hermanns tortoises (*Testudo hermanni*). *Arch. Virol.* 144, 1909-1922.
- Matin, J. P., Aubertin, A. M., Lecerf, F., and Kirn, A. (1981). Intracellular distribution and phosphorylation of virus-induced polypeptides in frog virus 3-infected cells. *Virology.* 110, 349-365.
- Martin, J. P., Aubertin, A. M., Tondre, L., and Kirn, A. (1984). Fate of frog virus 3 DNA replicated in the nucleus of arginine-deprived CHO cells. *J. Gen. Virol.* 65, 721-732.
- McAuslan, B. R., and Smith, W. (1968). DNA synthesis in frog virus 3-infected mammalian cells. *J. Virol.* 2, 1006-1015.

- Meehan, R., Lewis, J., Cross, S., Nan, X., Jeppesen, P., and Bird, A. (1992). Transcriptional repression by methylation of CpG. *J. Cell Sci.* 16, 9-14.
- Miller, R. C. (1975). Replication and molecular recombination of T4 phage. *Ann. Rev. Microbiol.* 29, 355-376.
- Moura Nunes J. F., Vigario, J. D., and Terrinka, A. M. (1975). Ultrastructural study of African swine fever virus replications in cultures of swine bone marrow cells. *Arch. Virol.* 49, 59-66.
- Müller, K., Tidona, C., and Darai, G. (1999). Identification of a gene cluster within the genome of Chilo iridescent virus encoding enzymes involved in viral DNA replication and processing. *Virus Genes.* 18, 243-264.
- Munnes, M., Schetter, C., Holker, I., and Doerfler, W. (1995). A fully 5'-CG-3' but not a 5'-CCGG-3' methylated late frog virus 3 promoter retains activity. *J. Virol.* 69, 2240-2247.
- Murti, K. G. and Goorha, R. (1983). Interaction of frog virus 3 with the cytoskeleton. I. Altered organization of microtubules, intermediate filaments, and microfilaments. *J. Cell Biol.* 96, 1248-1257.
- Murti, K. G., Porter, K. R., Goorha, R., Ulrich, M., and Wray, G. (1984). Interaction of frog virus 3 with the cytoskeleton. 2. Structure and composition of the virus assembly site. *Exp. Cell Res.* 154, 270-282.
- Naegèle, R. F., Granoff, A., and Darlington, R. W. (1974). The presence of the Lucké herpesvirus genome in induced tadpole tumors and its oncogenicity: Koch-Henle postulates fulfilled. *Proc. Natl. Acad. Sci. USA.* 71, 830-834.
- Nakayama, K., Irino, N., and Nakayama, H. (1985). The recQ gene of *Escherichia coli*K12: molecular cloning and isolation of insertion mutants. *Mol. Gen. Genet.* 200, 266-271.
- Parsons, R. L., Prasad, P. V., Harshey, R. M., and Jayaram, M. (1988). Step-arrest mutants of FLP recombinase: implications for the catalytic mechanism of DNA recombination. *Mol. Cell. Biol.* 8, 3303-3310.
- Persson, B., and Argos, P. (1994). Prediction of transmembrane segments in proteins utilising multiple sequence alignments. *J. Mol. Biol.* 237, 182-192.
- Porter, K. R. and Tucker, J. B. (1981). The ground substance of the living cell. *Scientific American.* 244, 56-67.

- Purifoy, D., Naegele, R. F., and Granoff, A. (1973). Viruses and renal carcinoma of *Rana pipiens*. XIV. Temperature-sensitive mutants of frog virus 3 with defective encapsidation. *Virology*. 54, 525-535.
- Raghow, R., and Granoff, A. (1979). Macromolecular synthesis in cells infected by frog virus 3. X. Inhibition of cellular protein synthesis by heat-inactivated virus. *Virology*. 98, 319-327.
- Raghow, R., and Granoff, A. (1980). Macromolecular synthesis in cells infected by frog virus 3. XIV. Characterization of the methylated nucleotide sequences in viral messenger RNAs. *Virology*. 107, 283-294.
- Ramachandran, R., Hartmann, C., Song, H. K., Huber, R., and Bochtler M. (2002). Functional interactions of HsIV (ClpQ) with the ATPase HsIU (ClpY). *Proc. Natl. Acad. Sci. USA*. 28, 7396-401.
- Razin, A., and Cedar, H. (1991). DNA methylation and gene repression. *Microbiological Reviews*. 55, 451-458.
- Reading, P. C., Moore, J. B., and Smith, G. L. (2003). Steroid hormone synthesis by vaccinia virus suppresses the inflammatory response to infection. *J. Exp. Med.* 197, 1269-1278.
- Rohozinski, J., and Goorha, R. (1992). A frog virus 3 gene codes for a protein containing the motif characteristic of the INT family of integrases. *Virology*. 186, 693-700.
- Schibler, U., Kelley, D. E., and Perry, R. P. (1977). Comparison of methylated sequences in messenger RNA and heterogeneous nuclear RNA from mouse L cells. *J. Mol. Biol.* 115, 695-714.
- Schmitt, M. P., Tondre, L., Kirn, A. and Aubertin, A.M. (1990). The nucleotide sequence of a delayed early gene (31K) of frog virus 3. *Nucleic Acids Res.* 18, 13.
- Schnitzler, P., and Darai, G. (1989). Characterization of the repetitive DNA elements in the genome of fish lymphocystis disease virus. *Virology*. 172, 32-41
- Schug, M. D., Wetterstrande, K. A., Gaudette, M. S., Lim, R. H., Hutter, C. M., and Aquadro, C. F. (1998). The distribution and frequency of microsatellite loci in *Drosophila melanogaster*. *Mol. Ecol.* 7, 57-70.
- Seki, T., Tada, S., Katada, T., and Enomoto, T. (1997). Cloning of a cDNA encoding a novel importin- α homologue, Qip1: discrimination of

- Qip1 and Rch1 from hSrp1 by their ability to interact with DNA helicase Q1/RecQL. *Biochem Biophys Res Commun.* 234, 48-53.
- Silverstein, S., Bachenheimer, S. L., Frenkel, N., and Roizman, B. (1973). Relationship between post-transcriptional adenylation of herpes virus RNA and messenger RNA abundance. *Proc. Natl. Acad. Sci. U S A.* 70, 2101-2104.
- Skalka, A. M. (1977). DNA replication-bacteriophage lambda. *Curr. Top. Microbiol. Immunol.* 78, 201-237.
- Selker, E. U. (1990). DNA methylation and chromatin structure: a view from below. *Trends Biochem. Sci.* 15, 103-107.
- Shen, J. C., Gray, M. D., Oshima, J., Kamath-Loeb, A. S., Fry, M., and Loeb, L. A. (1998a). Werner syndrome protein. I. DNA helicase and DNA exonuclease reside on the same polypeptide. *J. Biol. Chem.* 273, 34139-34144.
- Shen, J. C., Gray, M. D., Oshima, J., and Loeb, L. A. (1998b). Characterization of Werner syndrome protein DNA helicase activity: directionality, substrate dependence and stimulation by replication protein A. *Nucleic Acids Res.* 26, 2879-2885.
- Shin, J. H., Reeve, J. N., and Kelman, Z. (2005). Use of a restriction enzyme-digested PCR product as substrate for helicase assays. *Nucleic Acids Research.* 33e8, 1-5.
- Smith, W. R., McAuslan, B. R. (1969). Biophysical properties of frog virus 3 and its DNA: Fate of radioactive virus in early stages of infection. *J. Virol.* 4, 322-347.
- Spangler, C. M., and Essani, K. (1994). Transactivation of methylated HIV-LTR by a frog virus 3 protein. *Virology.* 204, 651-655.
- Sonnhammer, E.L.L., Heijne, G.V., and Krogh, A. (1998). A hidden Markov model for predicting transmembrane helices in protein sequences. *Int. Conf. Intell. Syst. Mol. Biol.* AAAI Press, Montreal, Canada, pp. 175-182.
- Stoltz, D. B. (1973). The structure of icosahedral cytoplasmic deoxyriboviruses. II. An alternative model. *J. Ultrastruct. Res.* 43, 58-74.

- Stoltzfus, C. M., Shatkin, A. J., and Banerjee, A. K. (1973). Absence of polyadenylic acid from reovirus messenger ribonucleic acid. *J. Biol. Chem.* 248, 7993-7998.
- Streisinger, G., Emrich, J., and Stahl, M. M. (1967). Chromosome structure in phage T4. III. Terminal redundancy and length determination. *Proc. Natl. Acad. Sci. USA.* 57, 292-295.
- Suzuki, N., Shiratori, M., Goto, M., and Furuichi, Y. (1999). Werner syndrome helicase contains a 5'->3' exonuclease activity that digests DNA and RNA strands in DNA/DNA and RNA/DNA duplexes dependent on unwinding. *Nucleic Acids Res.* 27, 2361-2368.
- Swofford, D. L. (2003). PAUP*. Phylogenetic Analysis Using Parsimony (*and Other Methods). Version 4. Sinauer Associates, Sunderland, Massachusetts.
- Tan, W. G. H., Barkman, T. J., Chinchar, V. G., and Essani, K. (2004). Comparative genomic analyses of frog virus 3, type species of the genus Ranavirus (family Iridoviridae). *Virology.* 323, 70-84.
- Tanner, N. K. (2003). The newly identified Q motif of DEAD box helicases is involved in adenine recognition. *Cell Cycle.* 2, 18-19.
- Tanner, N. K., Cordin, O., Banroques, J., Doère, M., and Linder, P. (2003). The Q motif: a newly identified motif in DEAD box helicases may regulate ATP binding and hydrolysis. *Mol. Cell.* 11, 127-128.
- Thompson, J. D., Gibson, T. J., Plewniak, F., Jeanmougin, F. and Higgins, D. G. (1997). The ClustalX windows interface: flexible strategies for multiple sequence alignment aided by quality analysis tools. *Nucleic Acids Research.* 24, 4876-4882.
- Thompson, J. P., Granoff, A., and Willis, D. B. (1986). Trans-activation of a methylated adenovirus promoter by a frog virus 3 protein. *Proc. Natl. Acad. Sci. USA.* 83, 7688-7692.
- Thompson, J. P., Granoff, A., and Willis, D. B. (1987). Infection with frog virus 3 allows transcription of DNA methylated at cytosine but not adenine residues. *Virology.* 166, 275-277.
- Tidona, C. A. and Darai, G. (1997). The complete DNA sequence of lymphocystis disease virus. *Virology.* 230, 207-216.

- Tidona, C. A., Schnitzler, P., Kehm, R., and Darai, G. (1998). Is the major capsid protein of iridoviruses a suitable target for the study of viral evolution? *Virus Genes*. 16, 59-66.
- Tondre, L., Tham, T. N., Mutin, H., and Aubertin, A.M. (1988). Molecular cloning and physical and translational mapping of the frog virus 3 genome. *Virology*. 162, 108-117.
- Tripier, F., Braunwald, J., Markovic, L., and Kirn, A. (1977). Frog virus 3 morphogenesis: effect of temperature and metabolic inhibitors. *J. Gen. Virol.* 37, 39-52.
- Tsai, C. T., Ting, J. W., Wu, M. H., Wu, M. F., Guo, I. C., and Chang, C. Y. (2005). Complete genome sequence of the grouper iridovirus and comparison of genomic organization with those of other iridoviruses. *J. Virol.* 79, 2010-2023.
- Tuteja, N., and Tuteja, Renu. (2004). Unraveling DNA helicases: motif, structure, mechanism and function. *Eur. J. Biochem.* 271, 1849-1863.
- Umezū, K., and Nakayama, H. (1993). RecQ DNA helicase of *Escherichia coli*. Characterization of the helix-unwinding activity with emphasis on the effect of single-stranded DNA-binding protein. *J. Mol. Biol.* 230, 1145-1150.
- Volpe, P., Iacovacci, P., Butler, R. H., and Ermenko, T. (1993). 5-methylcytosine in genes with methylation dependent regulation. *Federation of European Biochemical Societies Letters*. 329, 23-237.
- Watson, J. D. (1971). Origin of concatemeric T7 DNA. *Nature*. 239, 197-201.
- Williams, T., Chinchar, G., Darai, G., Hyatt, A., Kalkmakoff, J., and Seligg, V. (2000). Family Iridoviridae. In: *Virus Taxonomy – 7th Report of the international committee on taxonomy of viruses*, (Regentmortel *et al.*, Eds.), pp167-182, Academic Press, NY.
- Willis, D. B. (1985). *Current Topics in Microbiology and Immunology*. Iridoviridae. Springer-Verlag. Berlin-Heidelberg.
- Willis, D. B., Foglesong, D., and Granoff, A. (1984b). Nucleotide sequence of an immediate-early frog virus 3 gene. *J. Virol.* 53, 905-912.
- Willis, D. B., Goorha, R., Miles, M., and Granoff, A. (1977). Macromolecular synthesis in cells infected by frog virus 3. VII. Transcriptional and post-

- transcriptional regulation of virus gene expression. *J. Virol.* 24, 326-342.
- Willis, D. B., Goorha, R., and Granoff, A. (1979a). Macromolecular synthesis in cells infected by frog virus 3. XI. A ts mutant of frog virus 3 that is defective in late transcription. *Virology.* 98, 328-335
- Willis, D. B., Goorha, R., and Granoff, A. (1979b). Nongenetic reactivation of frog virus 3 DNA. *Virology.* 98, 476-479.
- Willis, D. B., Goorha, R., and Granoff, A. (1984a). DNA methyltransferase induced by frog virus 3. *J. Virol.* 49, 86-91
- Willis, D. B., and Granoff, A. (1976a). Macromolecular synthesis in cells infected by frog virus 3. IV. Regulation of virus-specific RNA synthesis. *Virology.* 70, 397-410
- Willis, D. B., and Granoff, A. (1976b). Macromolecular synthesis in cells infected by frog virus 3. V. The absence of polyadenylic acid in the majority of virus-specific RNA species. *Virology.* 73, 543-547.
- Willis, D. B., and Granoff, A. (1978). Macromolecular synthesis in cells infected by frog virus 3. IX. Two temporal classes of early viral RNA. *Virology.* 86, 443-453.
- Willis, D. B., and Granoff, A. (1980). Frog virus 3 DNA is heavily methylated at CpG sequences. *Virology.* 107, 250-257.
- Willis, D. B., and Granoff, A. (1985). trans activation of an immediate-early frog virus 3 promoter by a virion protein. *J. Virol.* 56, 495-501.
- Willis, D. B., and Thompson, J. P. (1986). The iridovirus frog virus 3: a model for trans-acting proteins. *Microbiological Sciences.* 3, 59-63.
- Willis, D. B., Thompson, J. P., Essani, K., and Goorha, R. (1989). Transcription of methylated viral DNA by eukaryotic RNA Polymerase II. *Cell Biophysics.* 15, 97-111.
- Wöfl, S., Schröder, M., and Witting, B. C. (1991). Lack of correlation between DNA methylation and transcriptional inactivation: The chicken lysozyme gene. *Proc. Natl. Acad. Sci. USA.* 88, 271-275.
- Yin, J., Kwon, Y. T., Varsgavsky, A., and Wang, W. (2004). RECQL4, mutated in the Rothmund-Thomson and RAPADILINO syndromes, interacts with ubiquitin ligases UBR1 and UBR2 of the N-end rule pathway. *Hum Mol Genet.* 13, 2421-2430.